

Disentangling physics and chemistry in AGB outflows: revealing degeneracies when adding complexity

Electronic supplementary information

Marie Van de Sande, Catherine Walsh, Tom J. Millar

The electronic supplementary information shows the fractional abundance profiles of all parent species and their daughters, along with all species that show a significant change in abundance when including a companion. It also includes the number of monolayers of dust and ice for all assumed GSDs and the ice and refractory coverage at the end of the outflow for the GSDs different to the MRN distribution. The table of contents contains links to the relevant sections for easy navigation.

Contents

1 Gas-phase tracers of dust-gas chemistry	2
1.1 O-rich outflows	2
1.2 C-rich outflows	9
2 Fractional abundances of gas-phase species	14
2.1 O-rich outflows	14
2.2 C-rich outflows	34
3 Grain surface coverage with ice and refractory material	71
3.1 O-rich outflows	71
3.1.1 Ice coverage	71
3.1.2 Refractory coverage	71
3.2 C-rich outflows	71
3.2.1 Ice coverage	71
3.2.2 Refractory coverage	71
4 Number of monolayers of ice and refractory material throughout the outflow	72
4.1 O-rich outflows	72
4.1.1 Ice coverage	72
4.1.2 Refractory coverage	72
4.2 C-rich outflows	72
4.2.1 Ice coverage	72
4.2.2 Refractory coverage	72

1 Gas-phase tracers of dust-gas chemistry

1.1 O-rich outflows

Fractional abundance profiles relative to H_2 for a selection of outflows with different outflow densities (columns) and companions (rows). Different line styles show different chemistries included. Dashed lines: gas-phase chemistry only, solid lines: including dust-gas chemistry. Different colours show different density structures and the inclusion of a companion. Black: smooth outflow without a companion, gray: porous outflow without a companion. When including a companion, different shades correspond to the value of R_{dust} . Darker shade: $R_{\text{dust}} = 2 R_*$, lighter shade: $R_{\text{dust}} = 5 R_*$. Purple: smooth outflow with a companion. Green: porous outflow with a companion, $f_{\text{ic}} = 0.0$, $f_{\text{vol}} = 0.3$, $l_* = 10^{13}$ cm. Orange: porous outflow with a companion, $f_{\text{ic}} = 0.1$, $f_{\text{vol}} = 0.5$, $l_* = 10^{13}$ cm. Blue: porous outflow with a companion, $f_{\text{ic}} = 0.3$, $f_{\text{vol}} = 0.3$, $l_* = 5 \times 10^{12}$ cm.

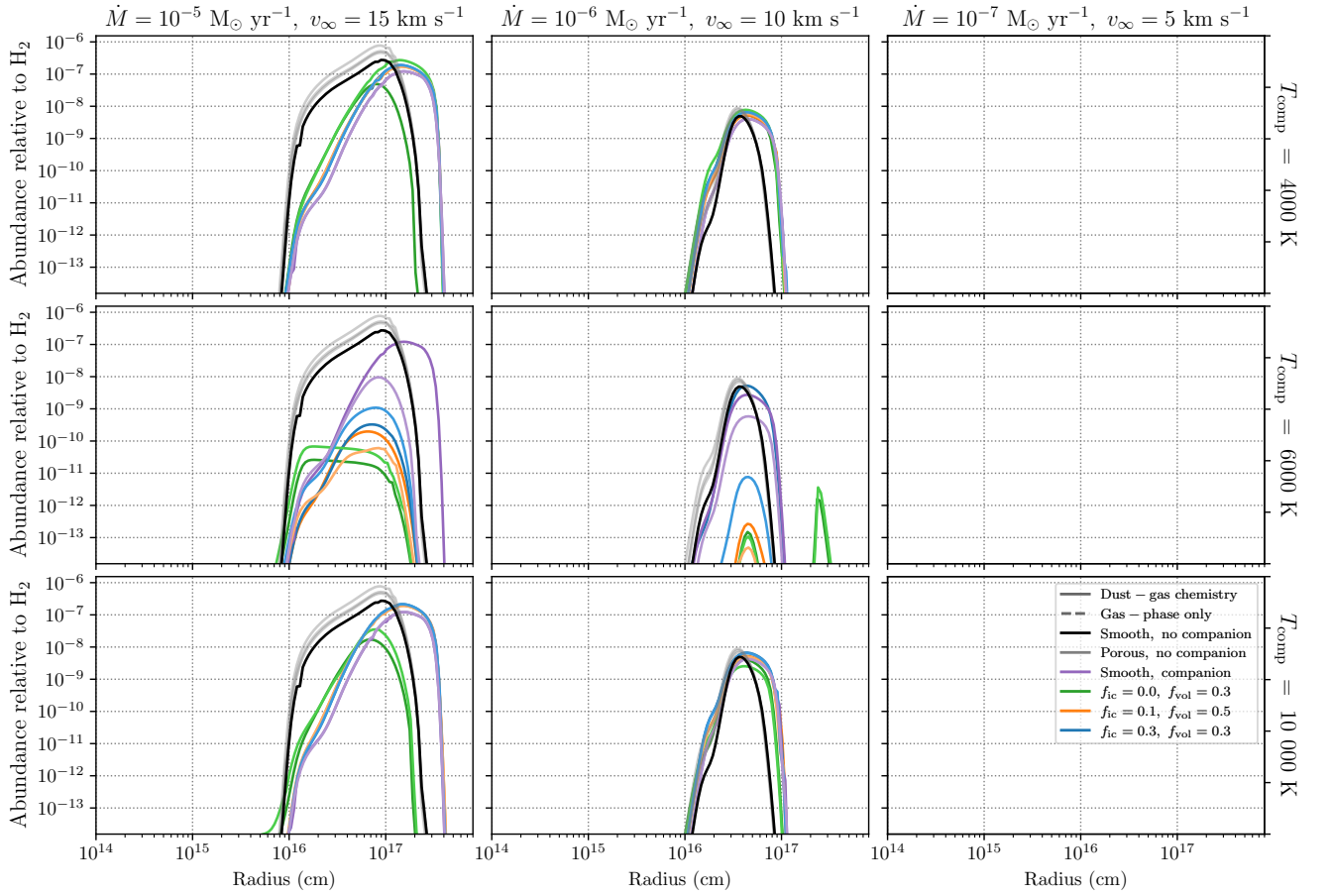


Figure 1: Fractional abundance of H_2O_2 relative to H_2 for a selection of O-rich outflows.

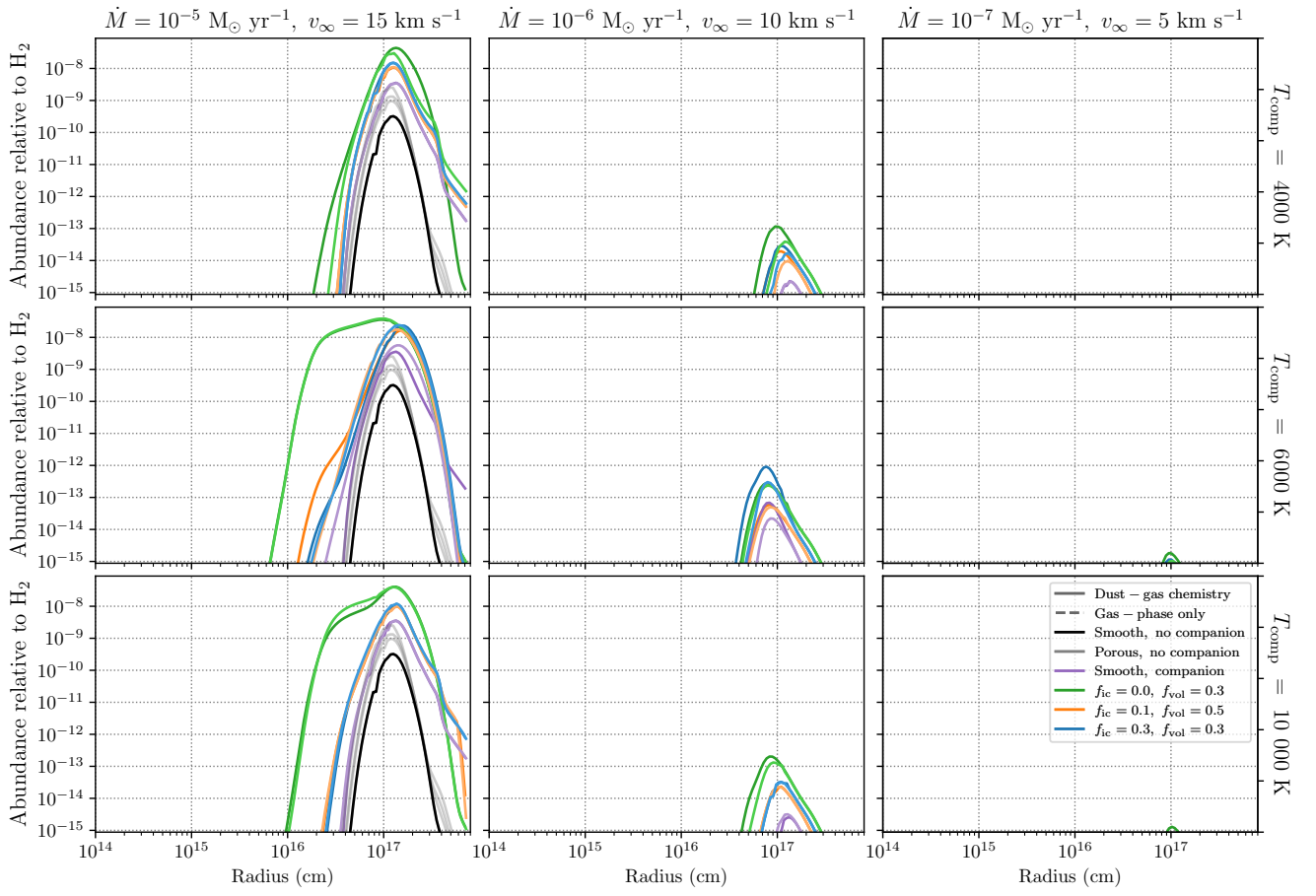


Figure 2: Fractional abundance of H_2SiO relative to H_2 for a selection of O-rich outflows.

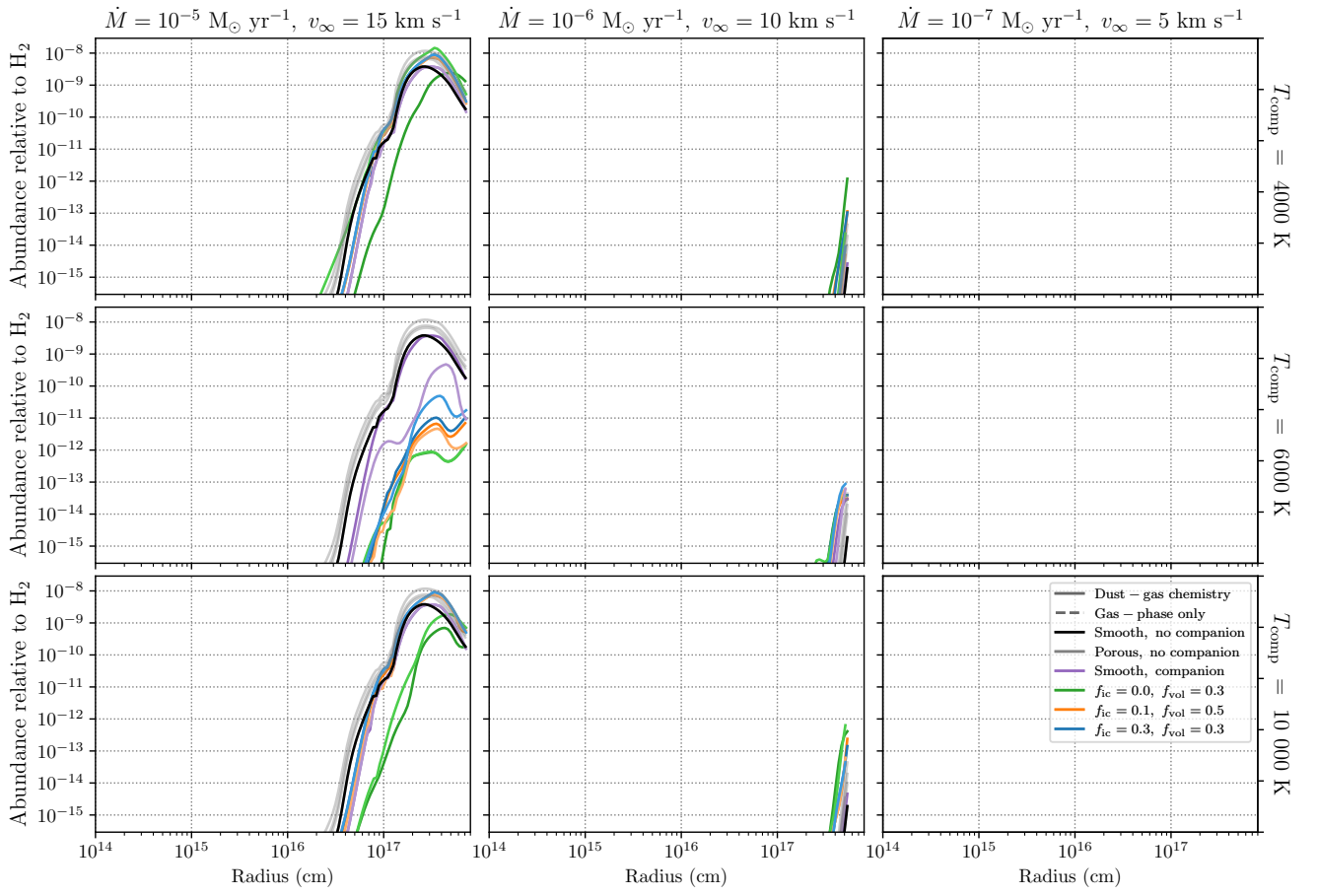


Figure 3: Fractional abundance of NH_2OH relative to H_2 for a selection of O-rich outflows.

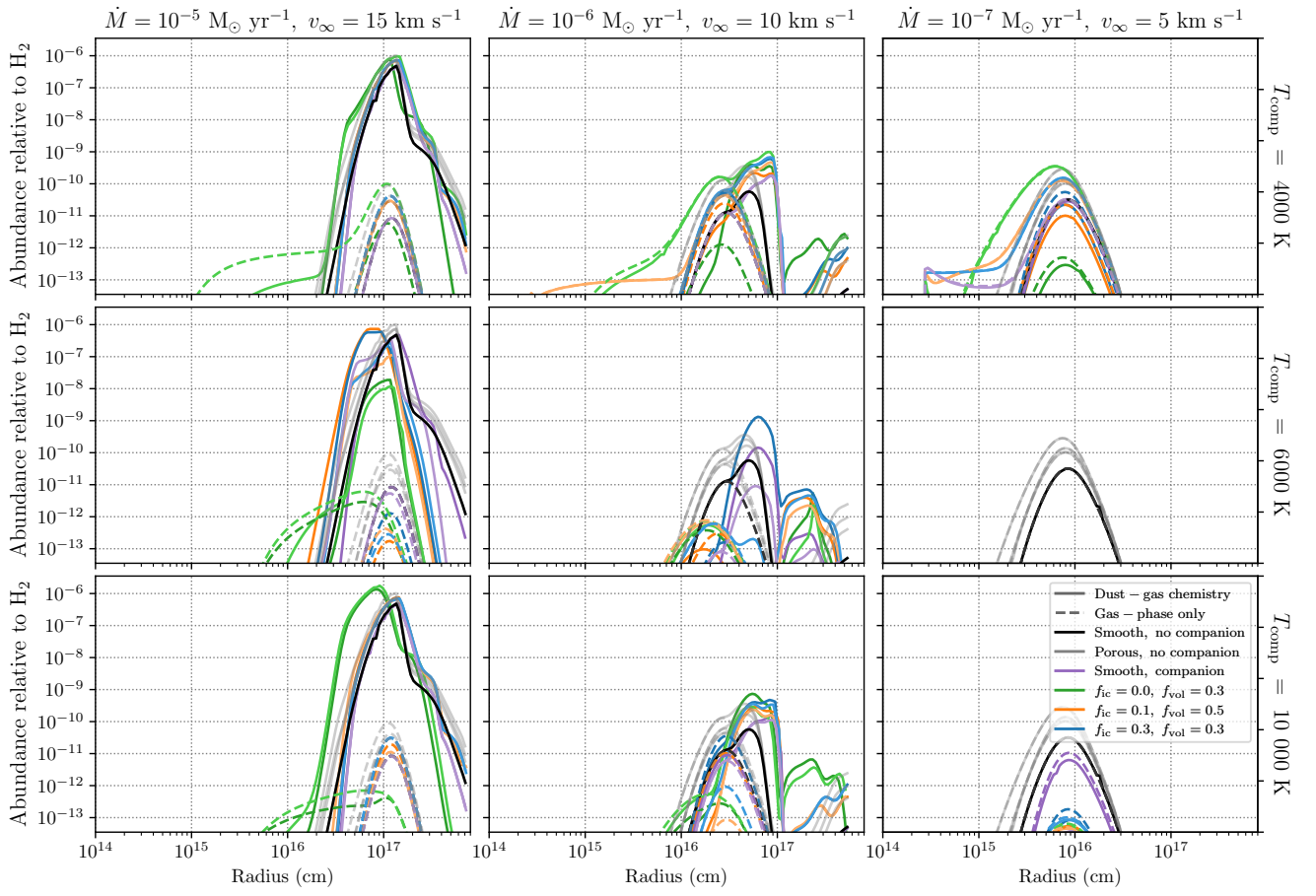


Figure 4: Fractional abundance of NO_2 relative to H_2 for a selection of O-rich outflows.

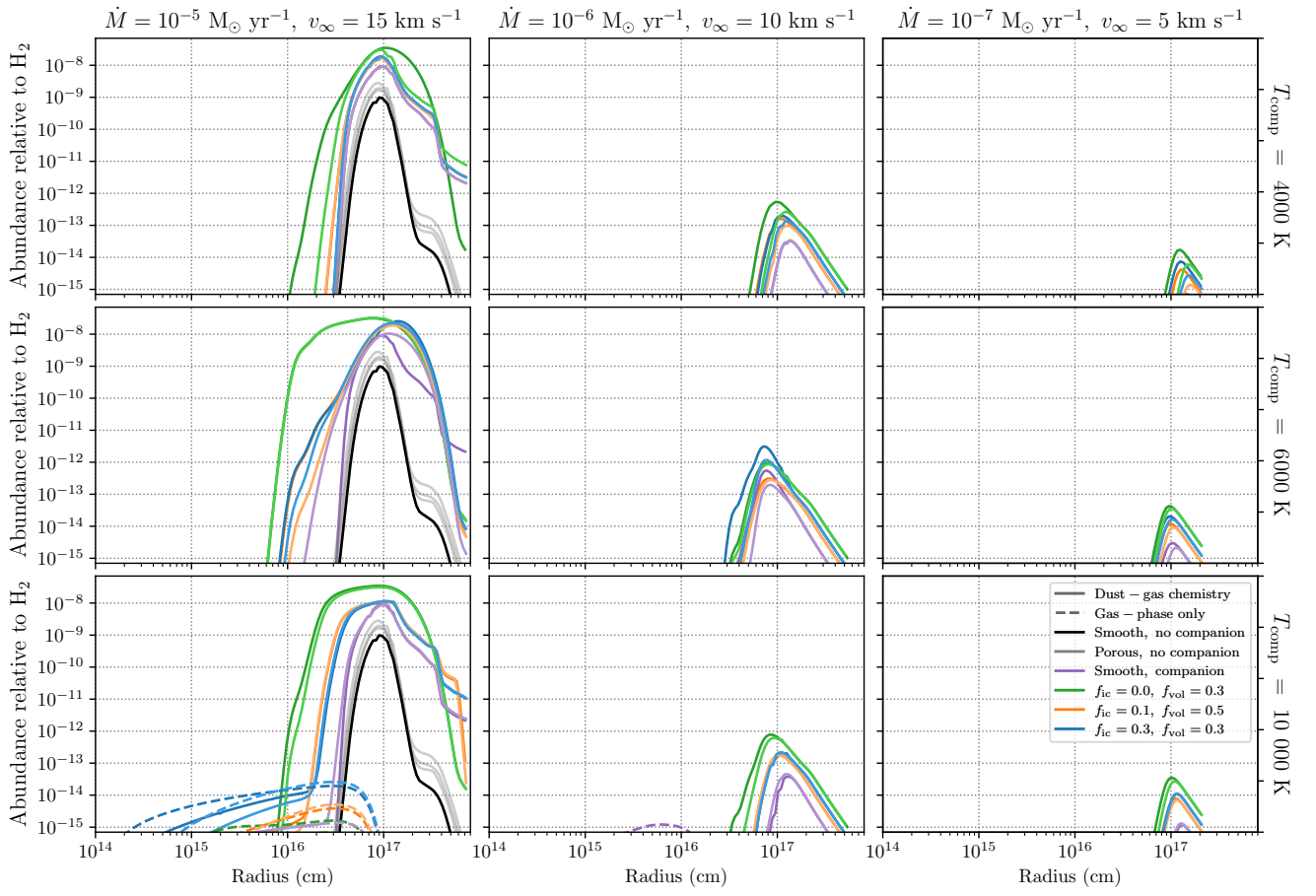


Figure 5: Fractional abundance of SiH_4 relative to H_2 for a selection of O-rich outflows.

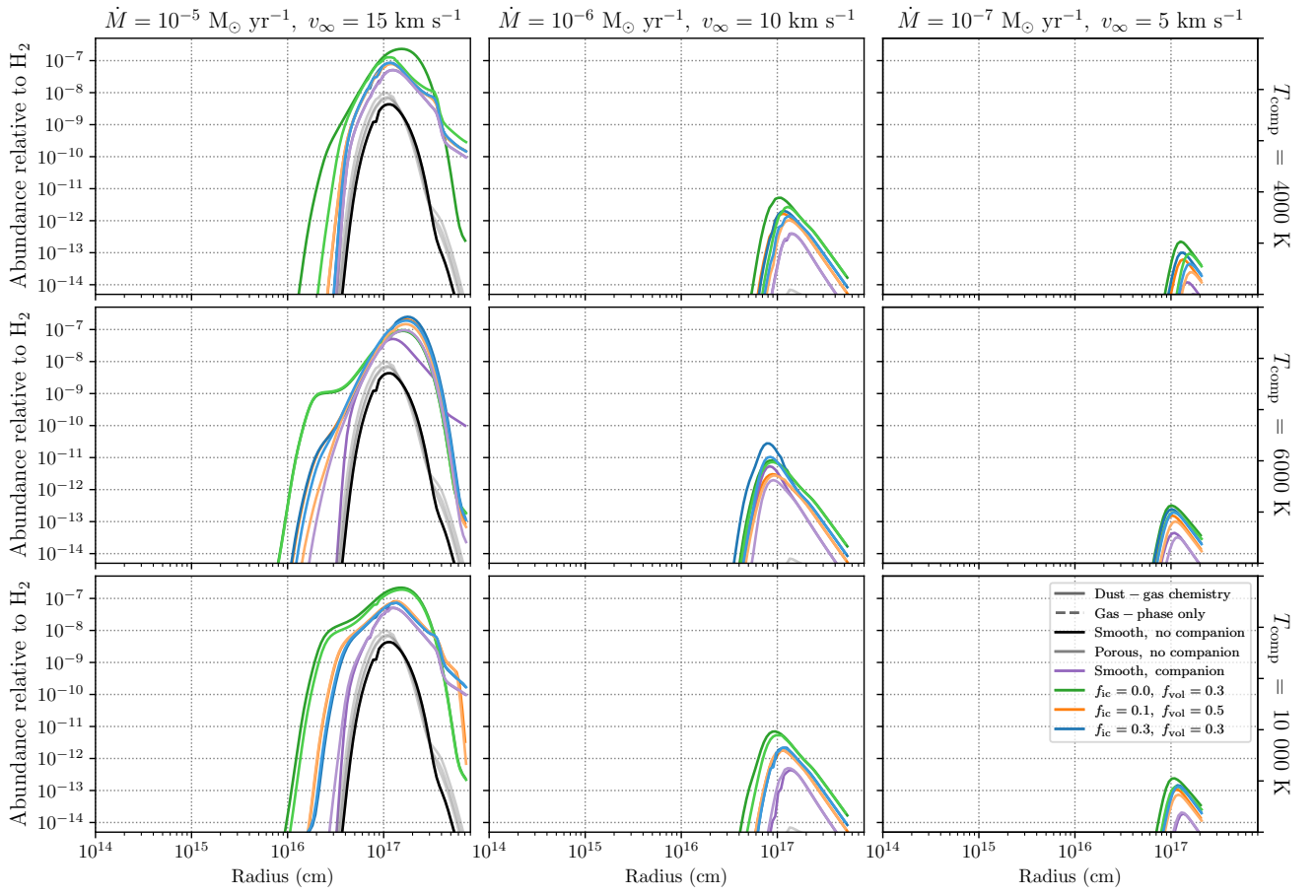


Figure 6: Fractional abundance of SiH_3 relative to H_2 for a selection of O-rich outflows.

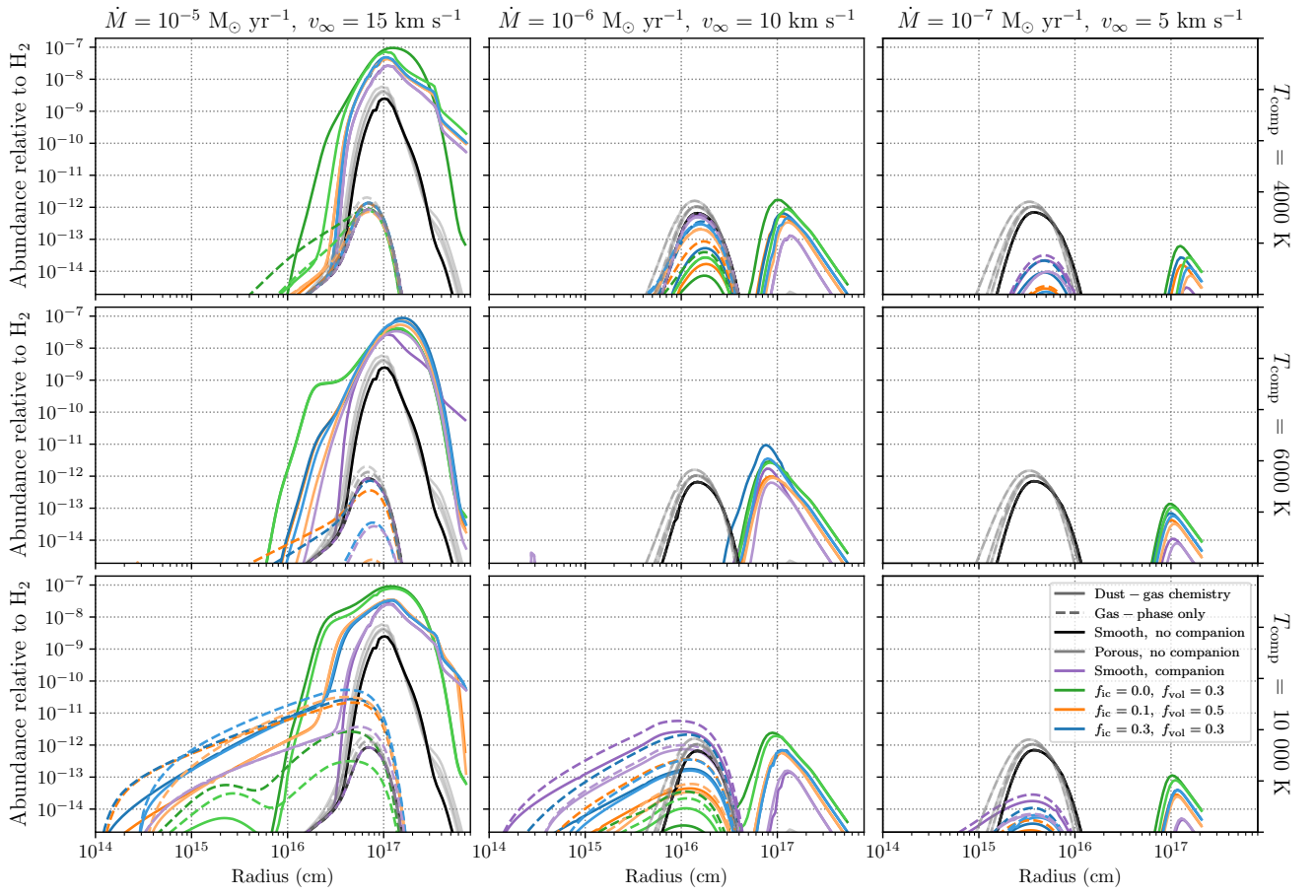


Figure 7: Fractional abundance of SiH₂ relative to H₂ for a selection of O-rich outflows.

1.2 C-rich outflows

Fractional abundance profiles relative to H_2 for a selection of outflows with different outflow densities (columns) and companions (rows). Different line styles show different chemistries included. Dashed lines: gas-phase chemistry only, solid lines: including dust-gas chemistry. Different colours show different density structures and the inclusion of a companion. Black: smooth outflow without a companion, gray: porous outflow without a companion. When including a companion, different shades correspond to the value of R_{dust} . Darker shade: $R_{\text{dust}} = 2 R_*$, lighter shade: $R_{\text{dust}} = 5 R_*$. Purple: smooth outflow with a companion. Green: porous outflow with a companion, $f_{\text{ic}} = 0.0$, $f_{\text{vol}} = 0.3$, $l_* = 10^{13}$ cm. Orange: porous outflow with a companion, $f_{\text{ic}} = 0.1$, $f_{\text{vol}} = 0.5$, $l_* = 10^{13}$ cm. Blue: porous outflow with a companion, $f_{\text{ic}} = 0.3$, $f_{\text{vol}} = 0.3$, $l_* = 5 \times 10^{12}$ cm.

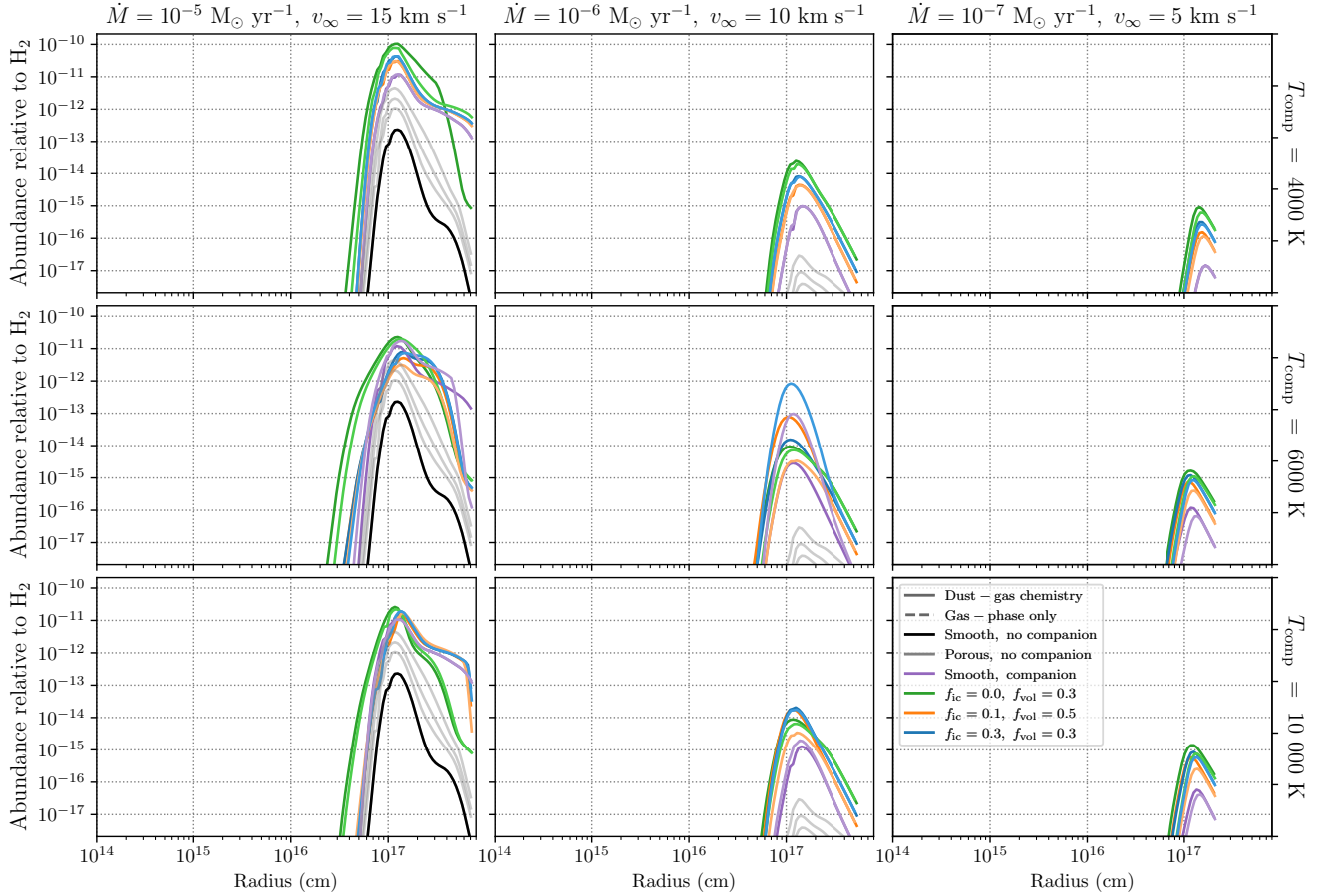


Figure 8: Fractional abundance of H_2SiO relative to H_2 for a selection of C-rich outflows.

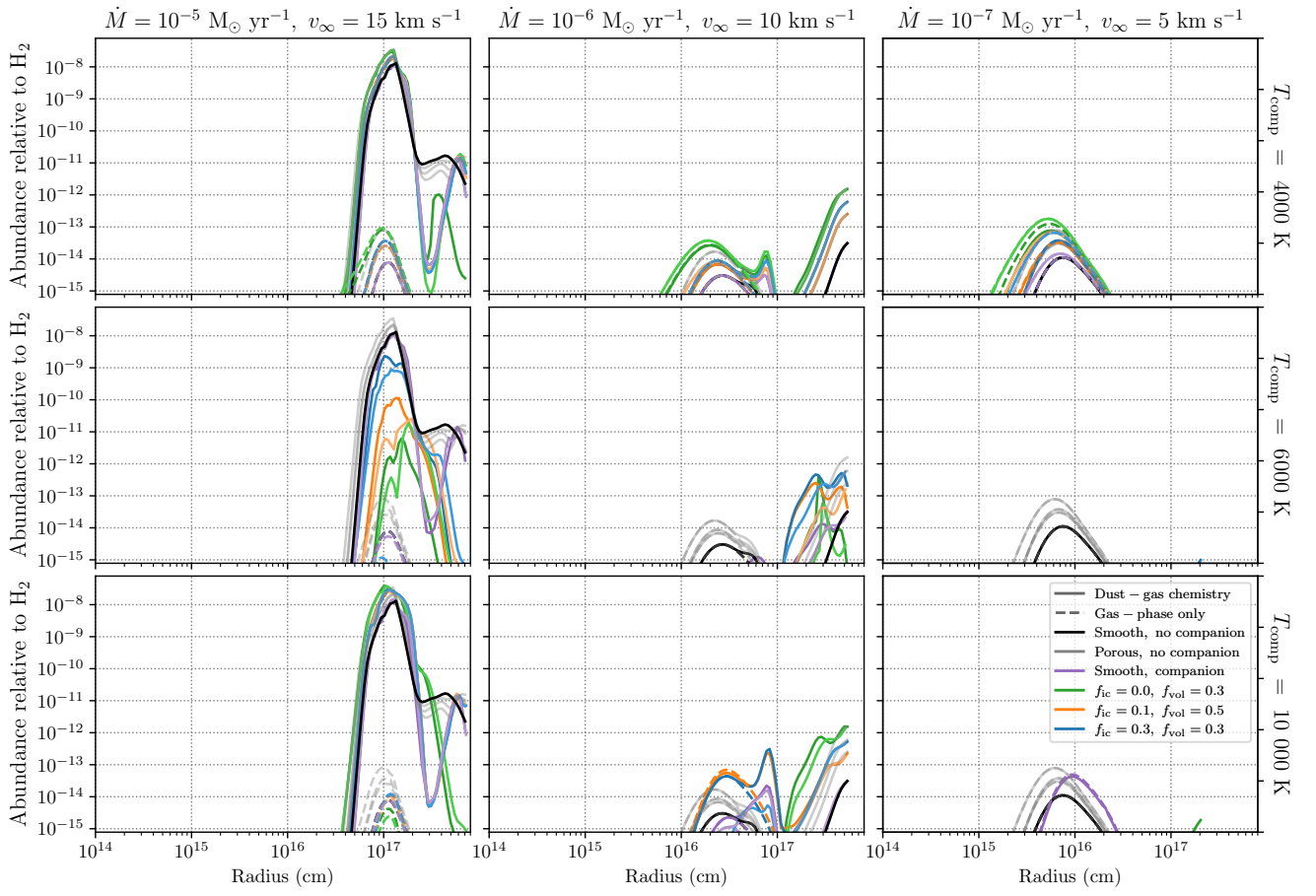


Figure 9: Fractional abundance of NO_2 relative to H_2 for a selection of C-rich outflows.

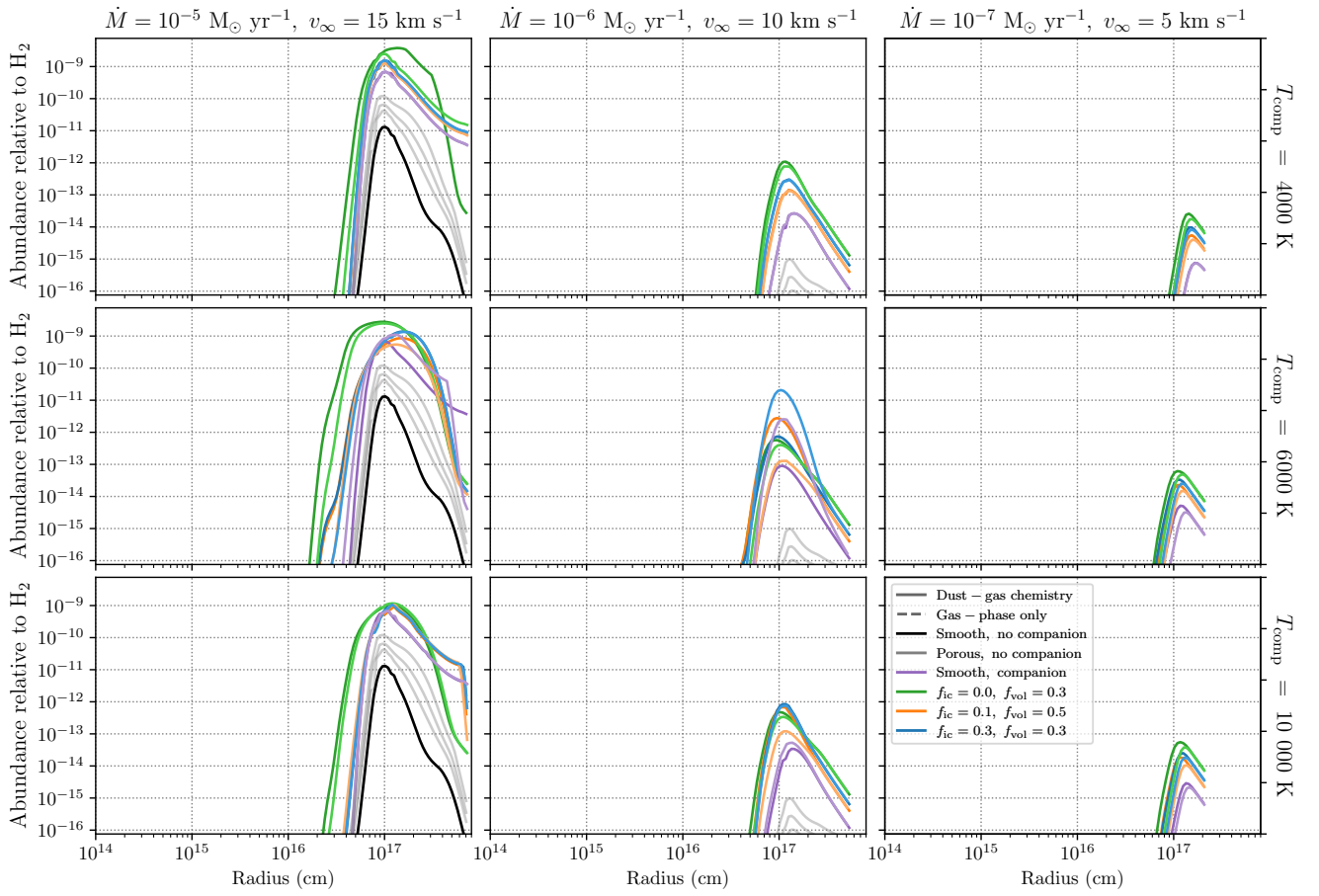


Figure 10: Fractional abundance of SiH_4 relative to H_2 for a selection of C-rich outflows.

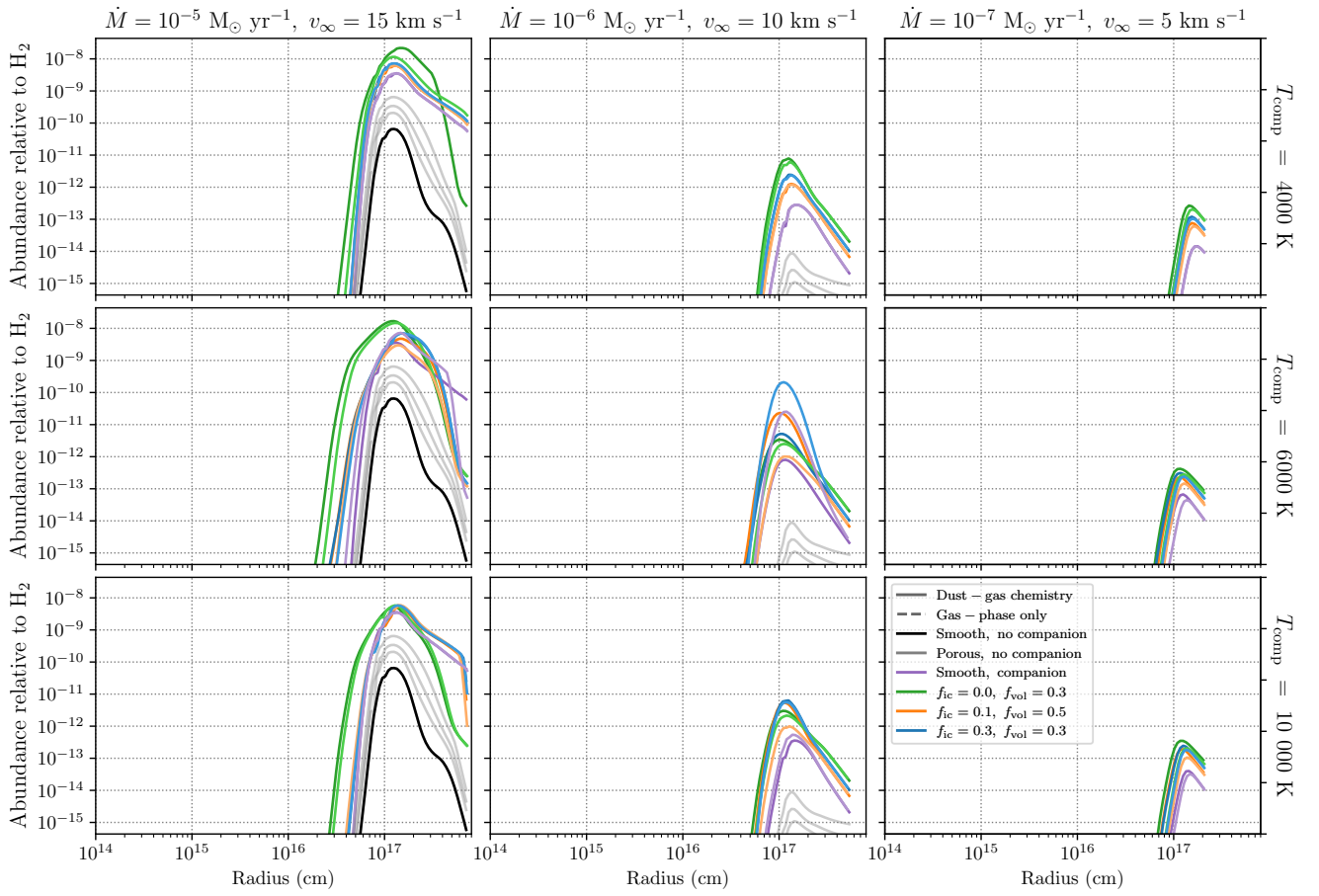


Figure 11: Fractional abundance of SiH_3 relative to H_2 for a selection of C-rich outflows.

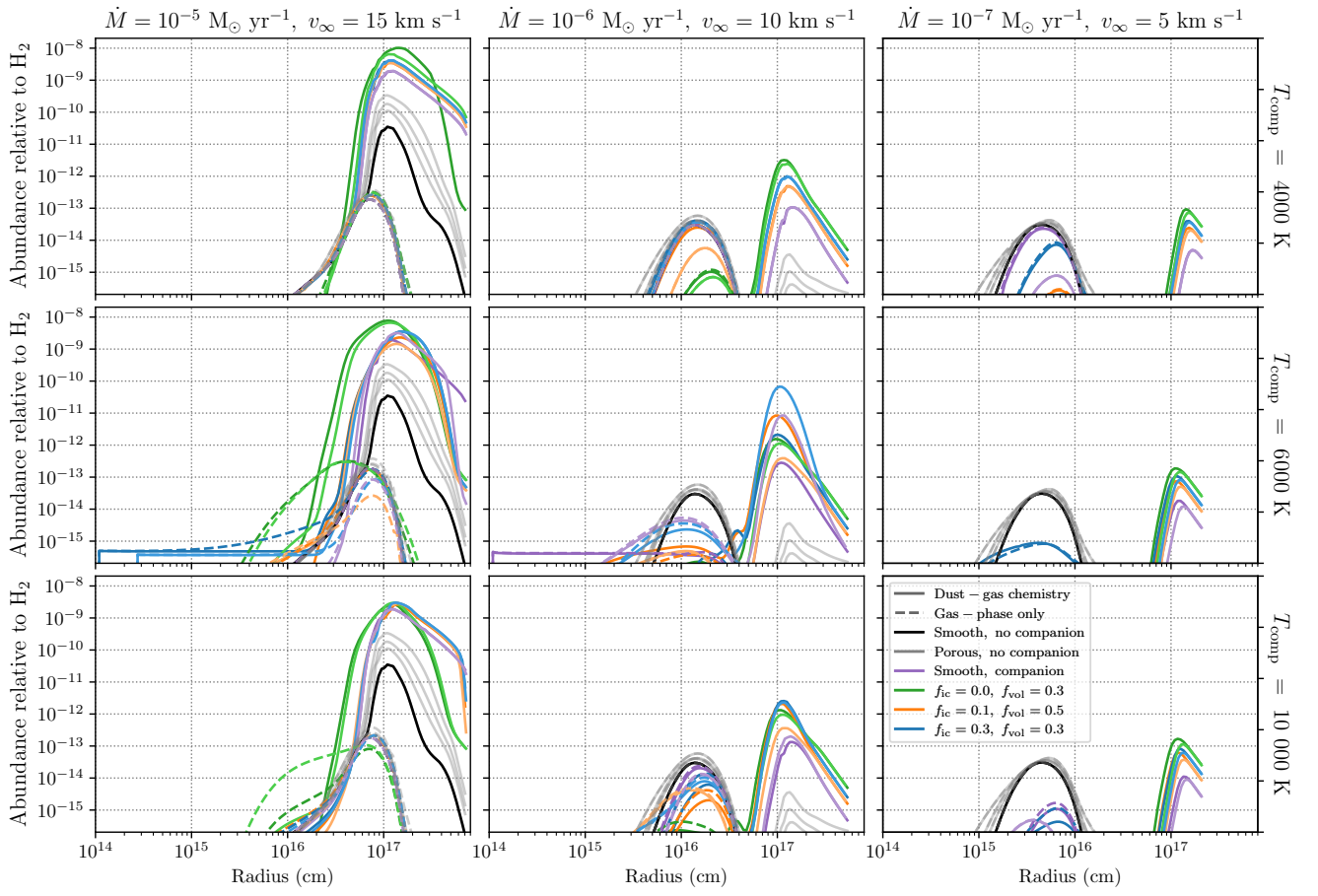


Figure 12: Fractional abundance of SiH₂ relative to H₂ for a selection of C-rich outflows.

2 Fractional abundances of gas-phase species

2.1 O-rich outflows

Fractional abundance profiles relative to H_2 for a selection of outflows with different outflow densities (columns) and companions (rows). Different line styles show different chemistries included. Dashed lines: gas-phase chemistry only, solid lines: including dust-gas chemistry. Different colours show different density structures and the inclusion of a companion. Black: smooth outflow without a companion, gray: porous outflow without a companion. When including a companion, different shades correspond to the value of R_{dust} . Darker shade: $R_{\text{dust}} = 2 R_*$, lighter shade: $R_{\text{dust}} = 5 R_*$. Purple: smooth outflow with a companion. Green: porous outflow with a companion, $f_{\text{ic}} = 0.0$, $f_{\text{vol}} = 0.3$, $l_* = 10^{13}$ cm. Orange: porous outflow with a companion, $f_{\text{ic}} = 0.1$, $f_{\text{vol}} = 0.5$, $l_* = 10^{13}$ cm. Blue: porous outflow with a companion, $f_{\text{ic}} = 0.3$, $f_{\text{vol}} = 0.3$, $l_* = 5 \times 10^{12}$ cm.

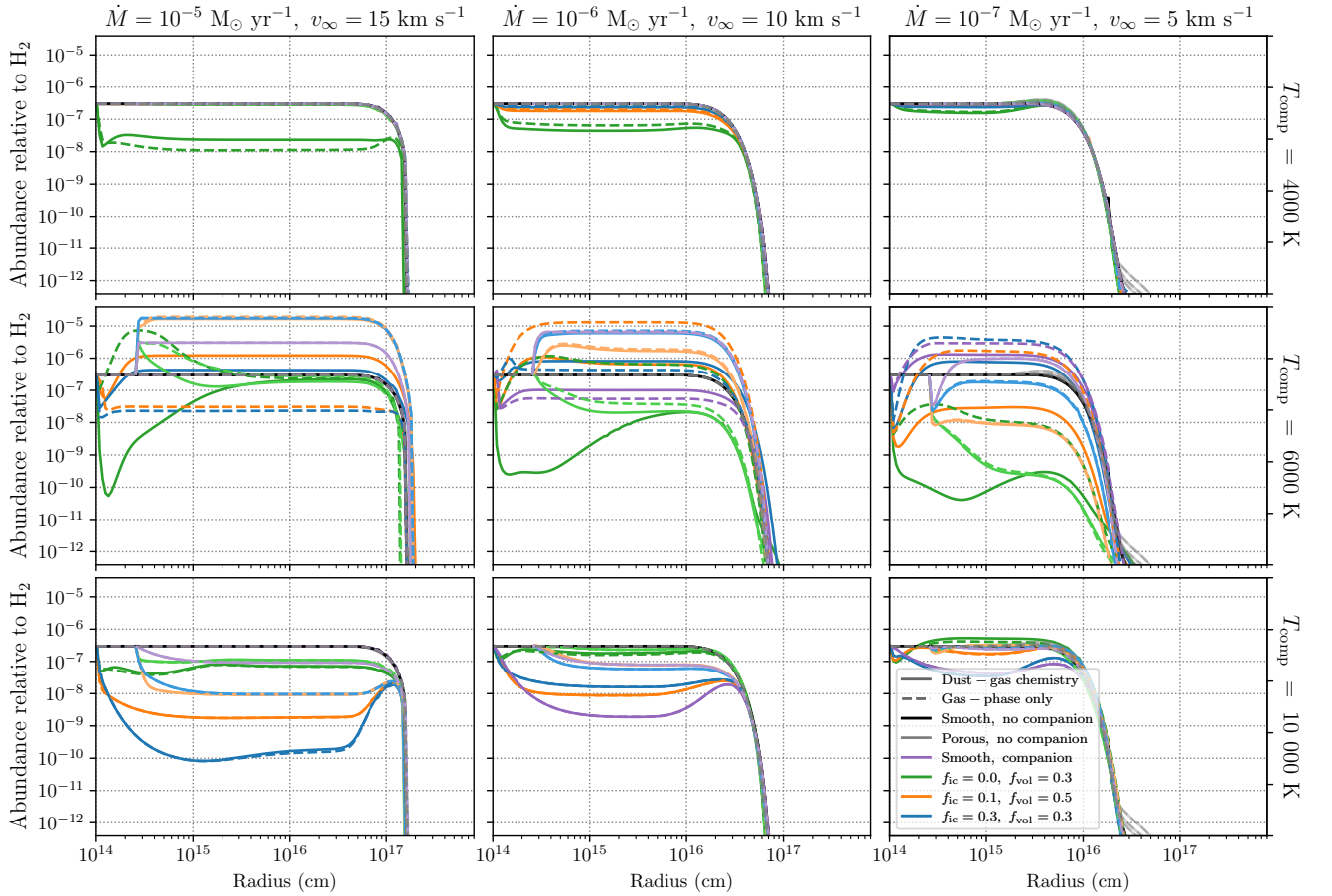


Figure 13: Fractional abundance of CO_2 relative to H_2 for a selection of O-rich outflows.

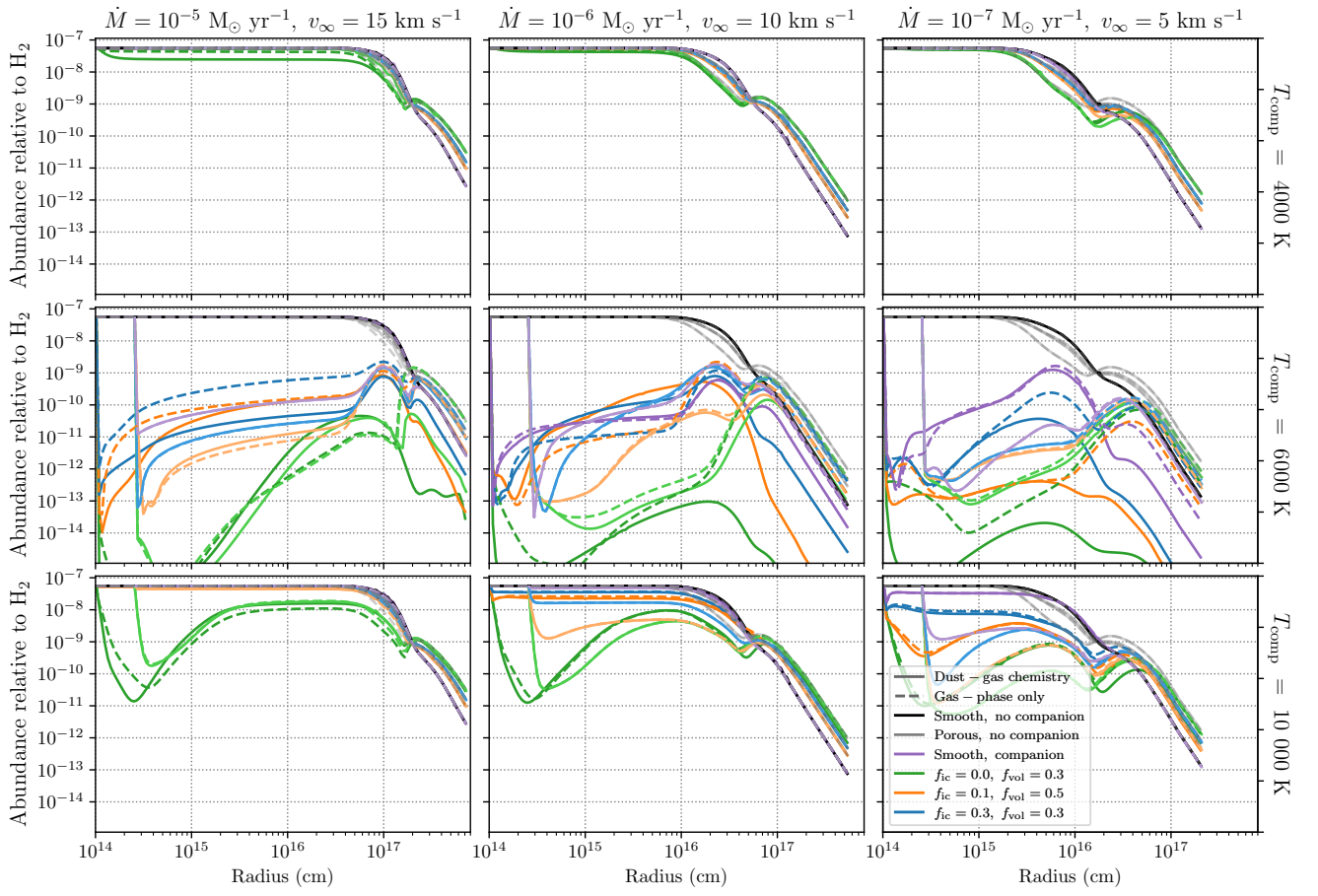


Figure 14: Fractional abundance of CS relative to H₂ for a selection of O-rich outflows.

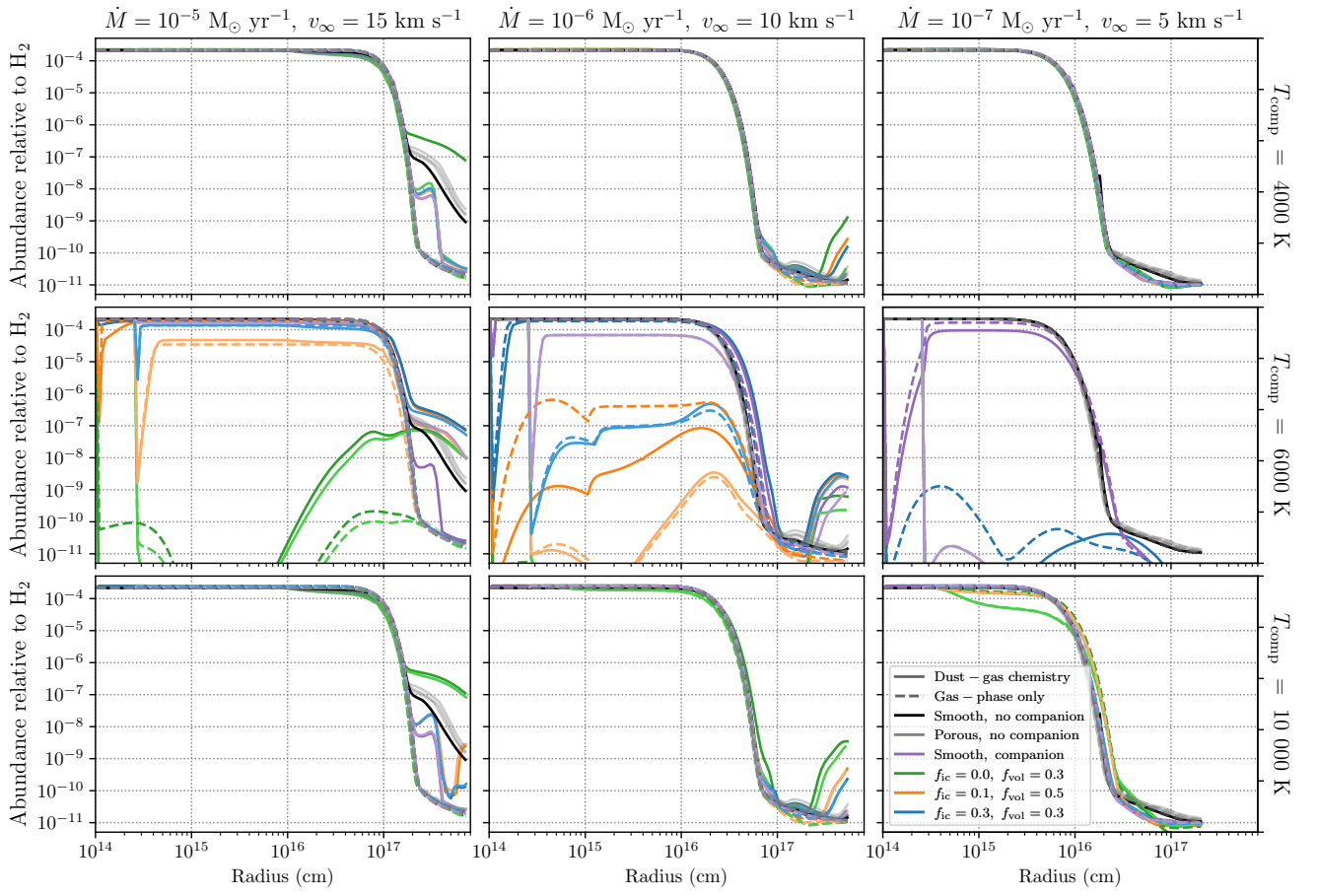


Figure 15: Fractional abundance of H_2O relative to H_2 for a selection of O-rich outflows.

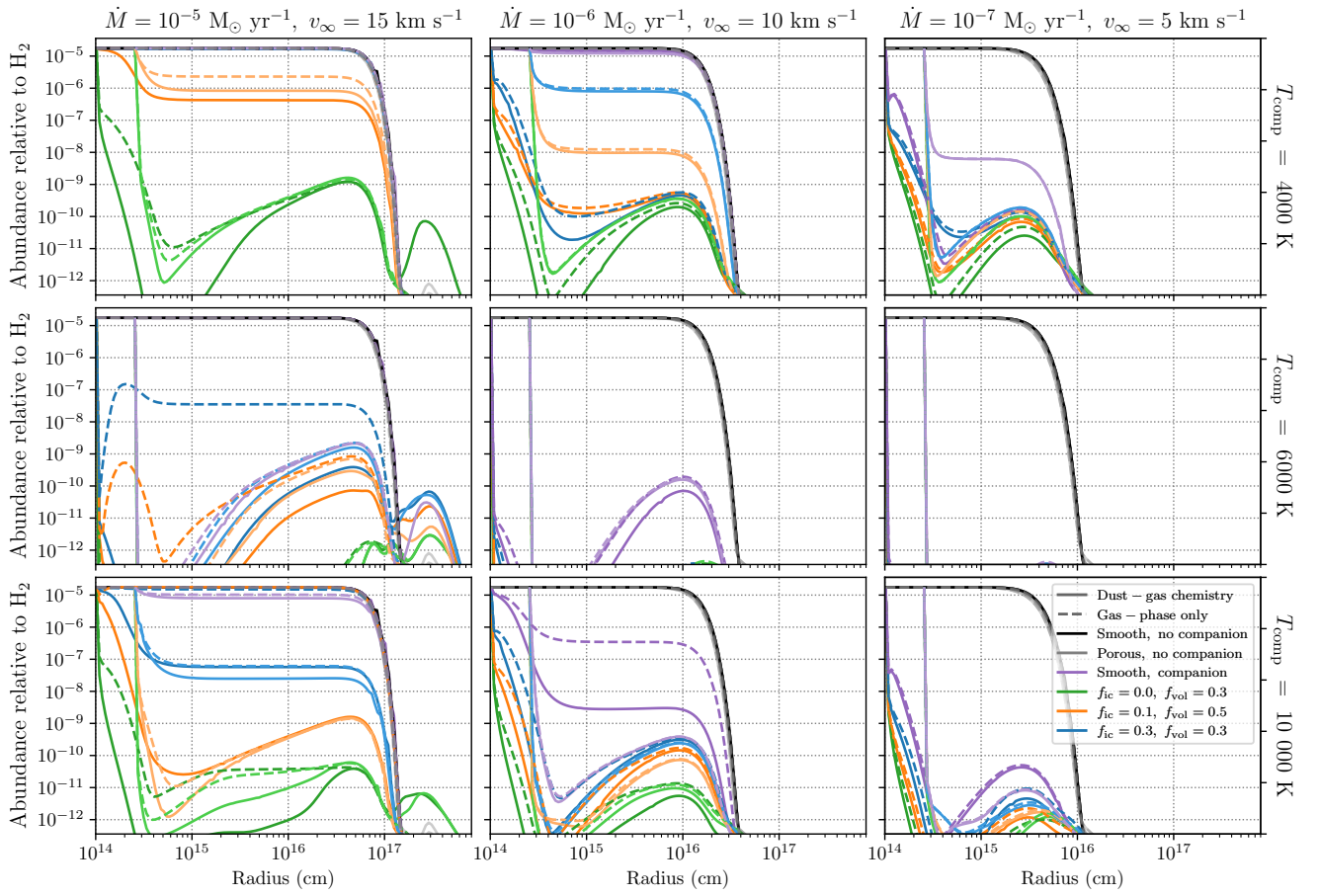


Figure 16: Fractional abundance of H_2S relative to H_2 for a selection of O-rich outflows.

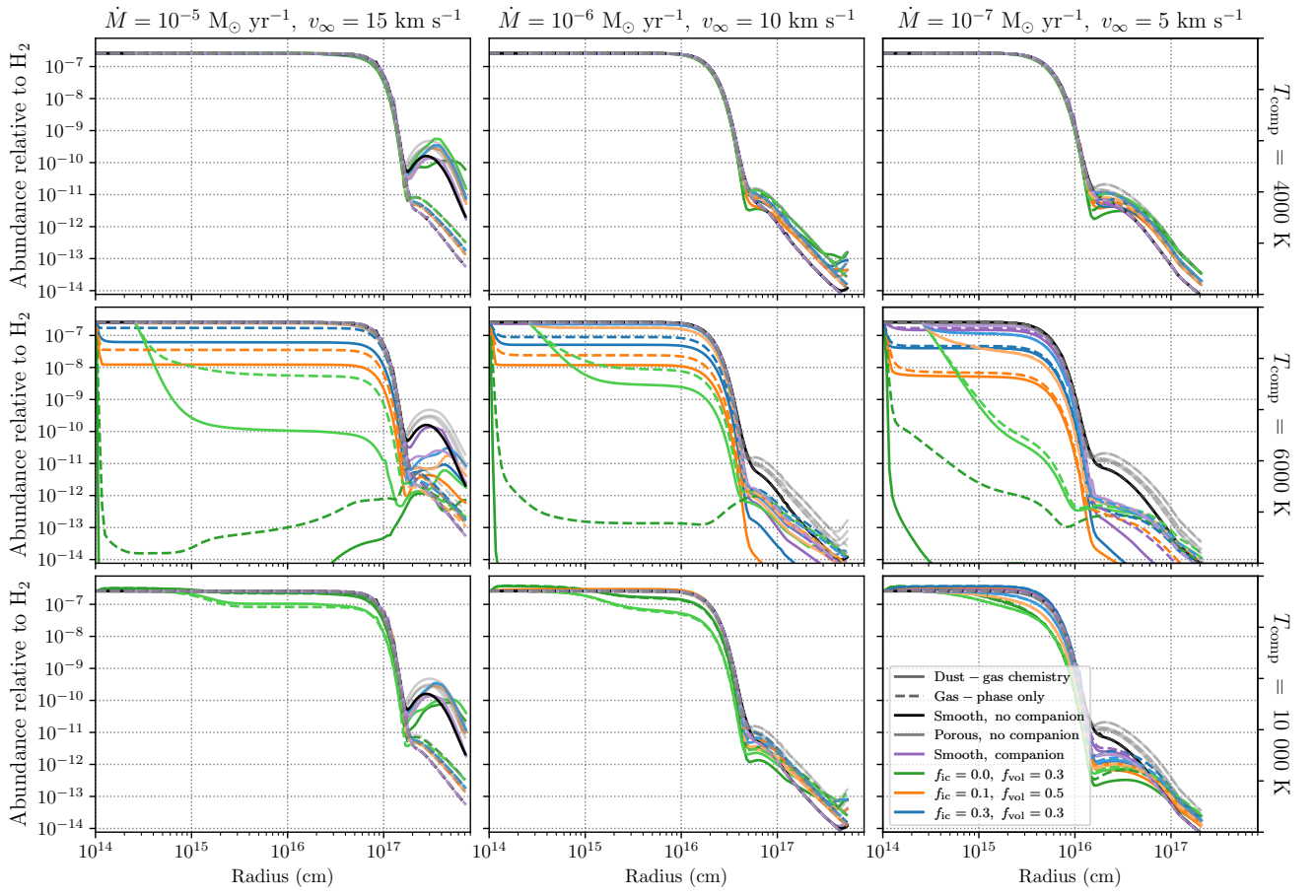


Figure 17: Fractional abundance of HCN relative to H_2 for a selection of O-rich outflows.

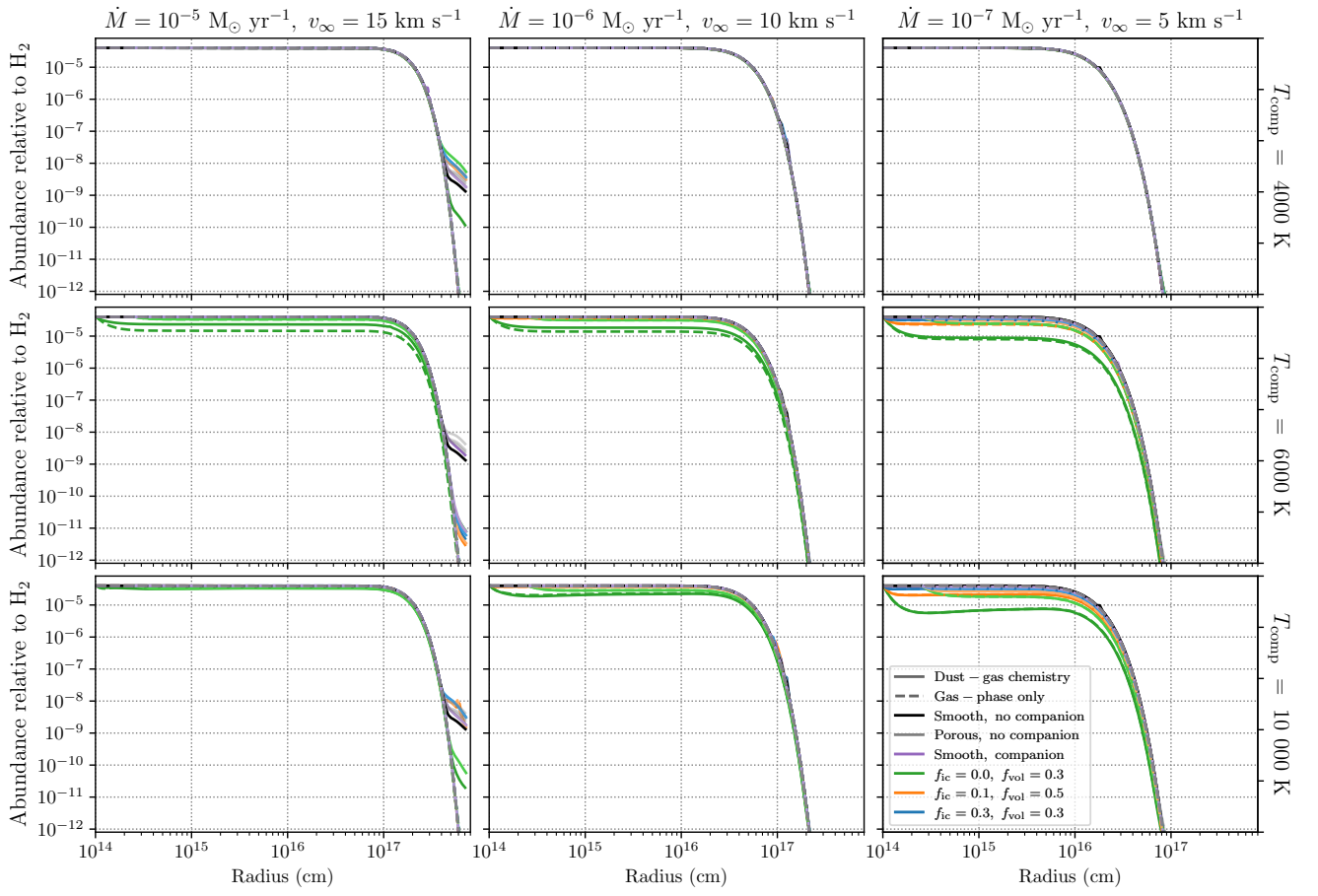


Figure 18: Fractional abundance of N_2 relative to H_2 for a selection of O-rich outflows.

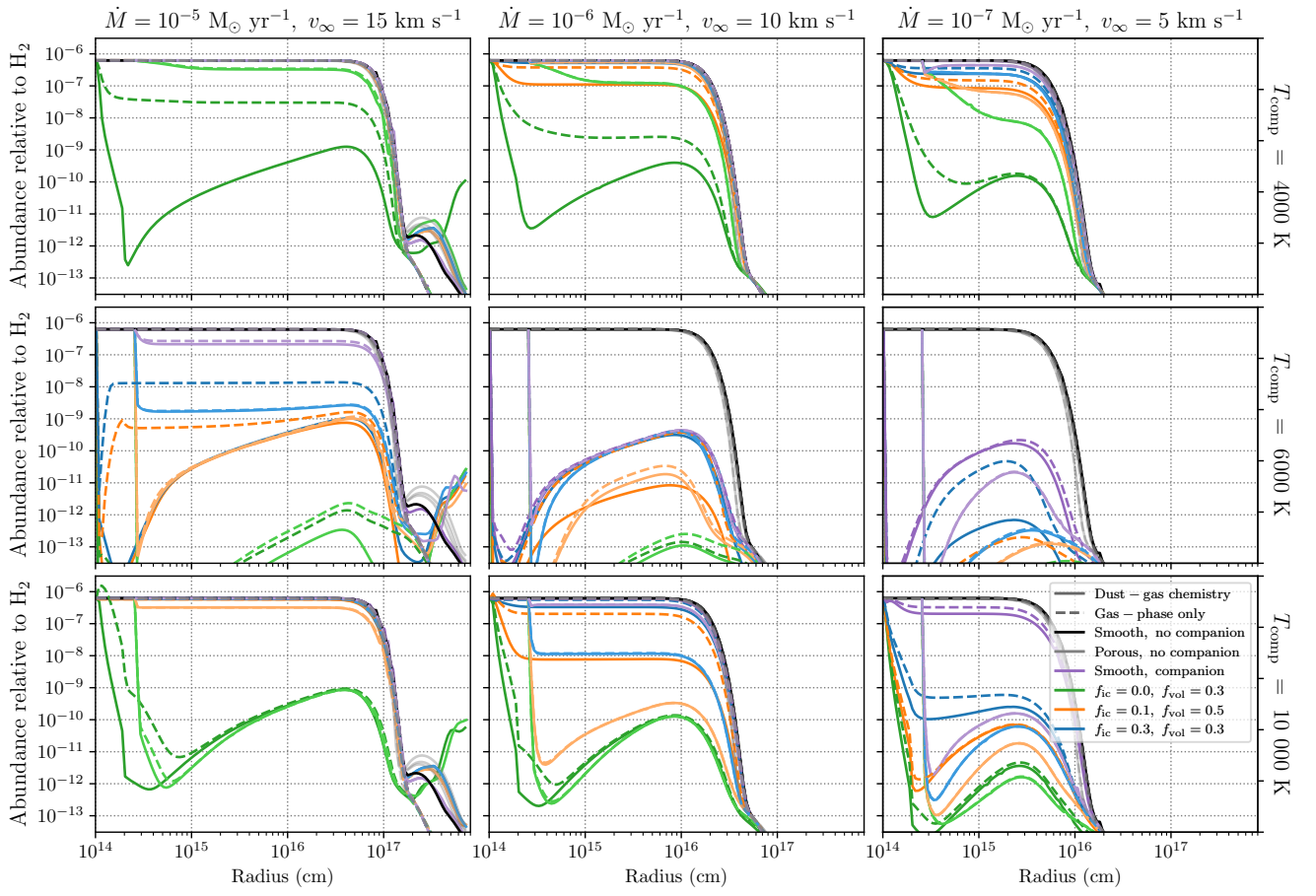


Figure 19: Fractional abundance of NH_3 relative to H_2 for a selection of O-rich outflows.

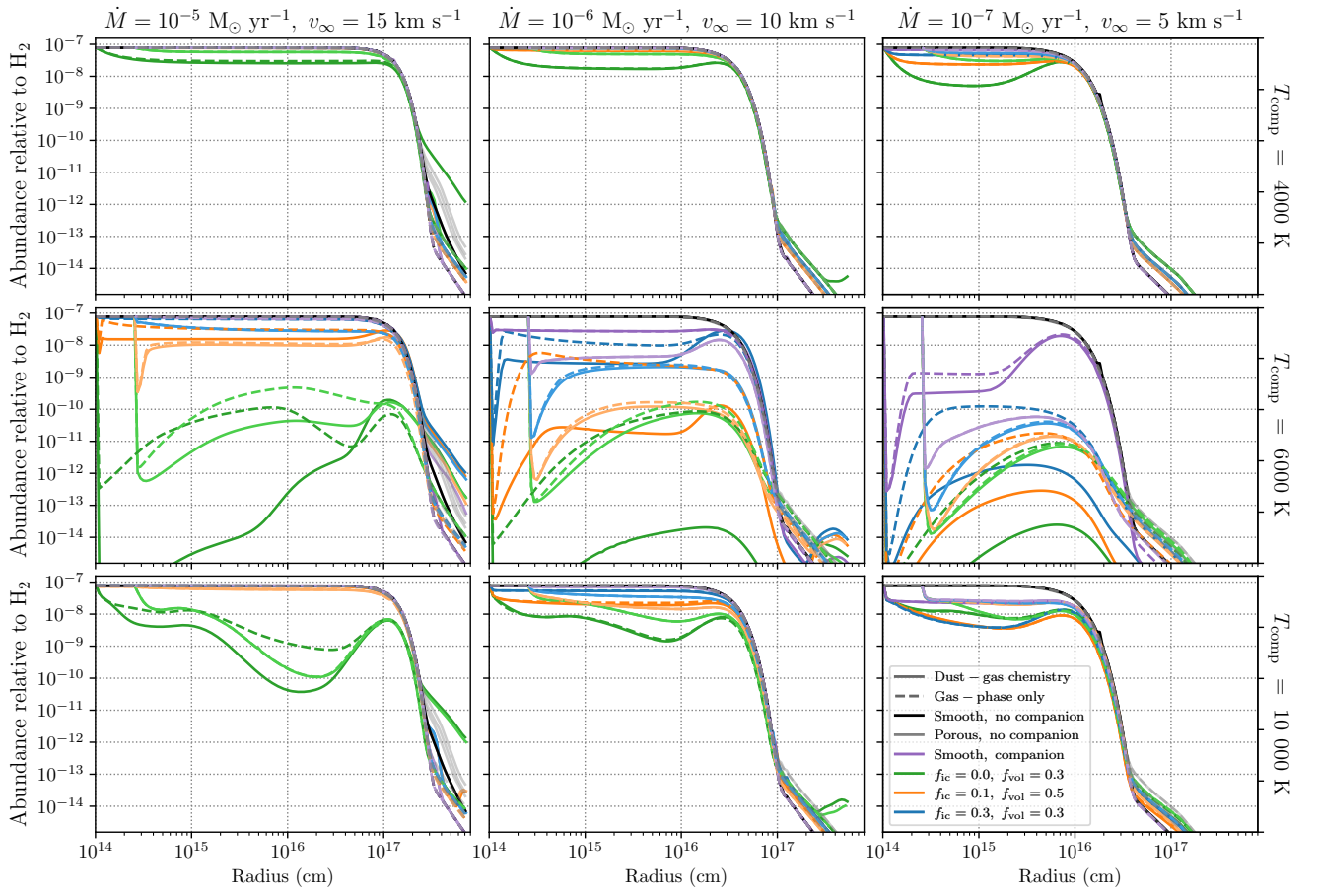


Figure 20: Fractional abundance of PO relative to H₂ for a selection of O-rich outflows.

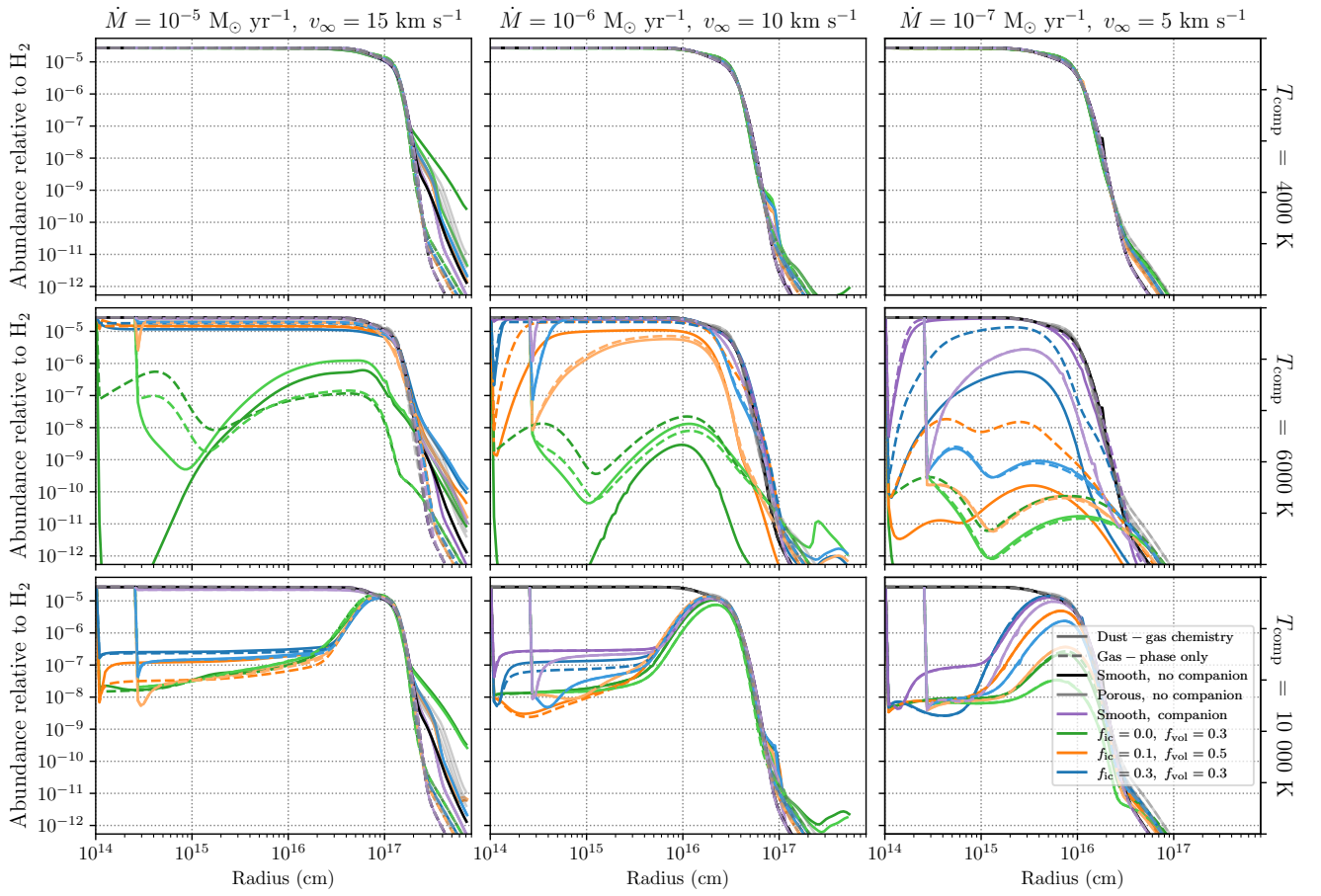


Figure 21: Fractional abundance of SiO relative to H_2 for a selection of O-rich outflows.

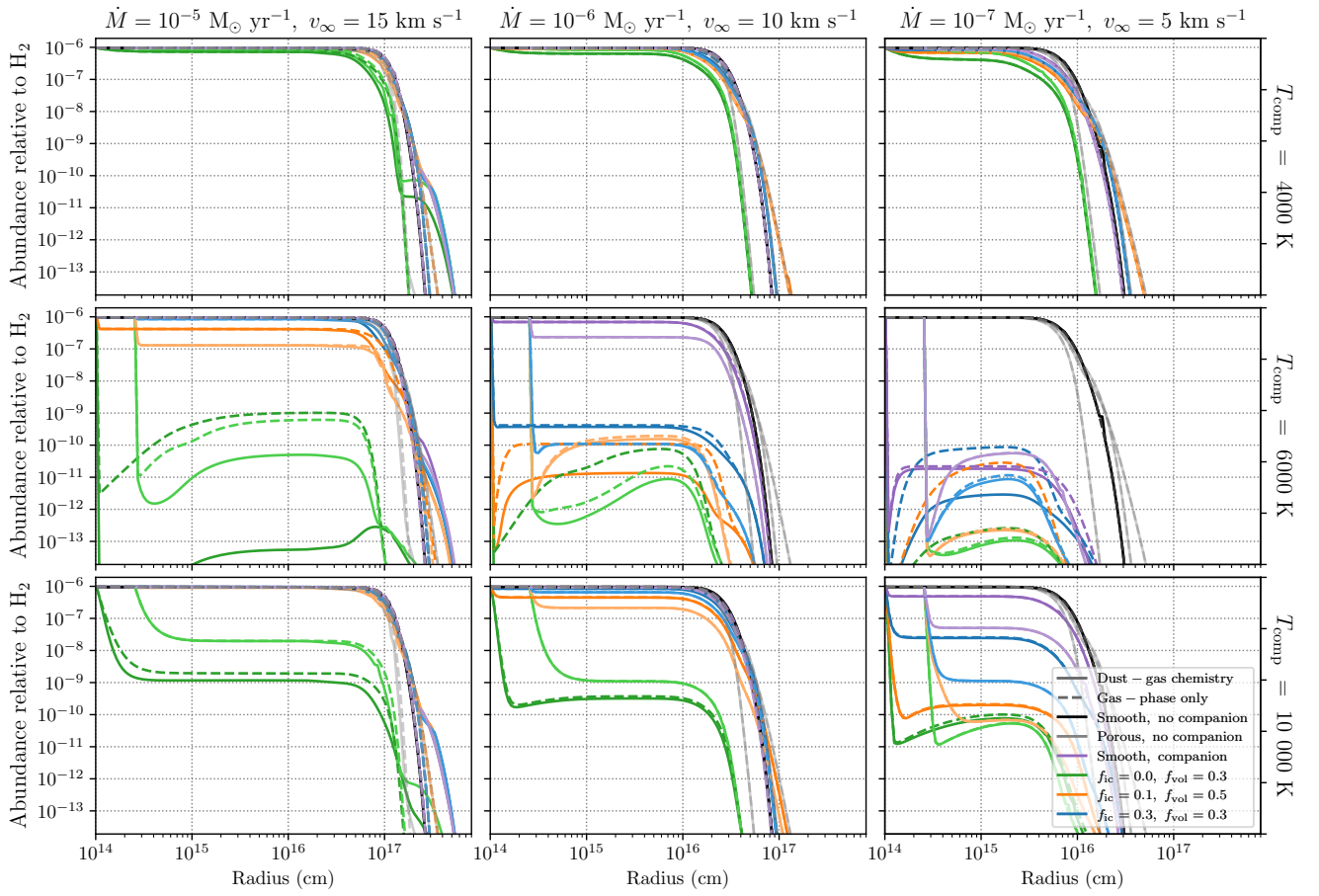


Figure 22: Fractional abundance of SiS relative to H₂ for a selection of O-rich outflows.

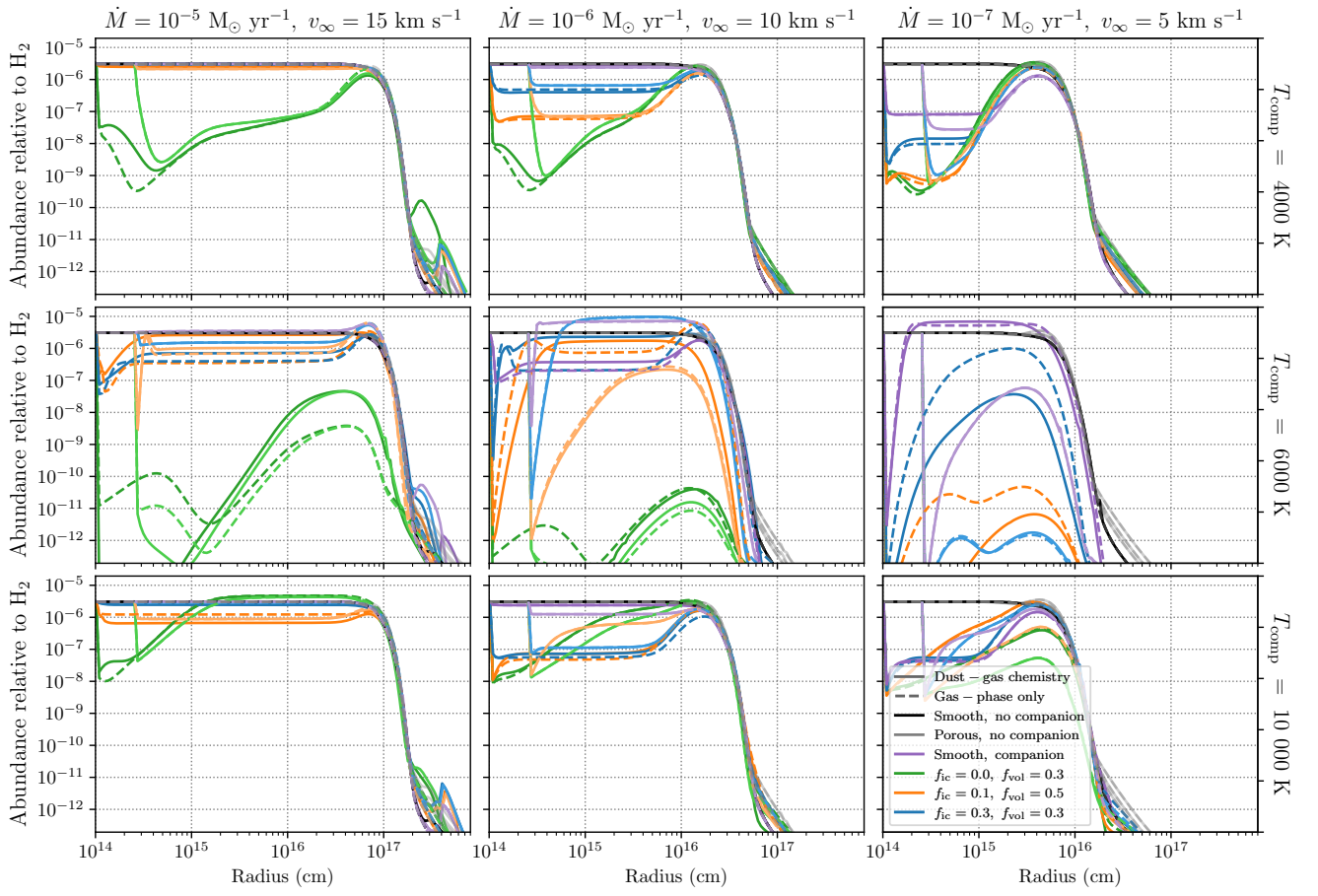


Figure 23: Fractional abundance of SO relative to H₂ for a selection of O-rich outflows.

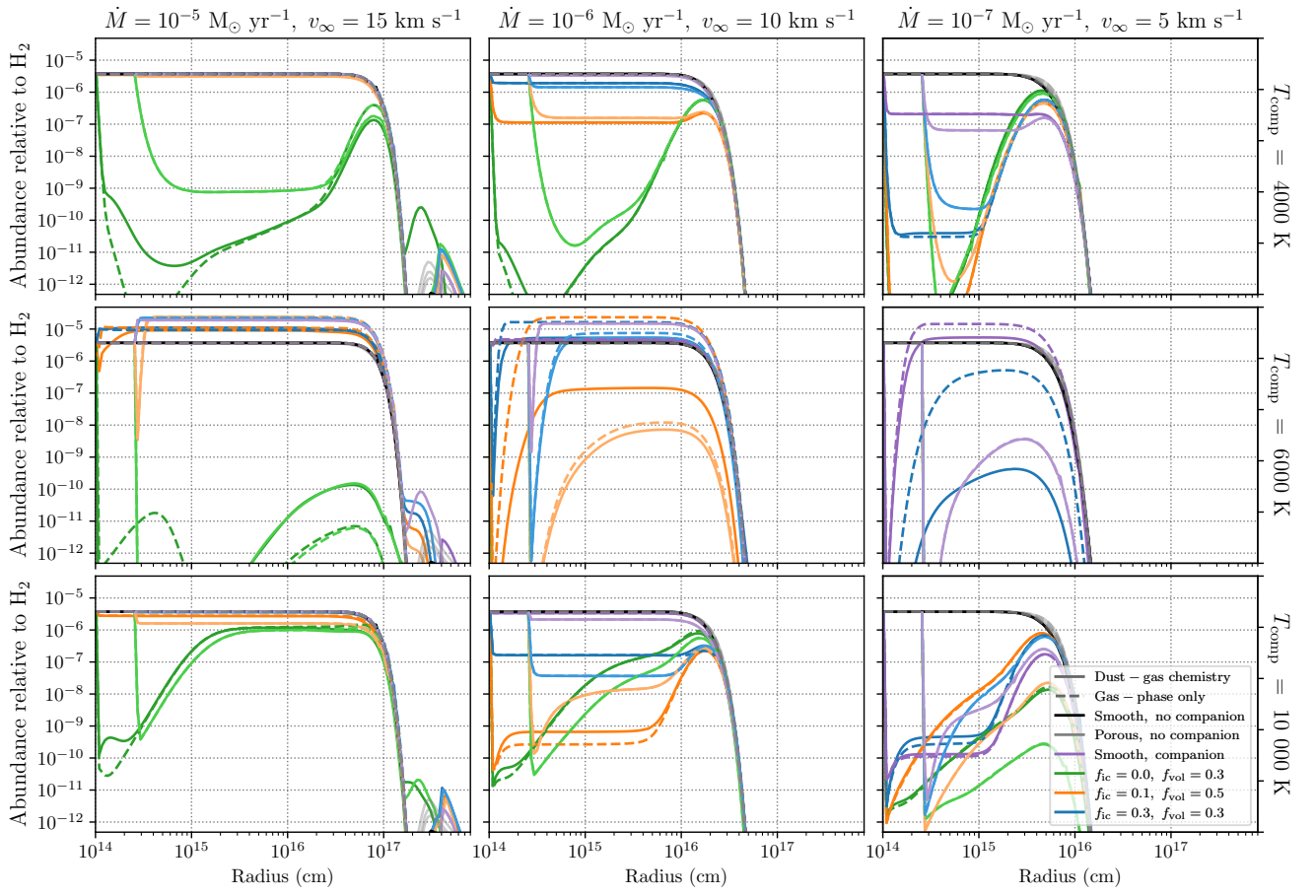


Figure 24: Fractional abundance of SO_2 relative to H_2 for a selection of O-rich outflows.

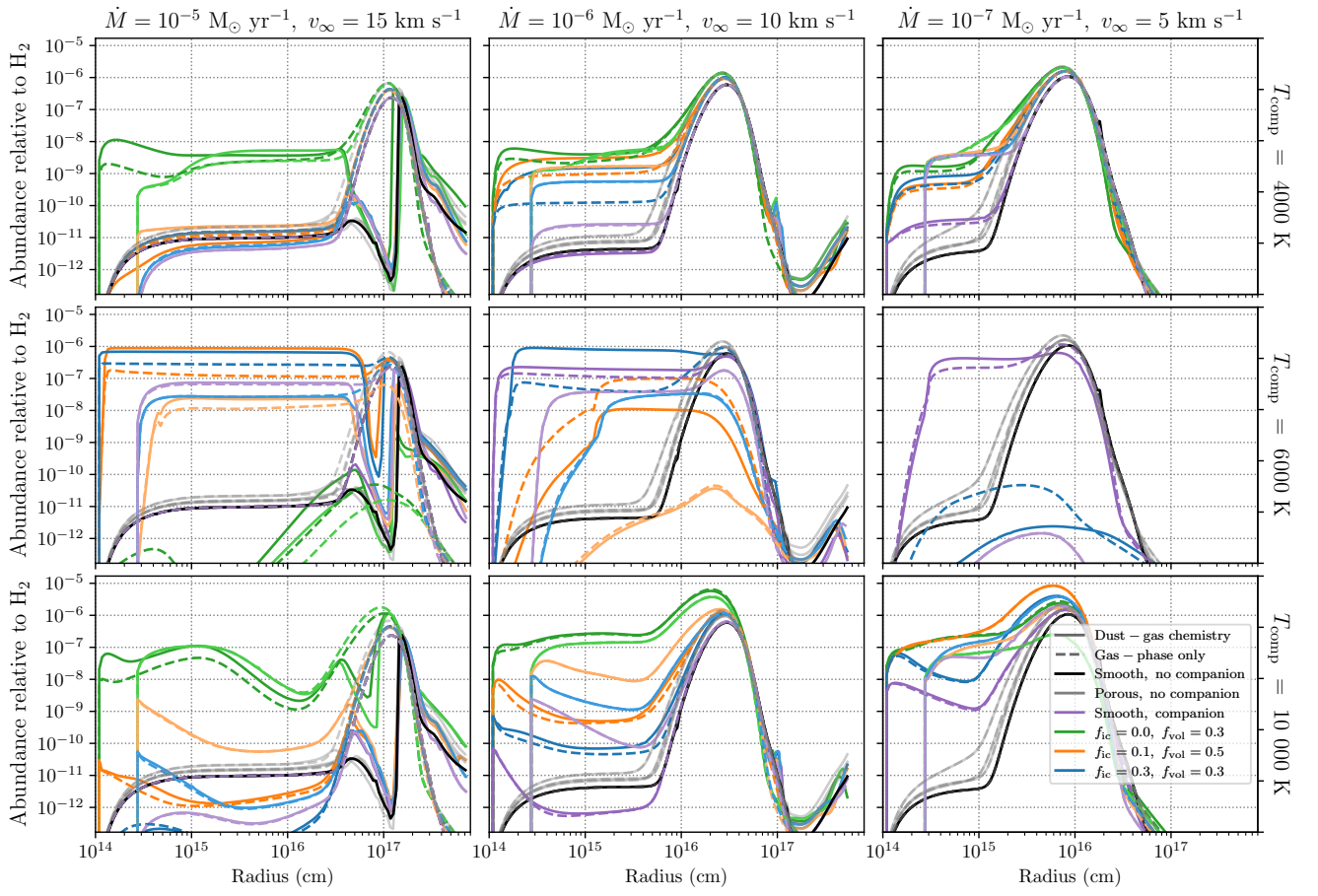


Figure 25: Fractional abundance of NO relative to H₂ for a selection of O-rich outflows.

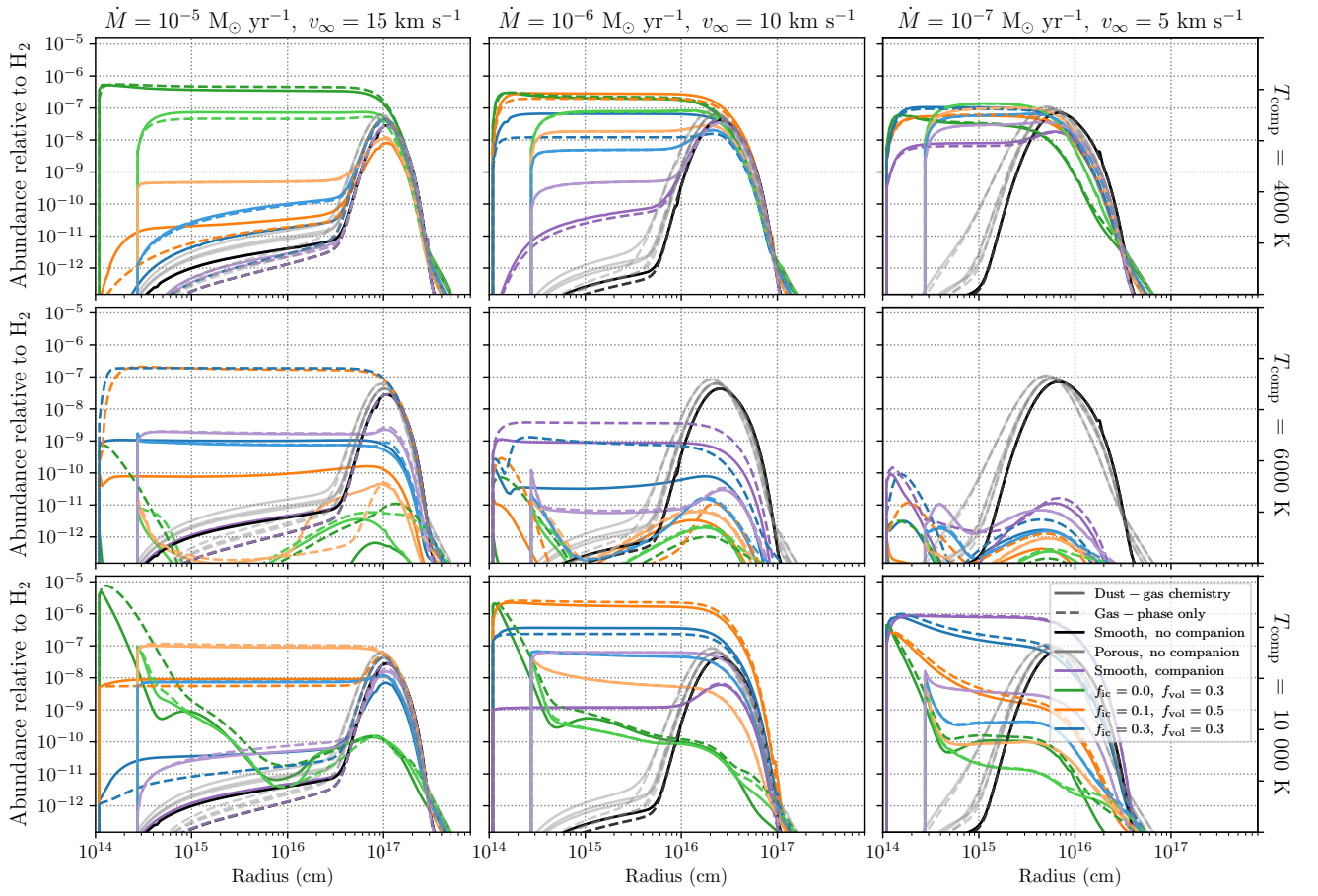


Figure 26: Fractional abundance of NS relative to H_2 for a selection of O-rich outflows.

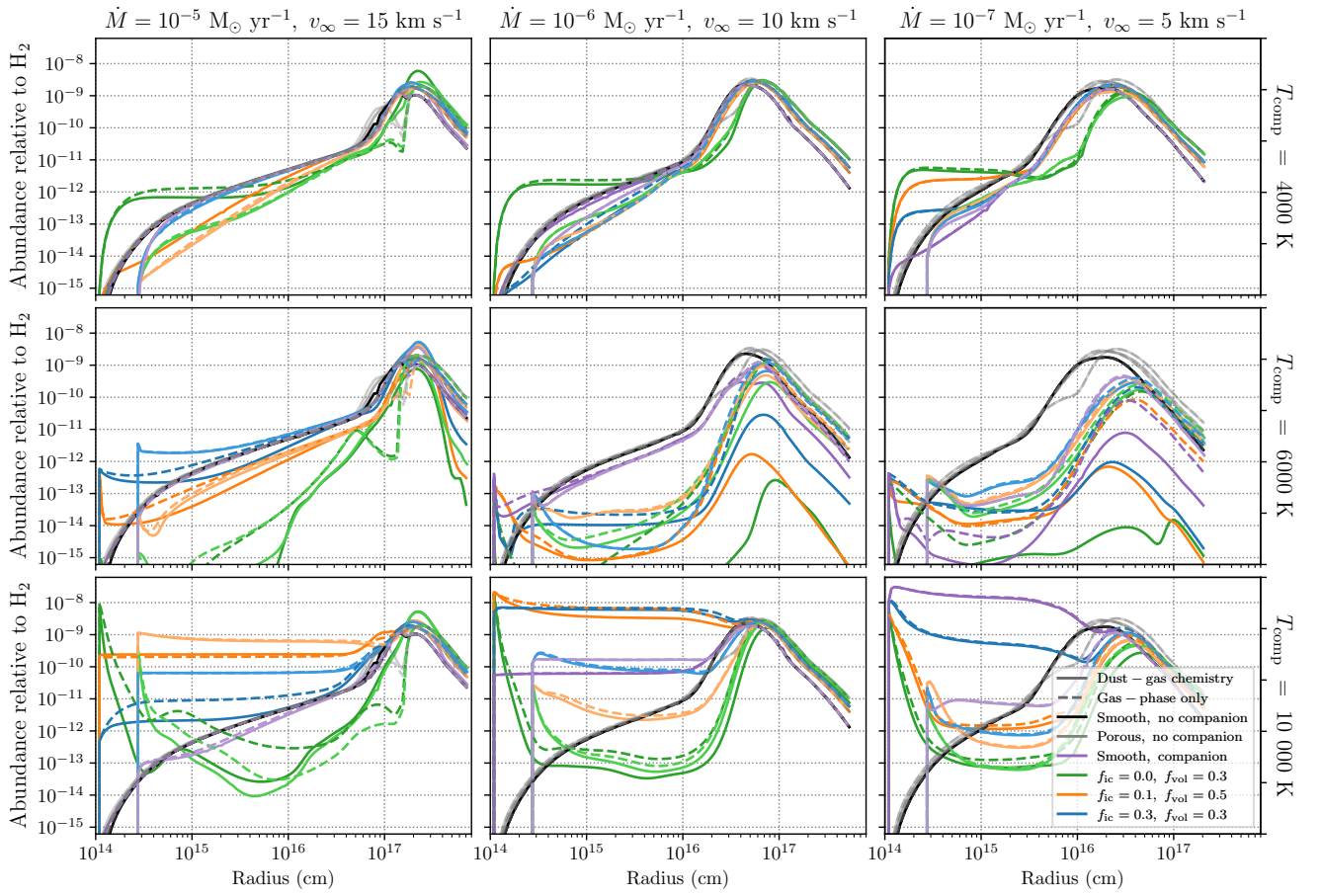


Figure 27: Fractional abundance of SiC relative to H_2 for a selection of O-rich outflows.

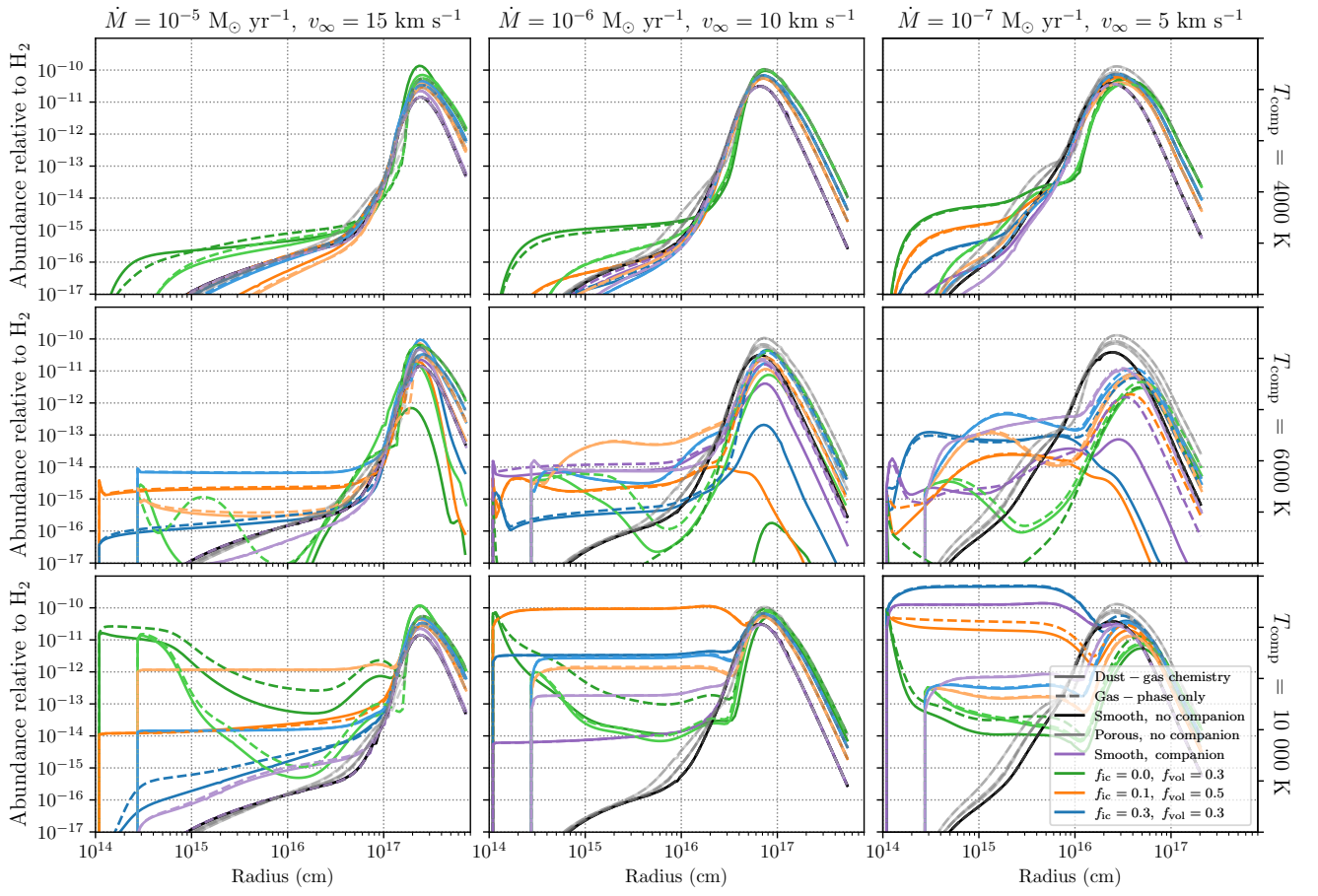


Figure 28: Fractional abundance of SiC_2 relative to H_2 for a selection of O-rich outflows.

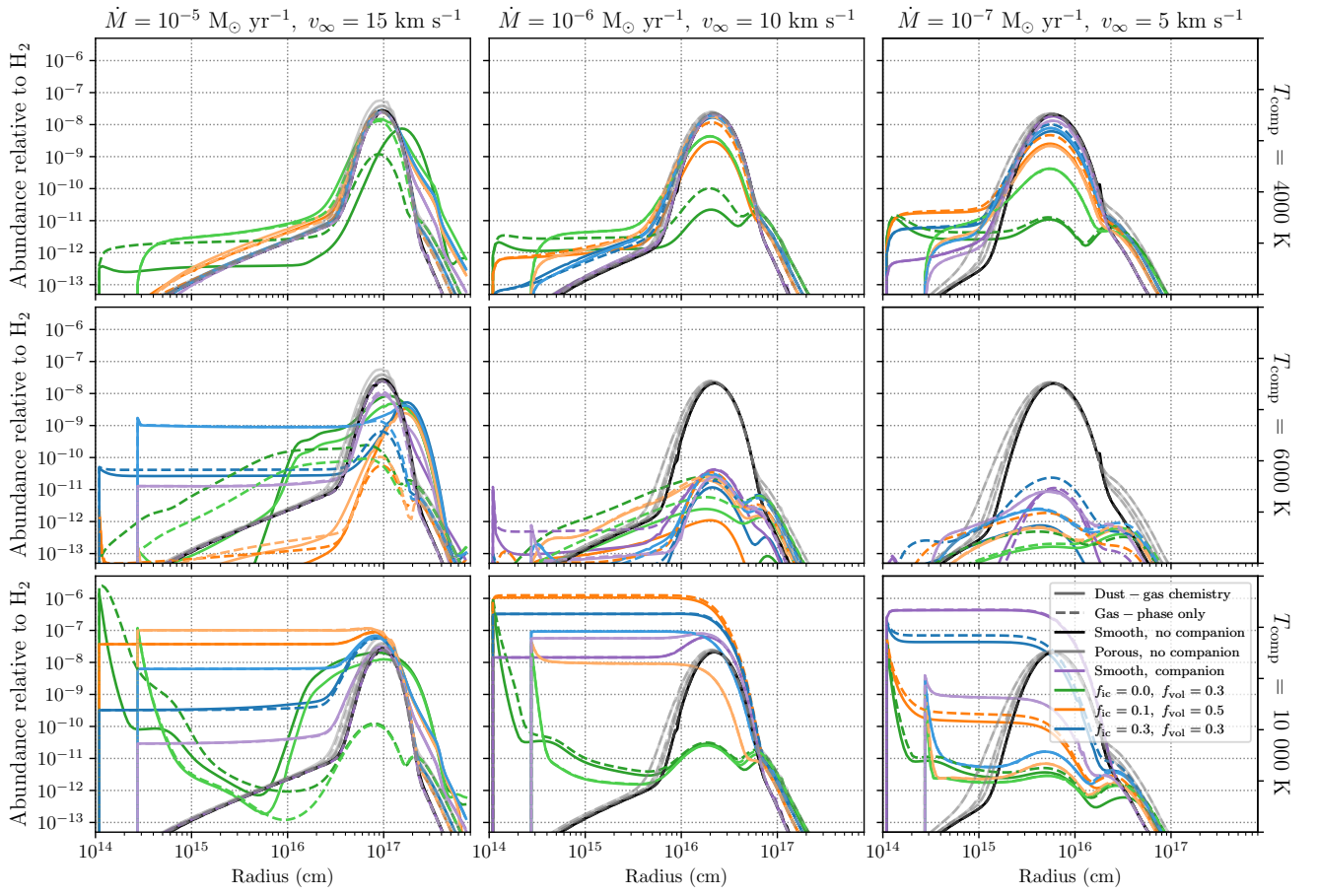


Figure 29: Fractional abundance of SiN relative to H_2 for a selection of O-rich outflows.

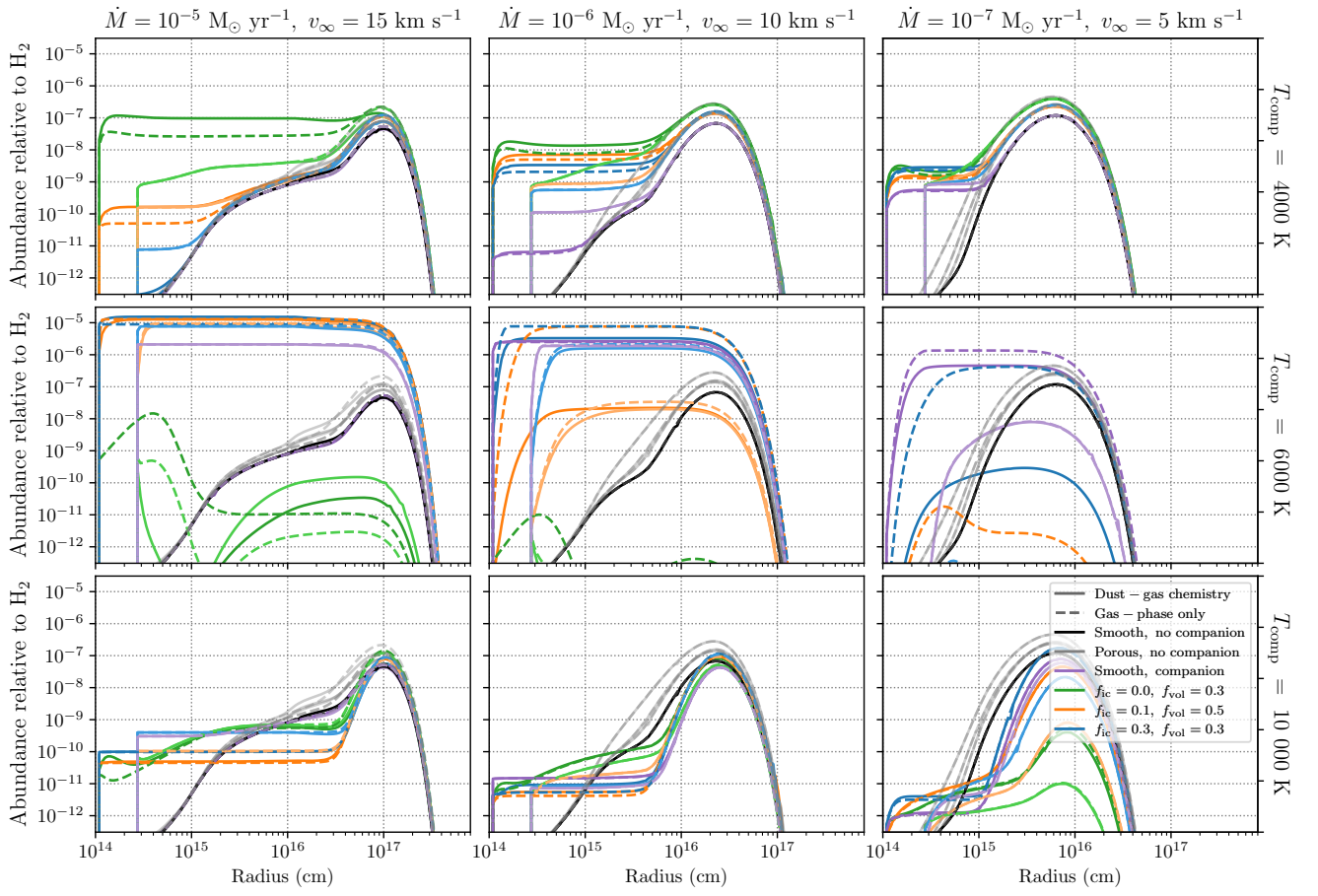


Figure 30: Fractional abundance of SiO_2 relative to H_2 for a selection of O-rich outflows.

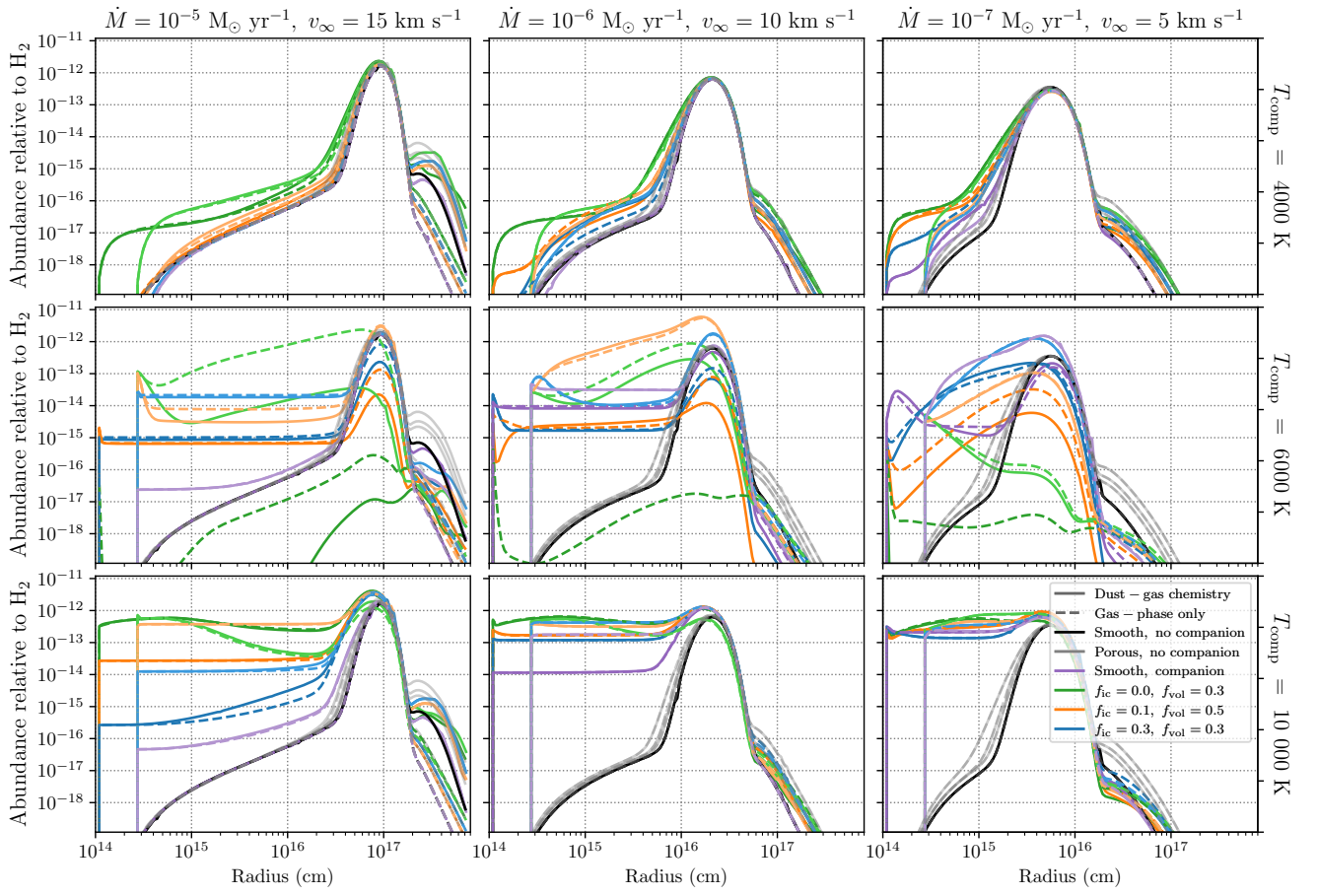


Figure 31: Fractional abundance of SiNC relative to H₂ for a selection of O-rich outflows.

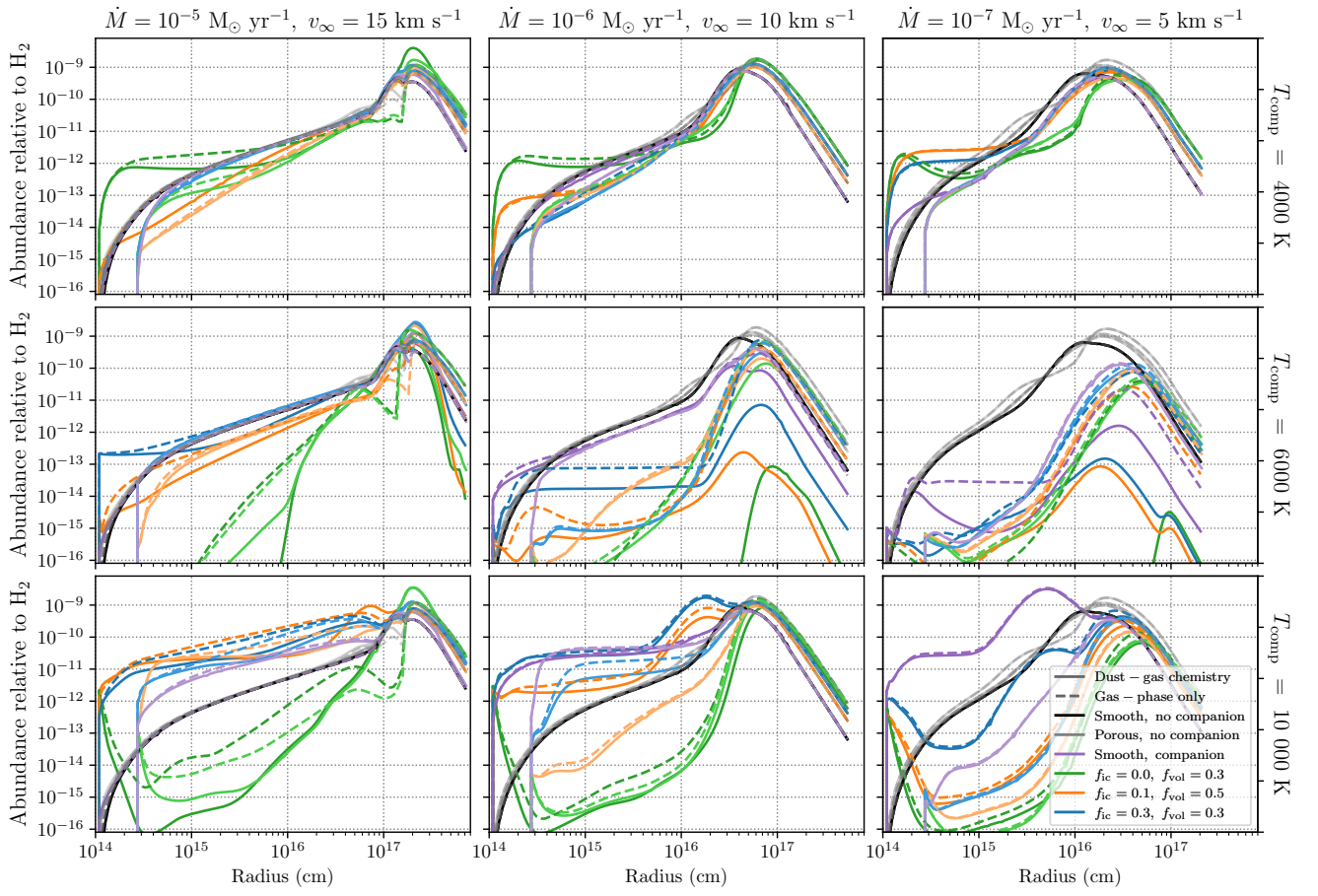


Figure 32: Fractional abundance of HCSi relative to H₂ for a selection of O-rich outflows.

2.2 C-rich outflows

Fractional abundance profiles relative to H_2 for a selection of outflows with different outflow densities (columns) and companions (rows). Different line styles show different chemistries included. Dashed lines: gas-phase chemistry only, solid lines: including dust-gas chemistry. Different colours show different density structures and the inclusion of a companion. Black: smooth outflow without a companion, gray: porous outflow without a companion. When including a companion, different shades correspond to the value of R_{dust} . Darker shade: $R_{\text{dust}} = 2 R_*$, lighter shade: $R_{\text{dust}} = 5 R_*$. Purple: smooth outflow with a companion. Green: porous outflow with a companion, $f_{\text{ic}} = 0.0$, $f_{\text{vol}} = 0.3$, $l_* = 10^{13}$ cm. Orange: porous outflow with a companion, $f_{\text{ic}} = 0.1$, $f_{\text{vol}} = 0.5$, $l_* = 10^{13}$ cm. Blue: porous outflow with a companion, $f_{\text{ic}} = 0.3$, $f_{\text{vol}} = 0.3$, $l_* = 5 \times 10^{12}$ cm.

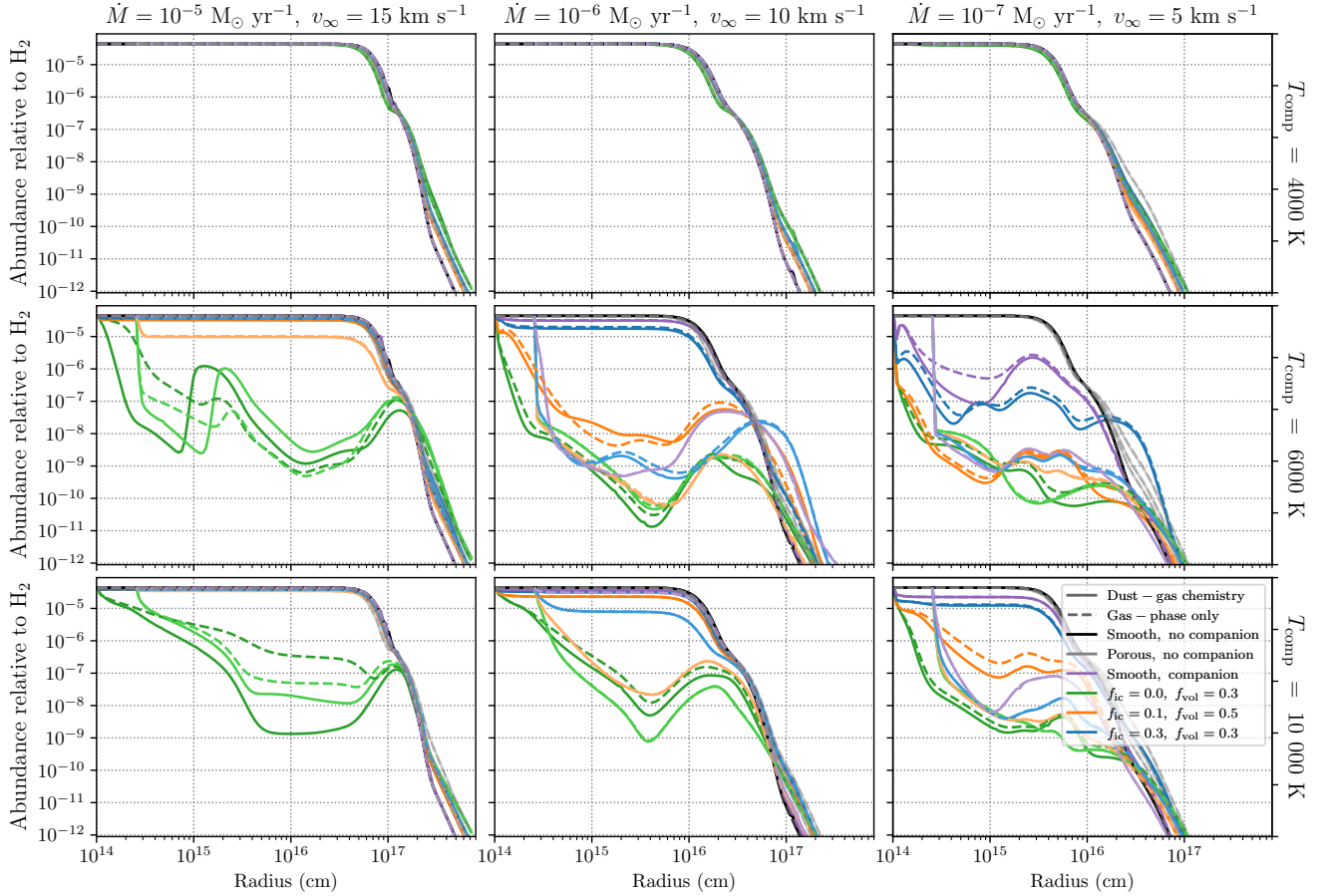


Figure 33: Fractional abundance of C_2H_2 relative to H_2 for a selection of C-rich outflows.

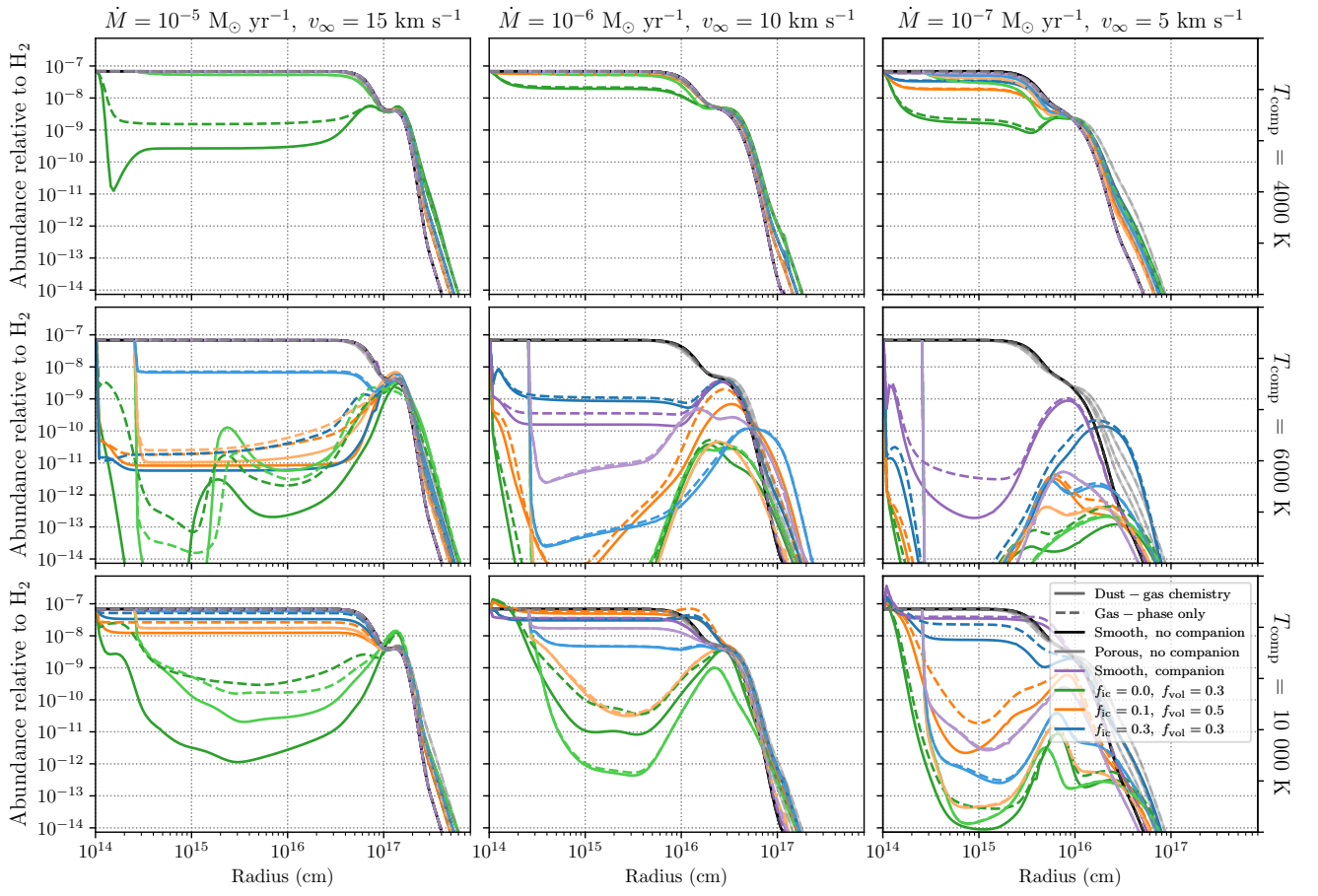


Figure 34: Fractional abundance of C_2H_4 relative to H_2 for a selection of C-rich outflows.

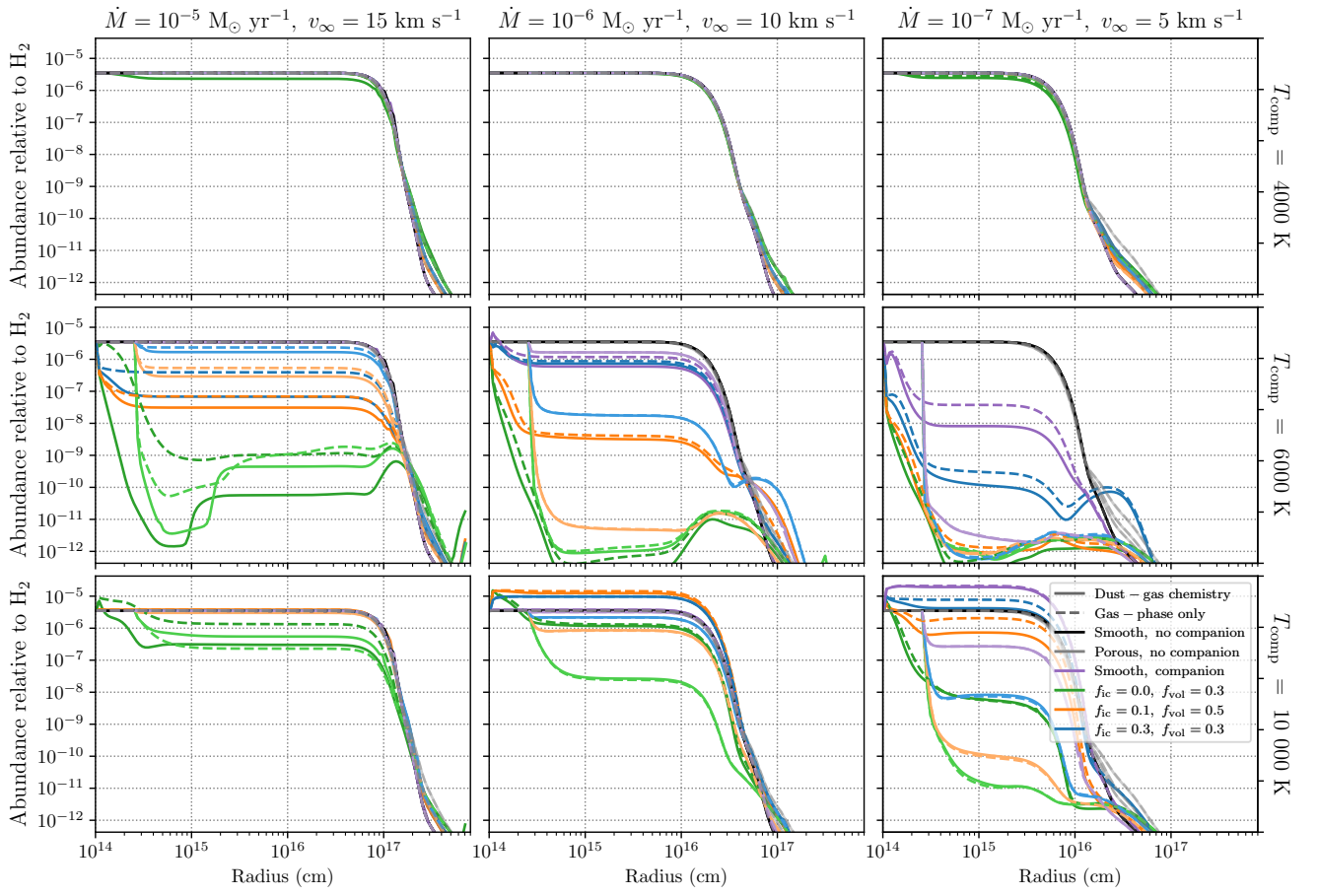


Figure 35: Fractional abundance of CH₄ relative to H₂ for a selection of C-rich outflows.

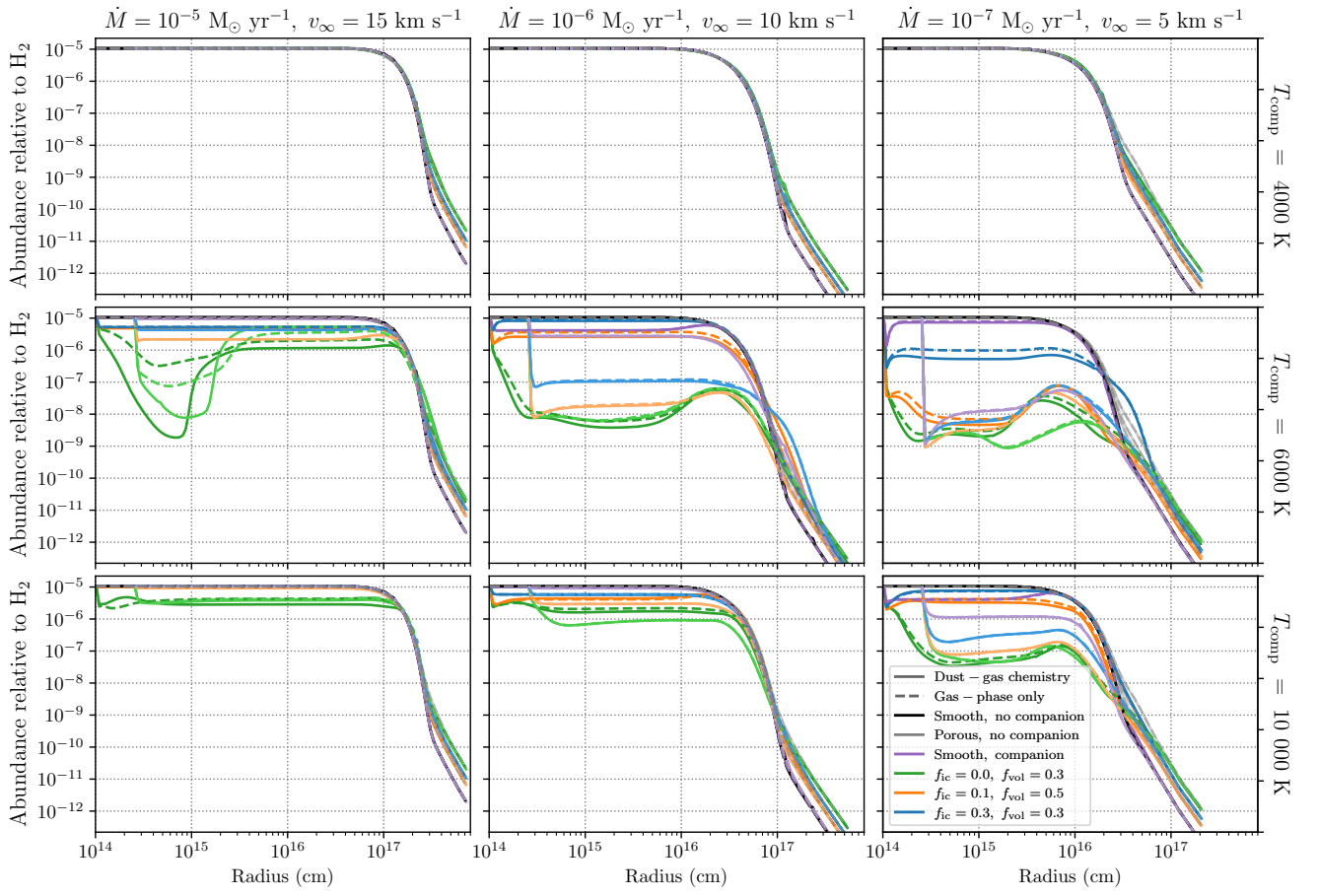


Figure 36: Fractional abundance of CS relative to H₂ for a selection of C-rich outflows.

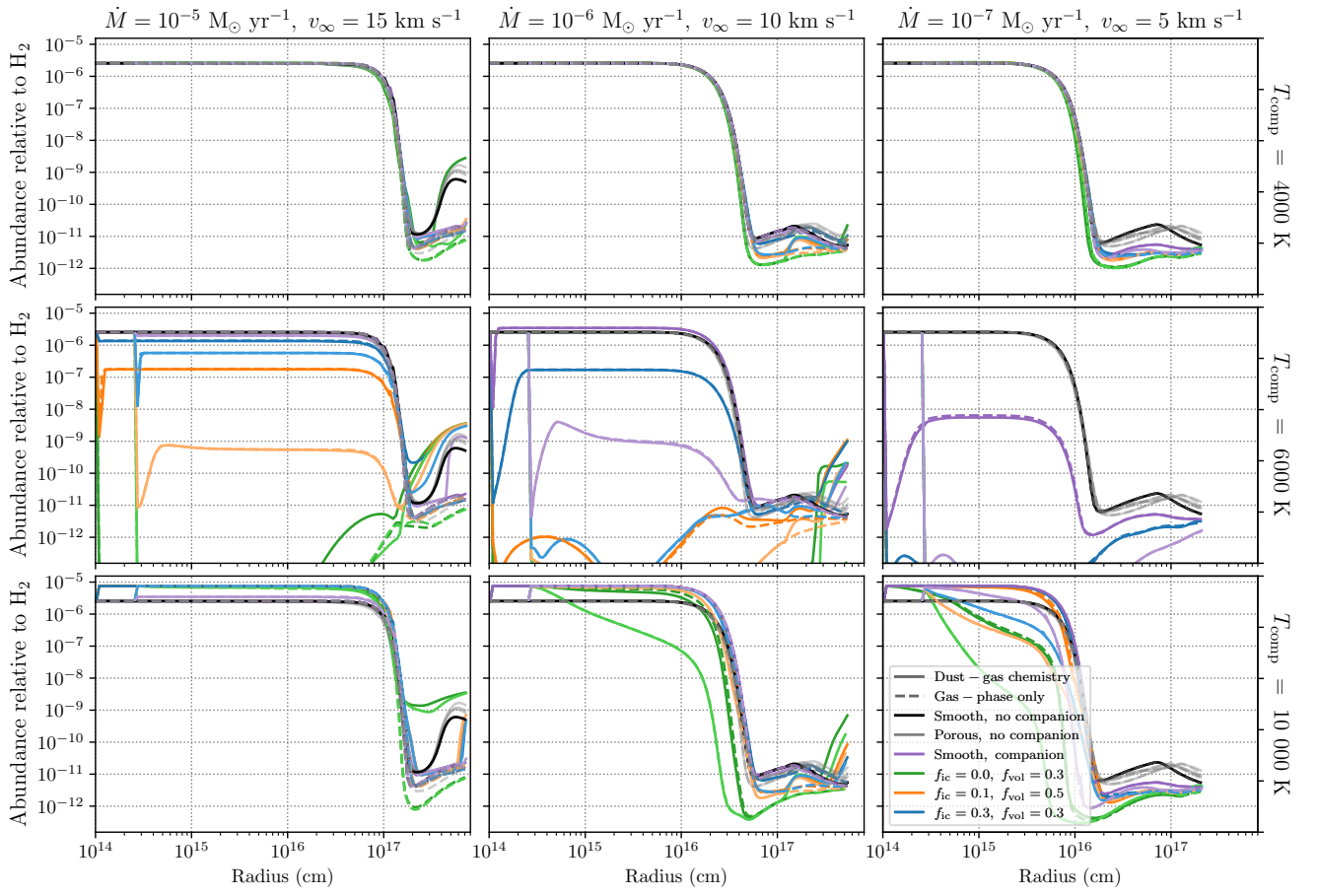


Figure 37: Fractional abundance of H_2O relative to H_2 for a selection of C-rich outflows.

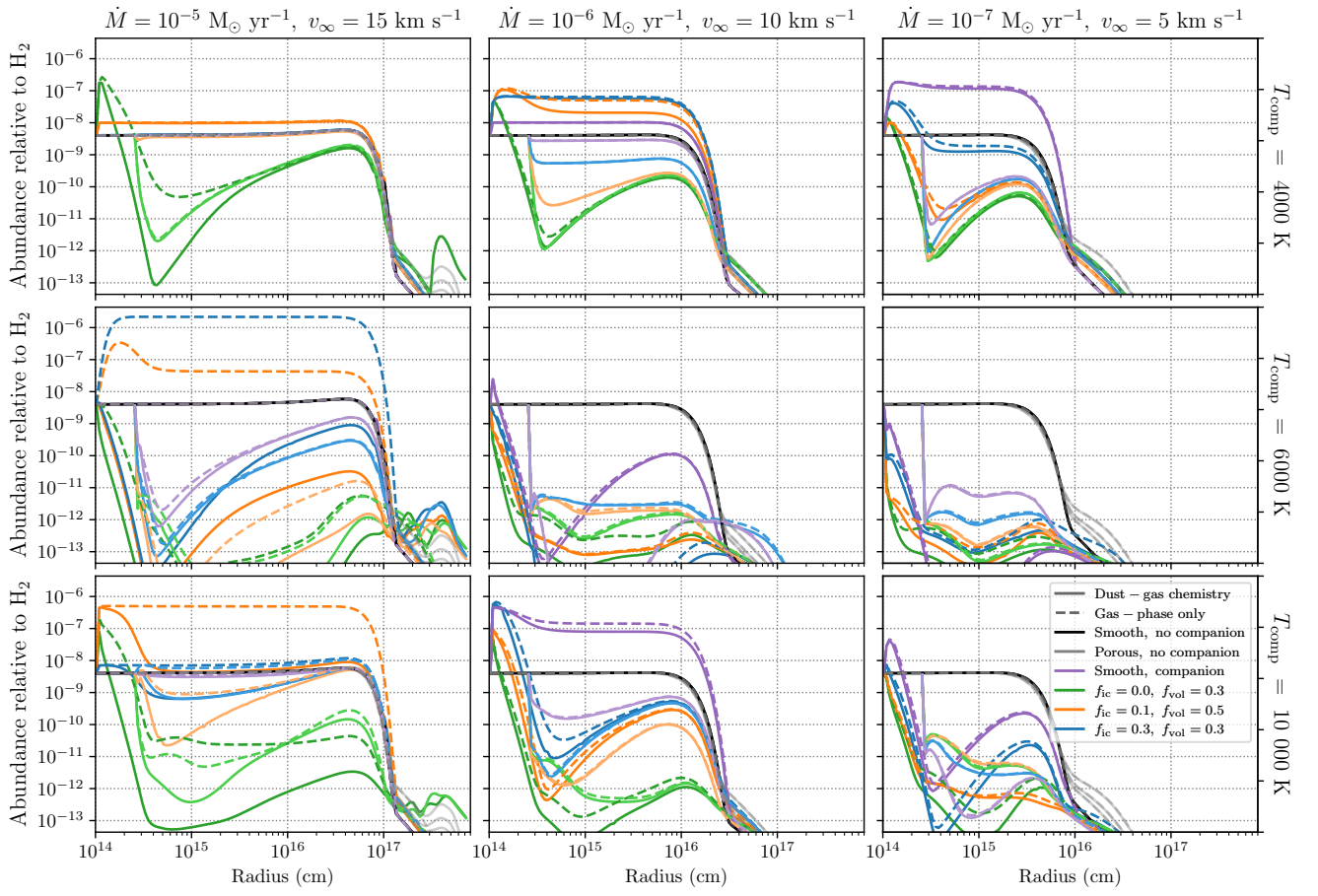


Figure 38: Fractional abundance of H_2S relative to H_2 for a selection of C-rich outflows.

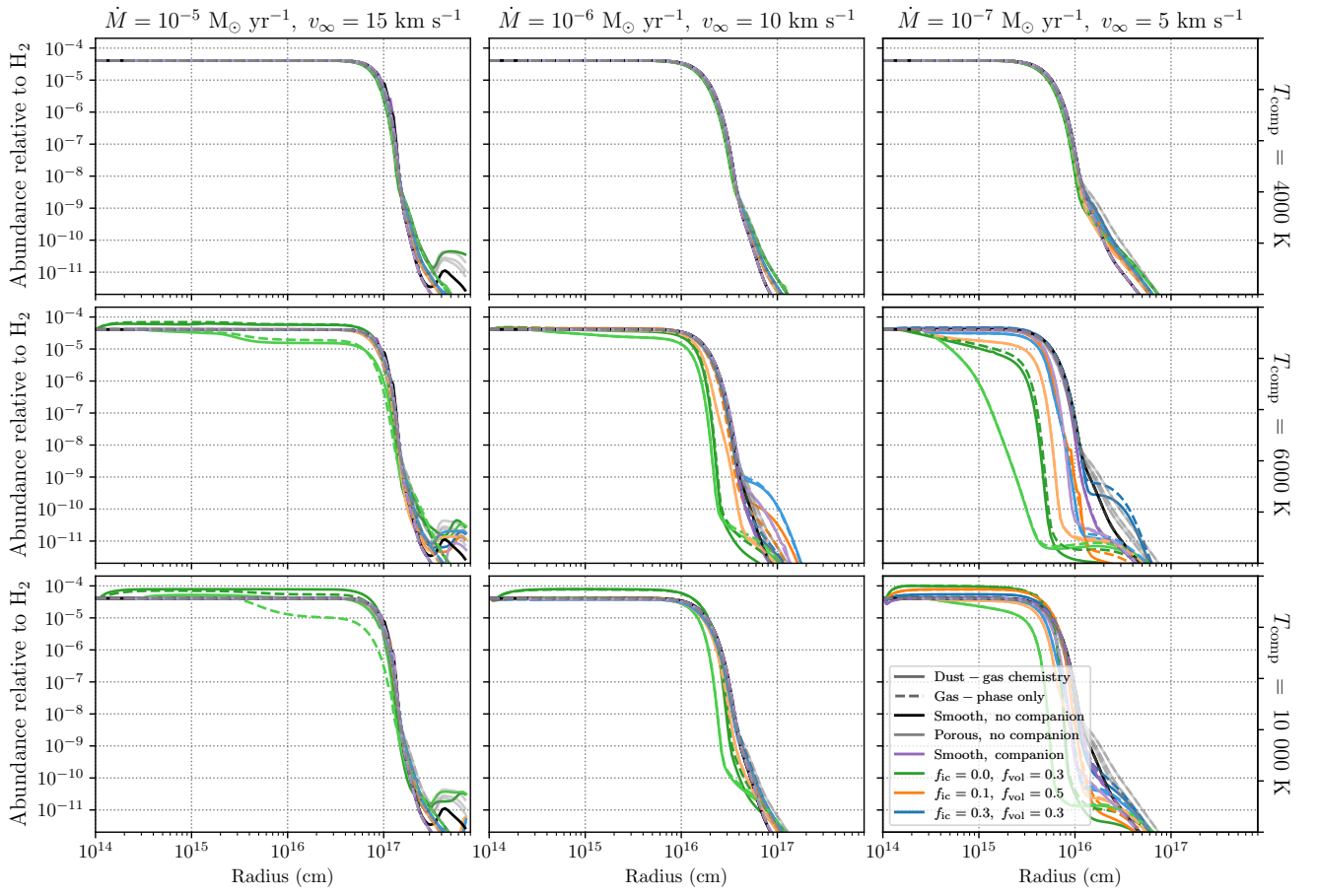


Figure 39: Fractional abundance of HCN relative to H₂ for a selection of C-rich outflows.

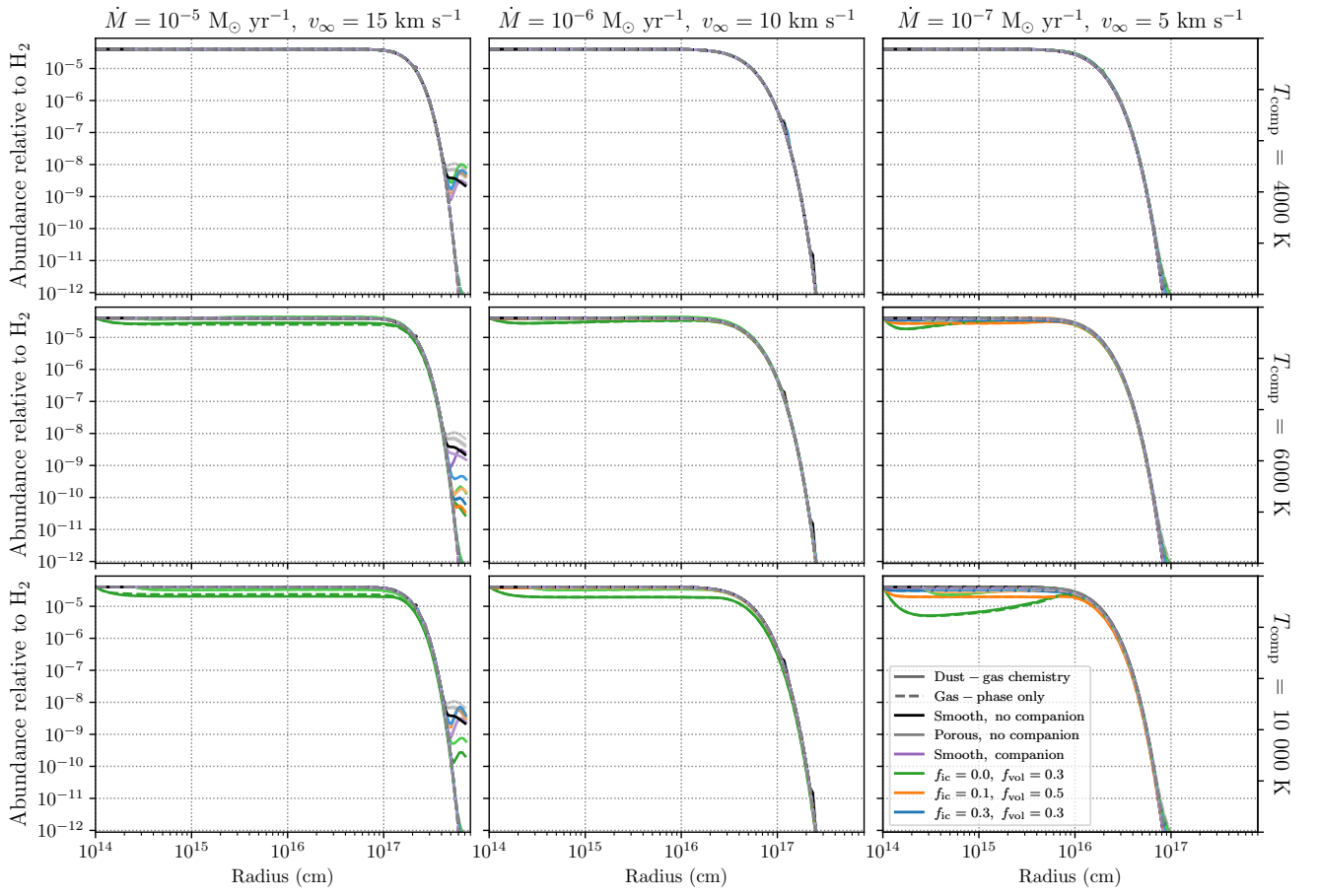


Figure 40: Fractional abundance of N_2 relative to H_2 for a selection of C-rich outflows.

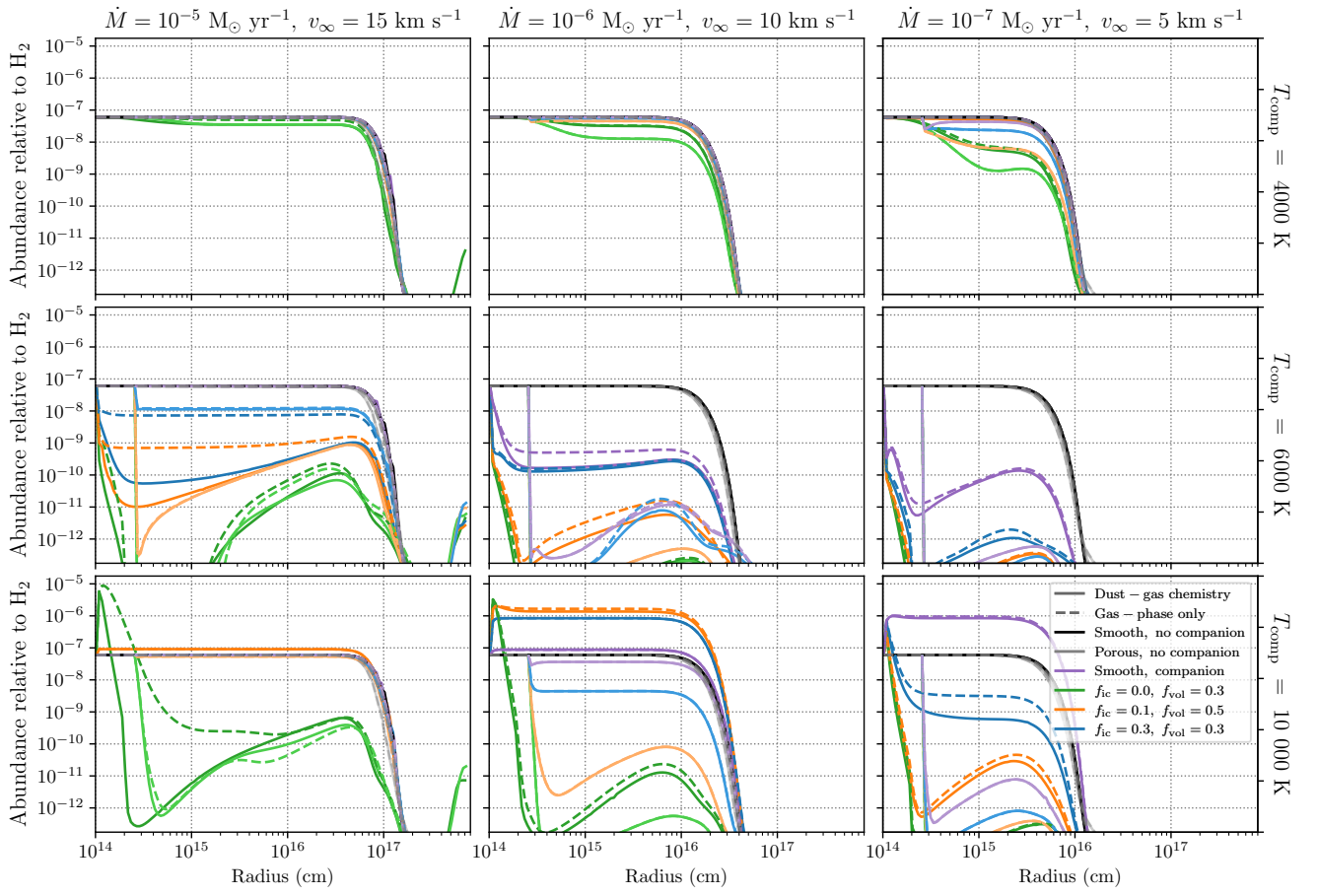


Figure 41: Fractional abundance of NH_3 relative to H_2 for a selection of C-rich outflows.

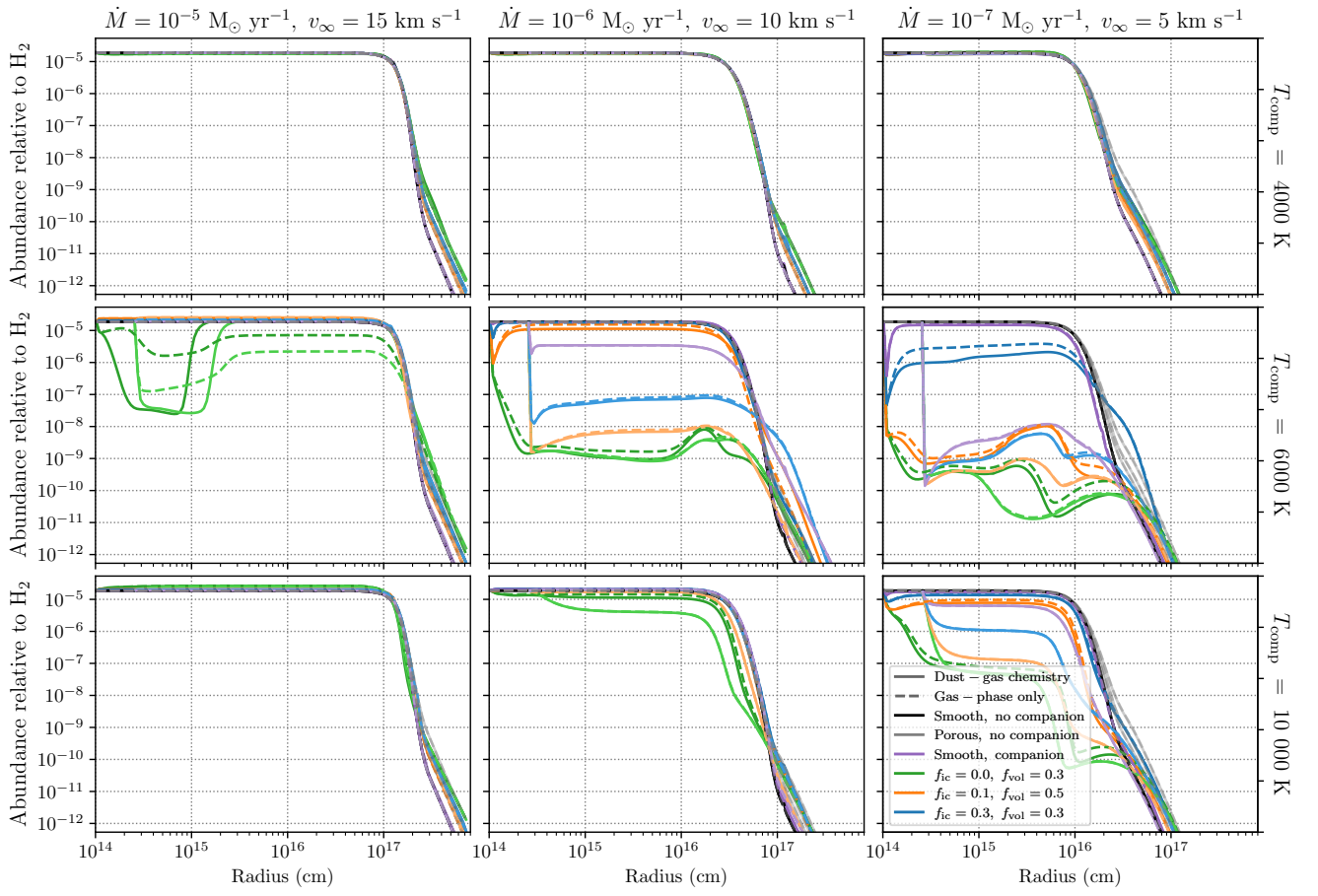


Figure 42: Fractional abundance of SiC₂ relative to H₂ for a selection of C-rich outflows.

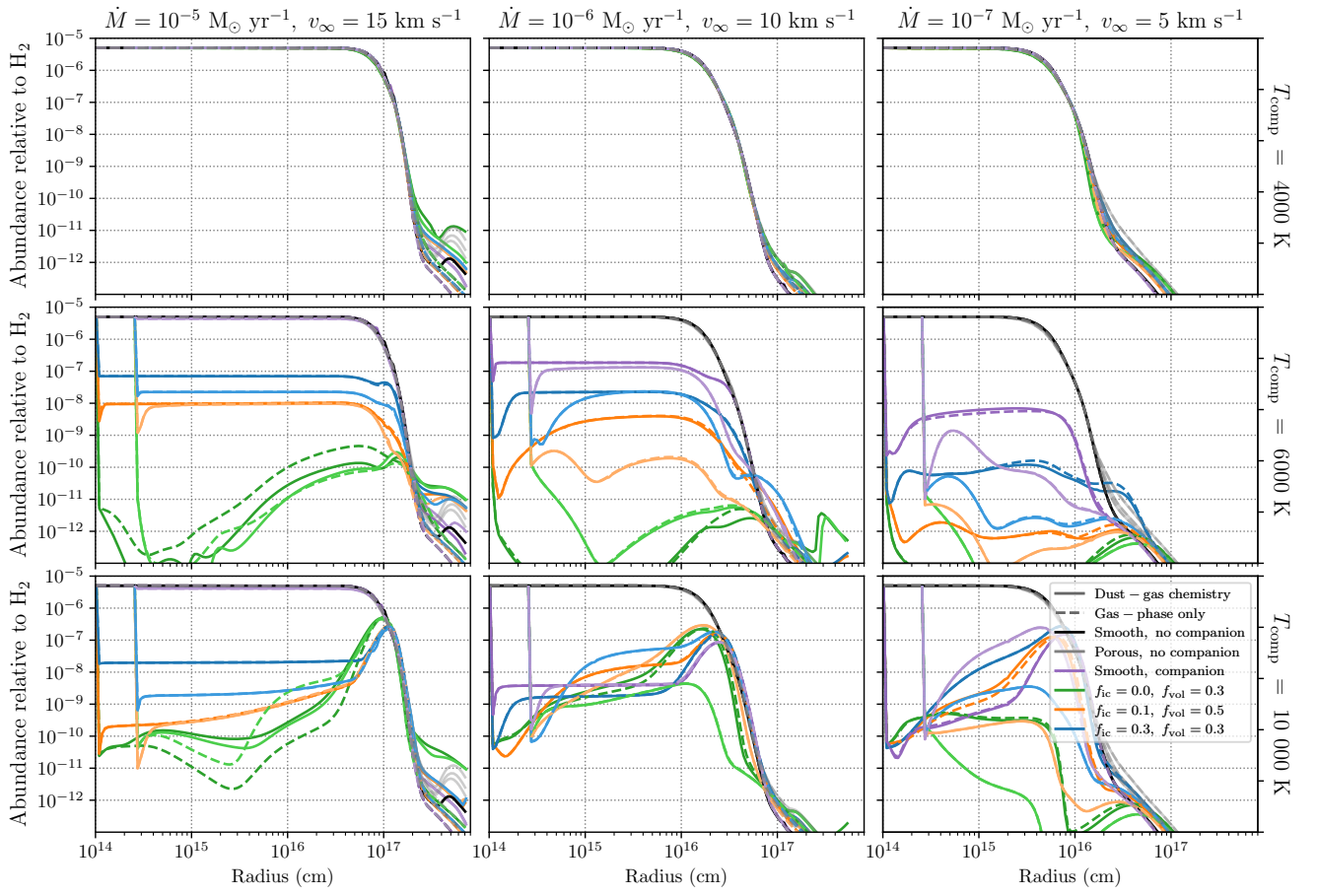


Figure 43: Fractional abundance of SiO relative to H₂ for a selection of C-rich outflows.

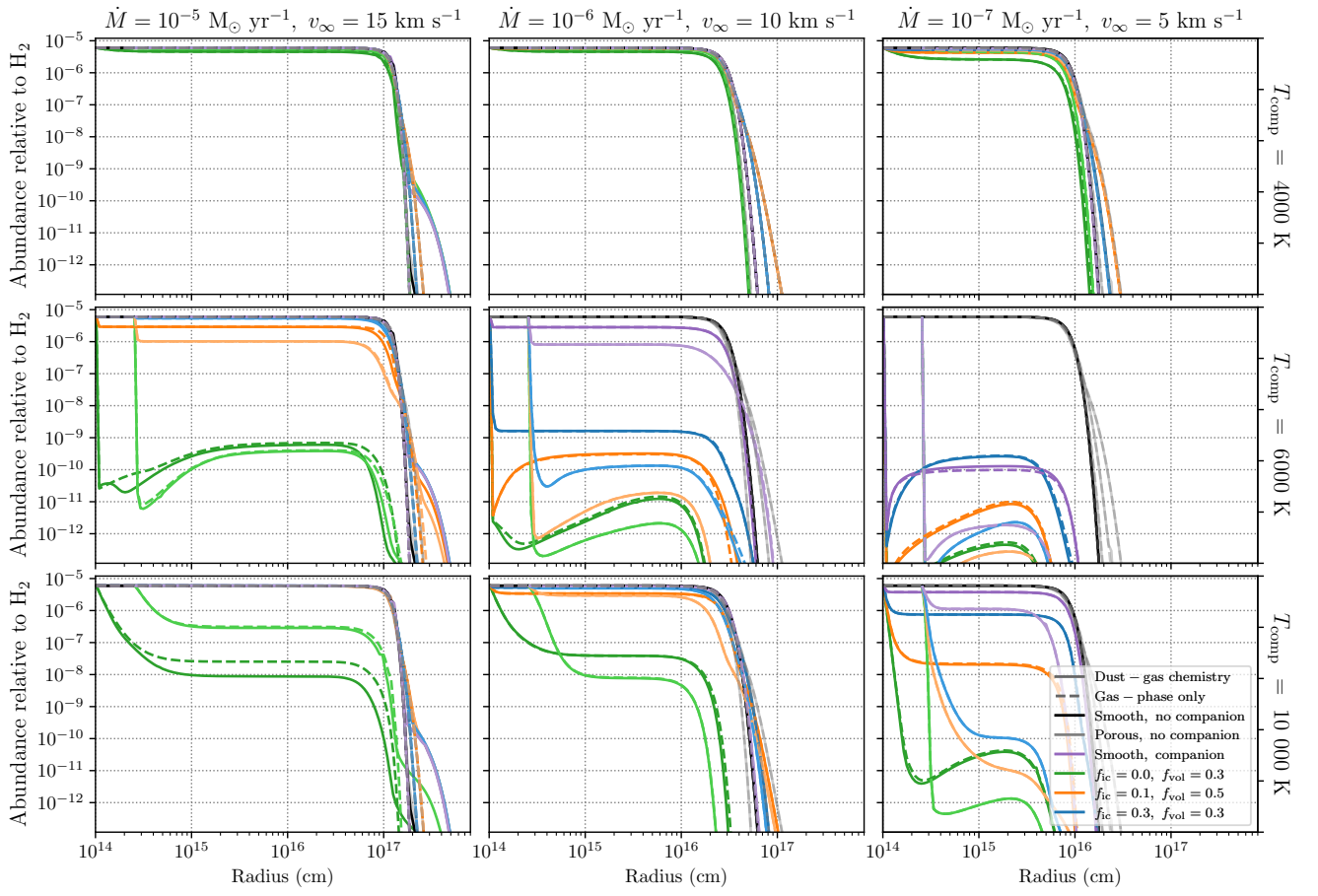


Figure 44: Fractional abundance of SiS relative to H₂ for a selection of C-rich outflows.

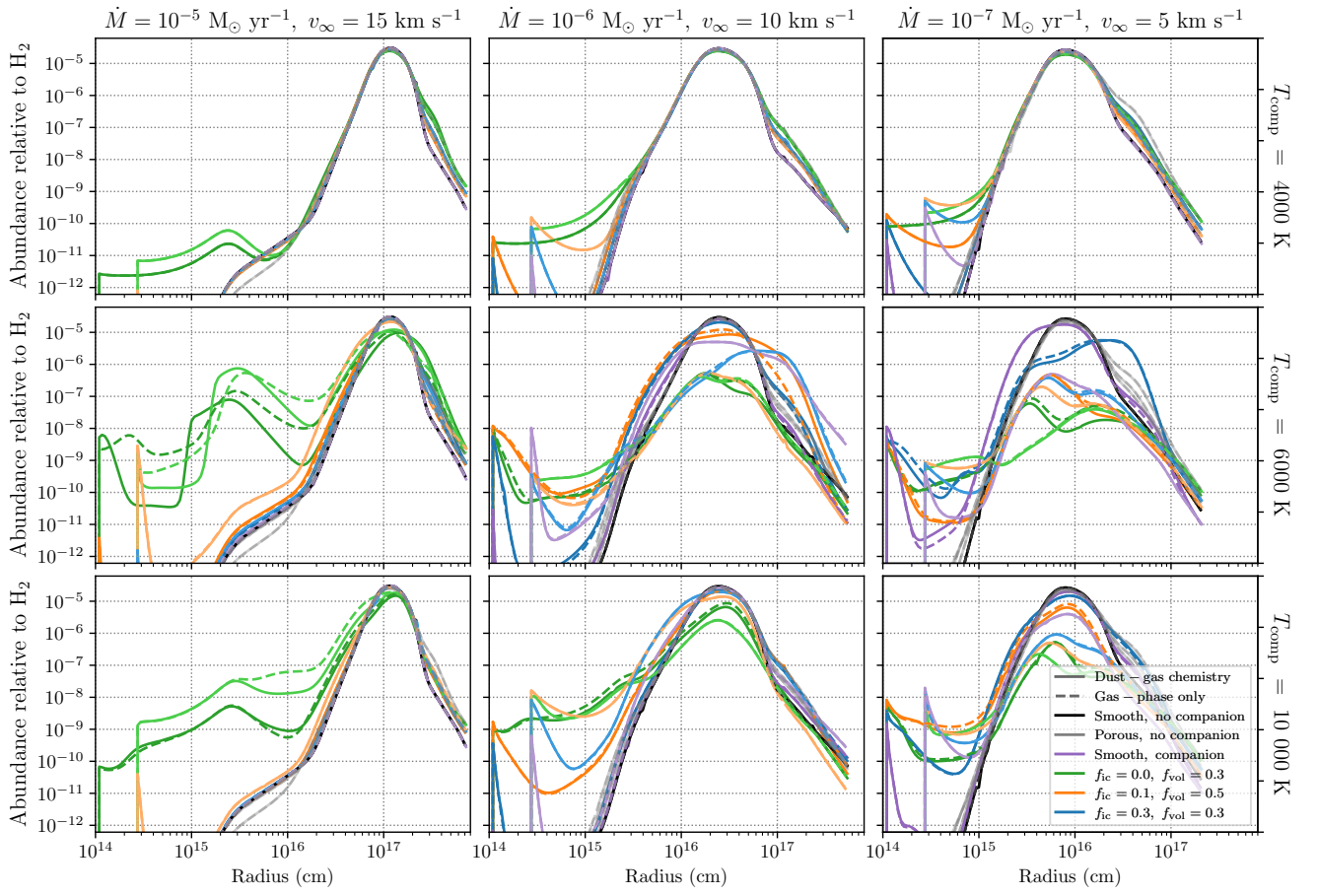


Figure 45: Fractional abundance of C_2 relative to H_2 for a selection of C-rich outflows.

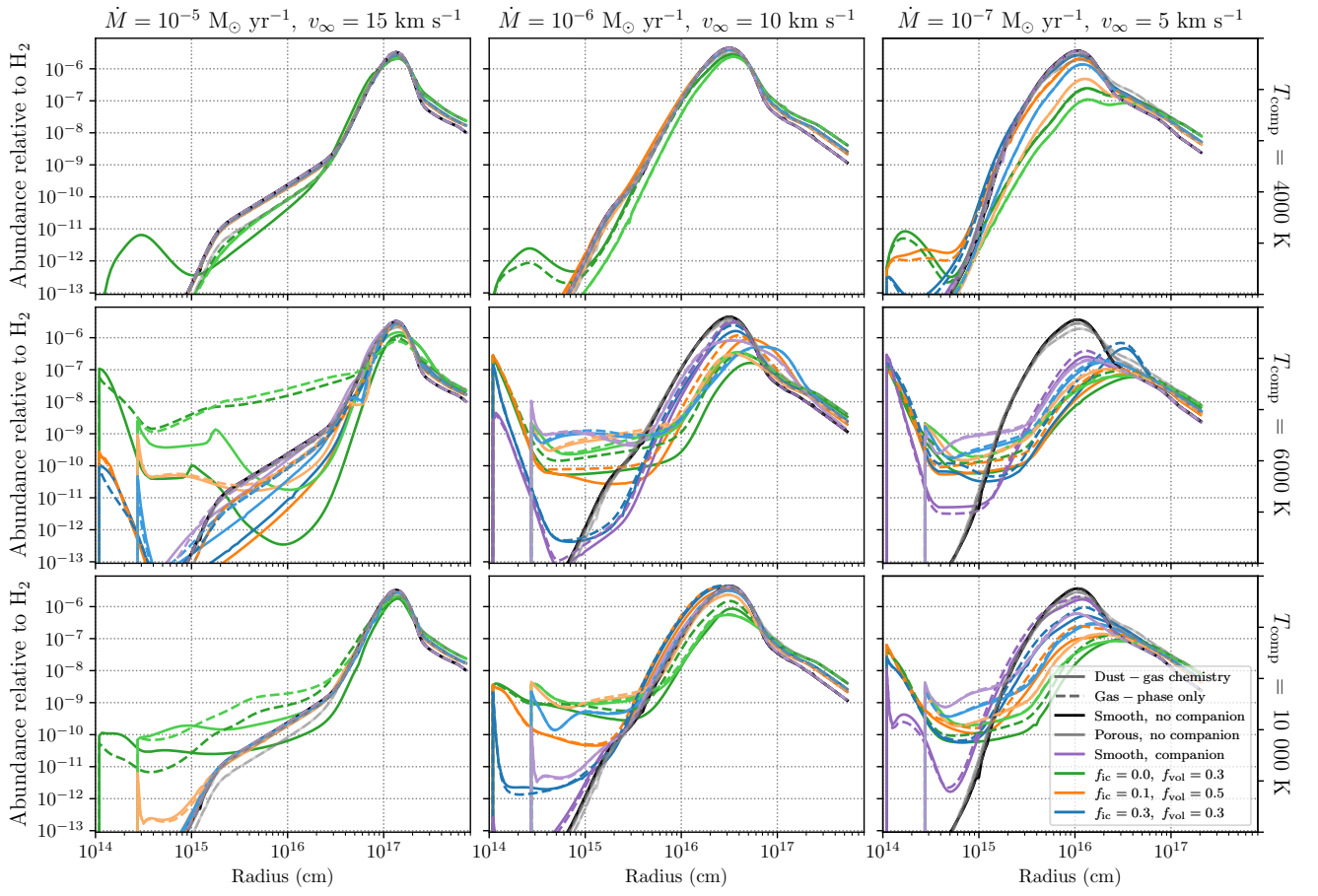


Figure 46: Fractional abundance of CH relative to H₂ for a selection of C-rich outflows.

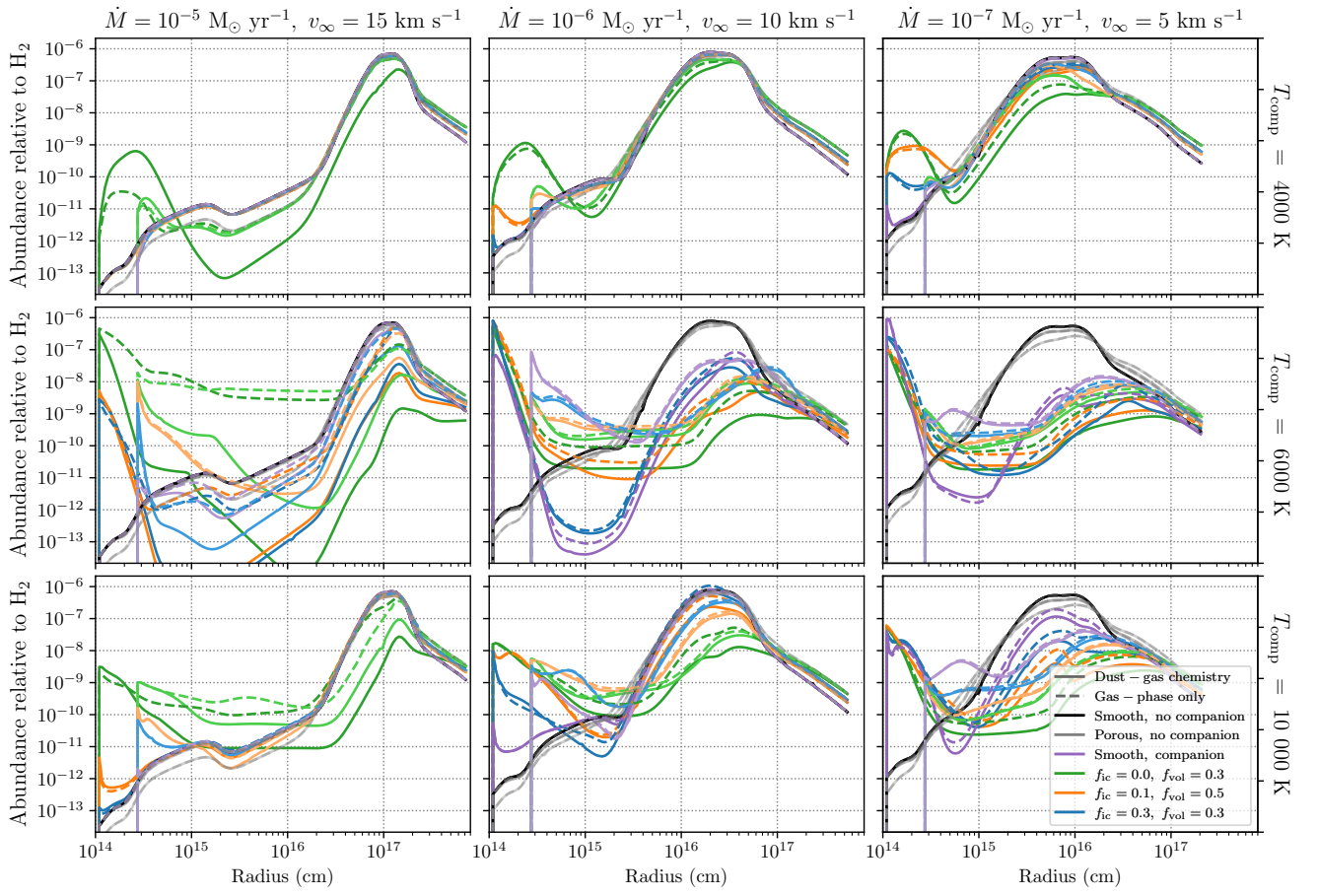


Figure 47: Fractional abundance of CH₂ relative to H₂ for a selection of C-rich outflows.

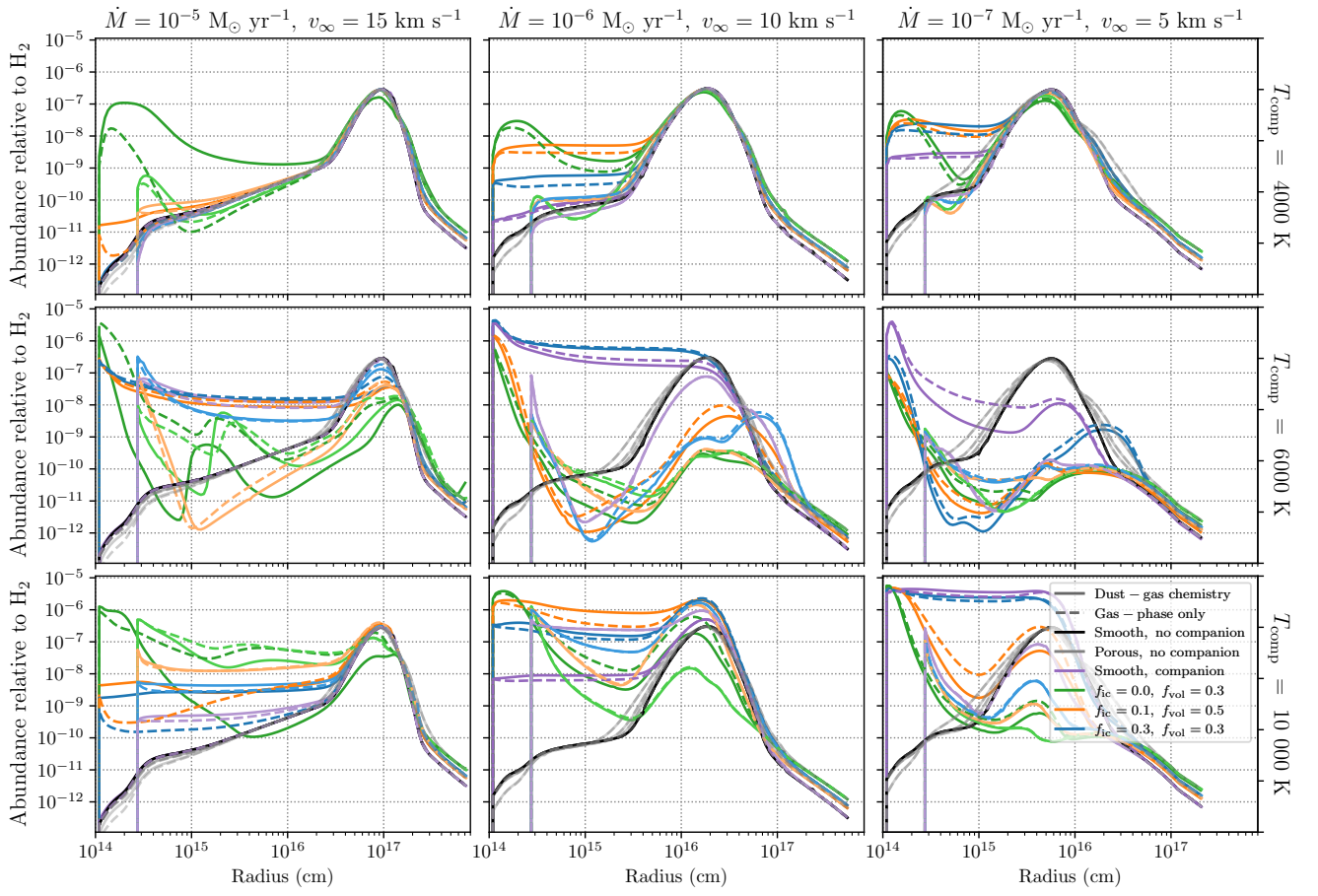


Figure 48: Fractional abundance of CH_3 relative to H_2 for a selection of C-rich outflows.

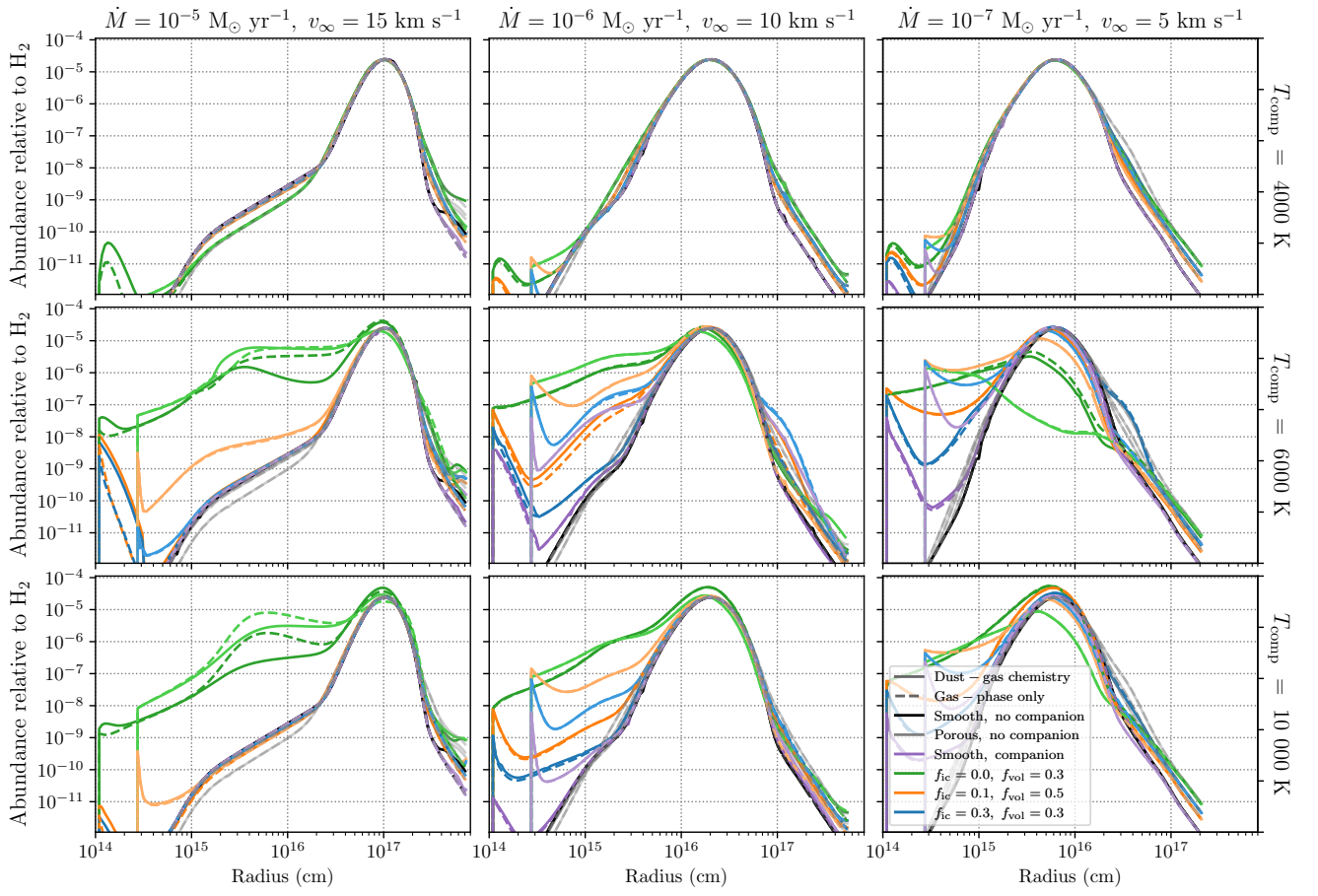


Figure 49: Fractional abundance of CN relative to H₂ for a selection of C-rich outflows.

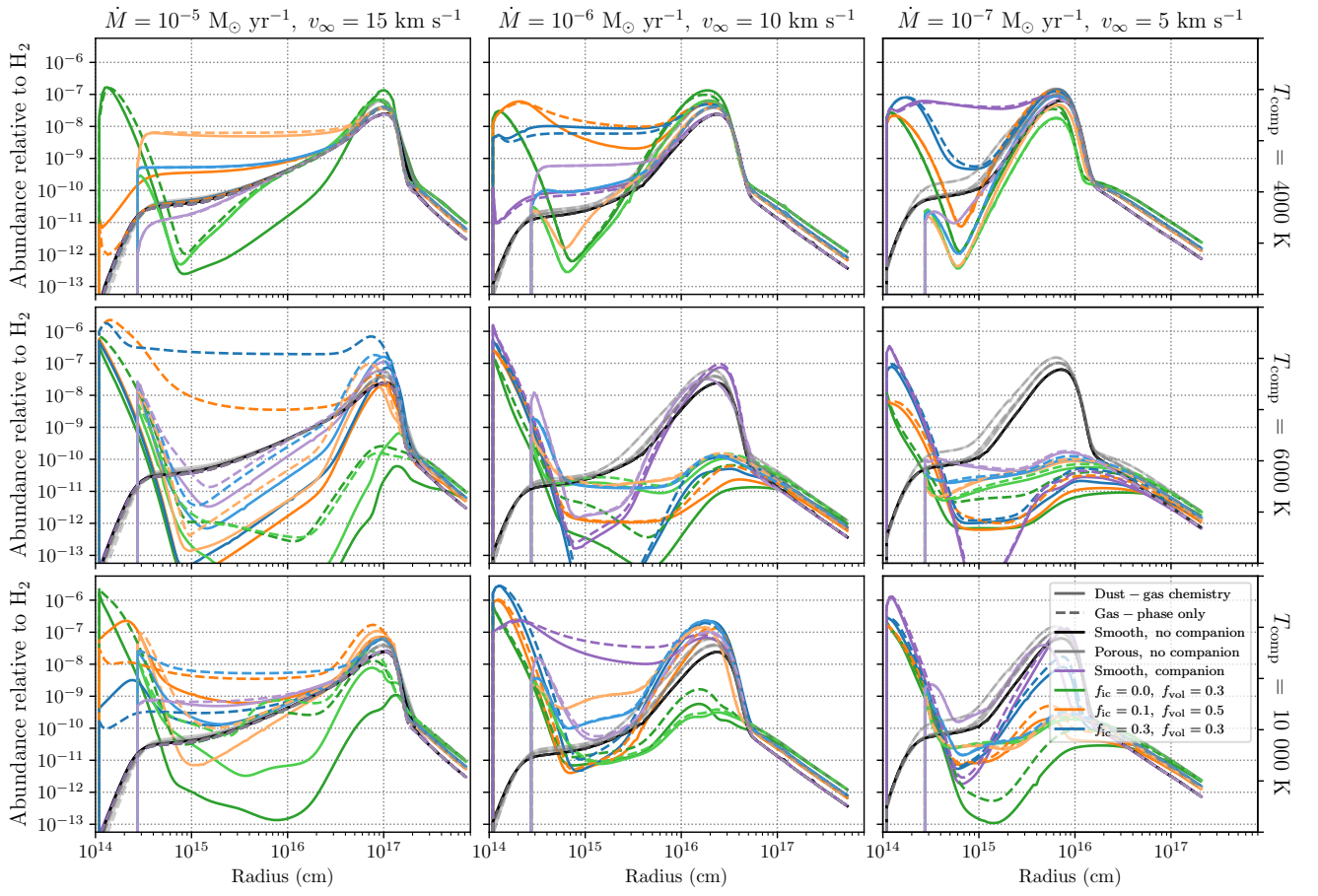


Figure 50: Fractional abundance of HS relative to H₂ for a selection of C-rich outflows.

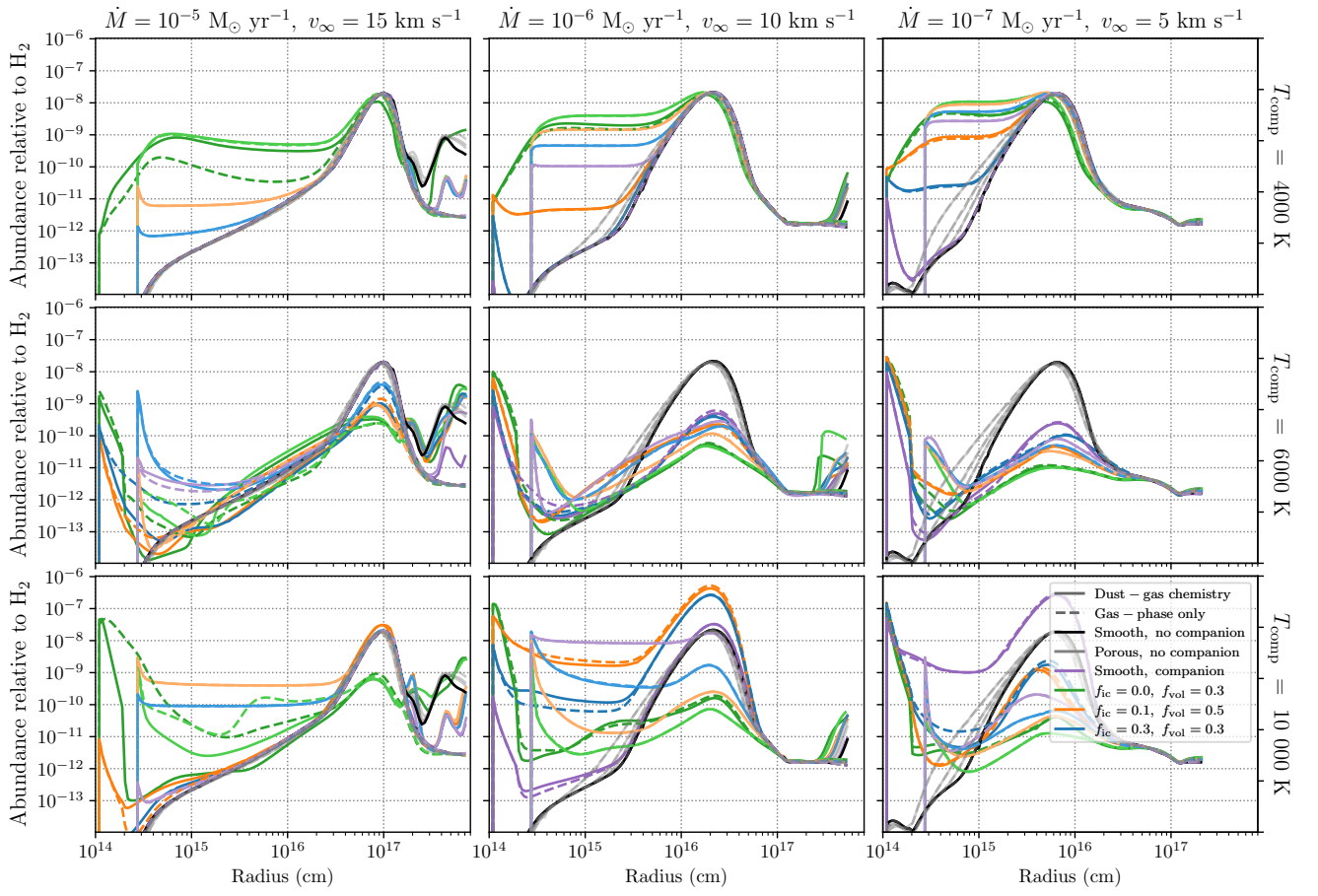


Figure 51: Fractional abundance of NH relative to H₂ for a selection of C-rich outflows.

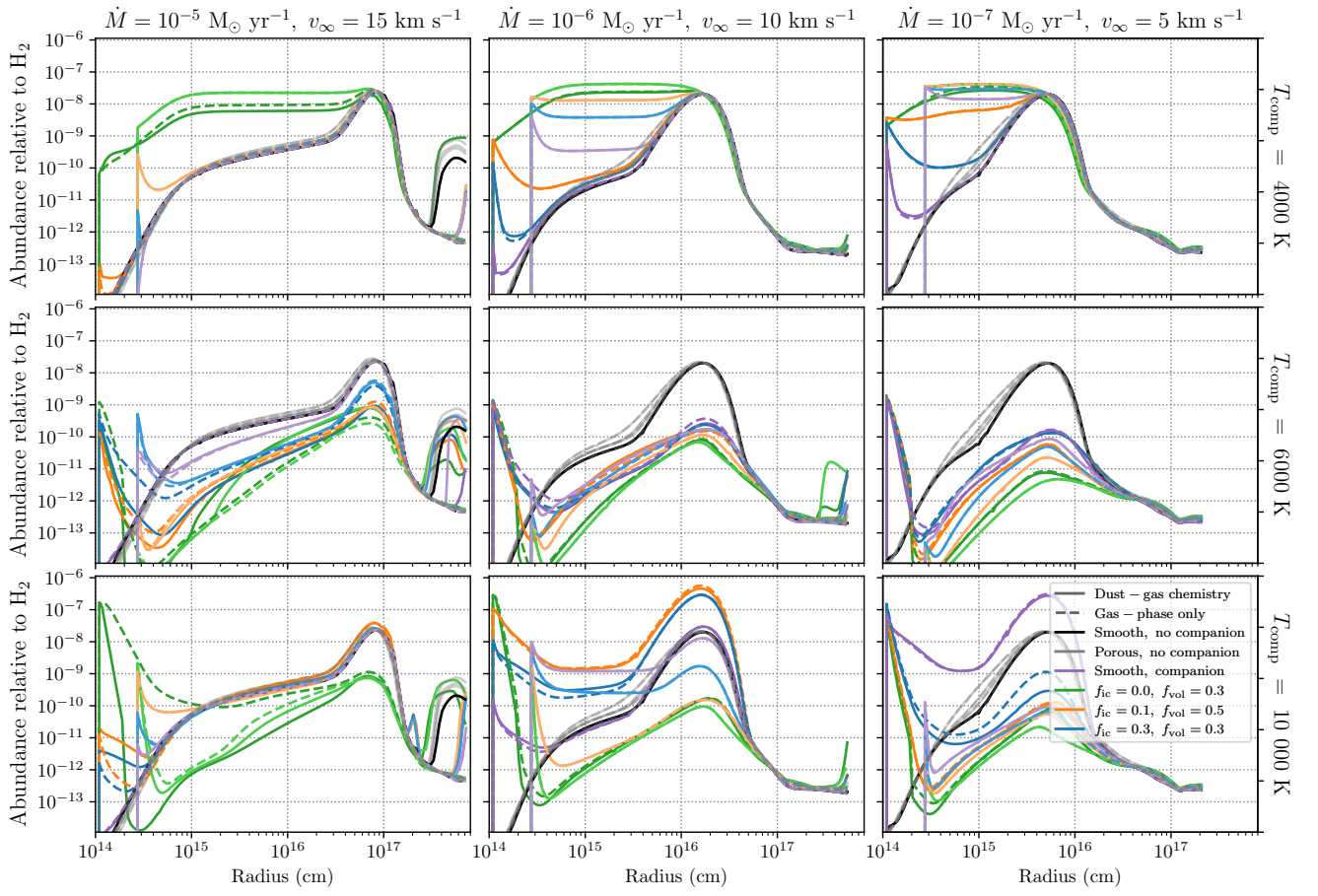


Figure 52: Fractional abundance of NH_2 relative to H_2 for a selection of C-rich outflows.

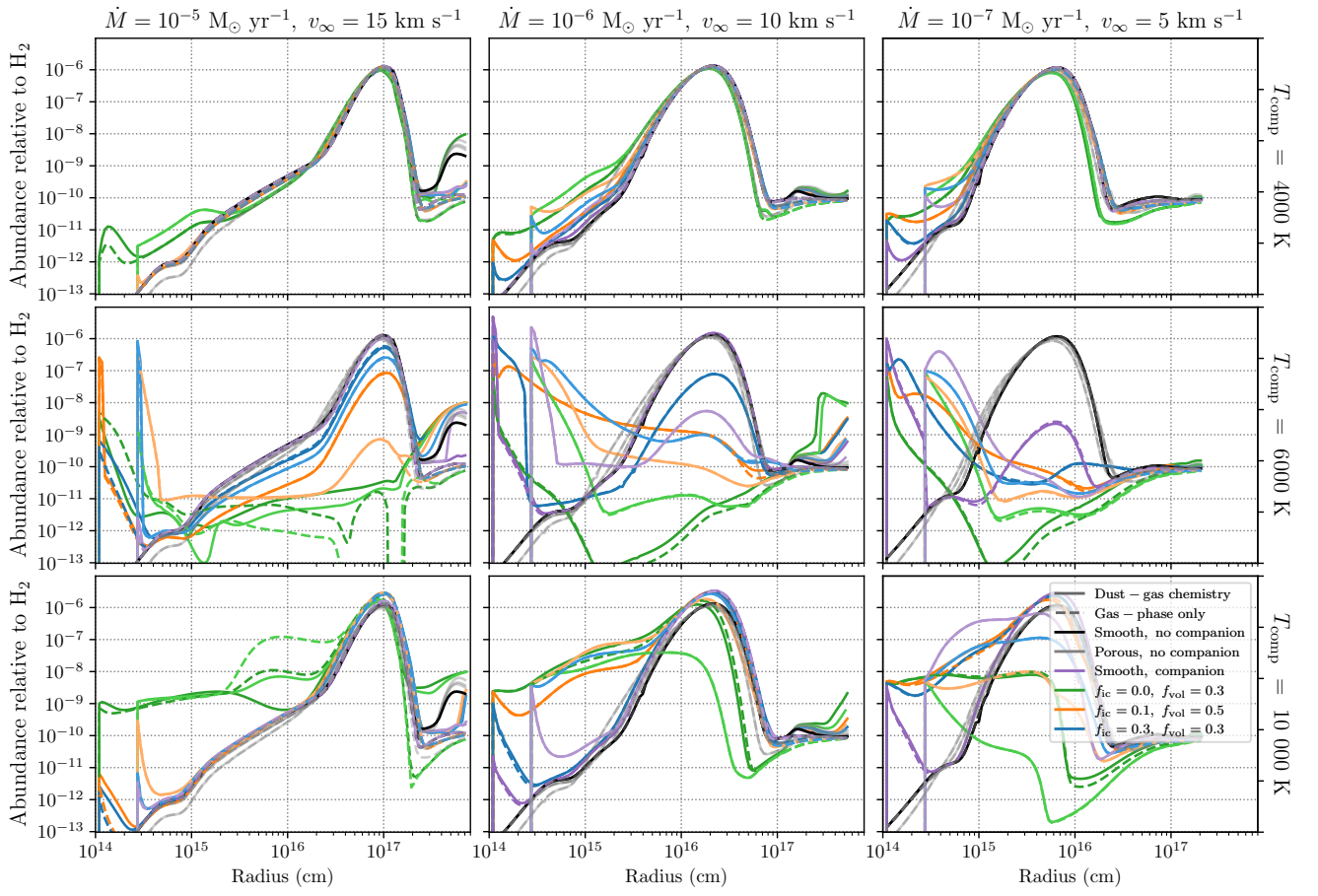


Figure 53: Fractional abundance of OH relative to H_2 for a selection of C-rich outflows.

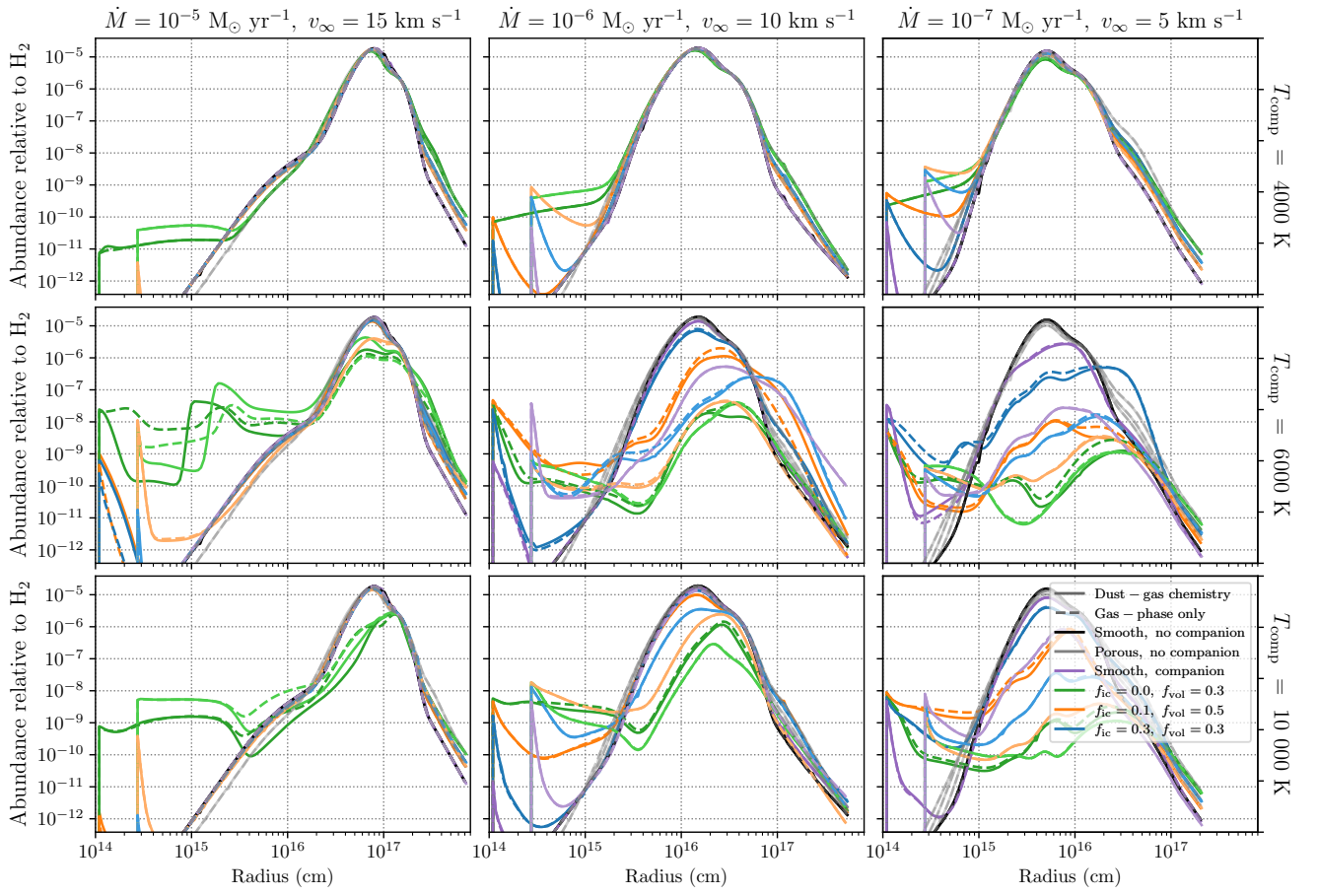


Figure 54: Fractional abundance of C_2H relative to H_2 for a selection of C-rich outflows.

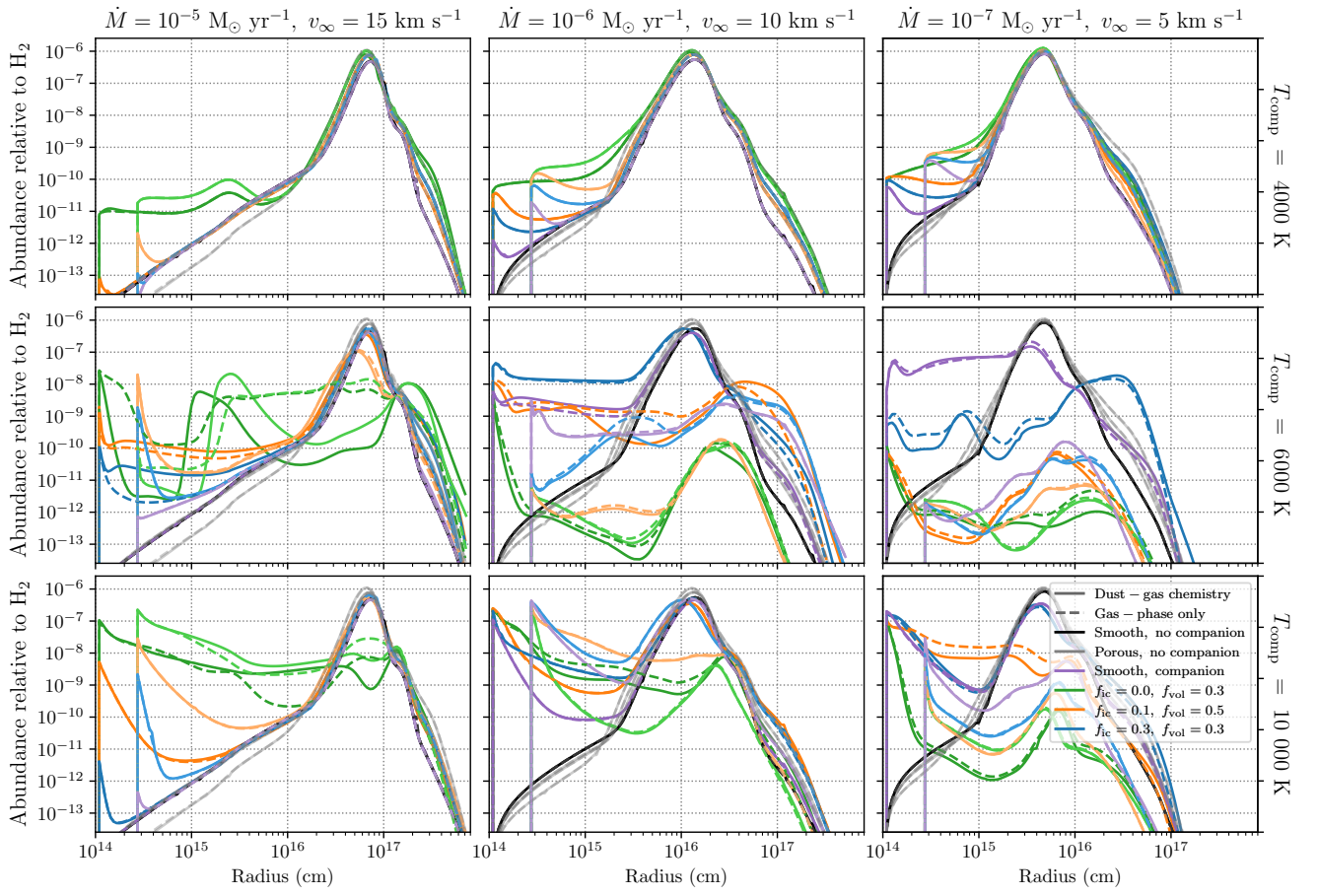


Figure 55: Fractional abundance of C_4H relative to H_2 for a selection of C-rich outflows.

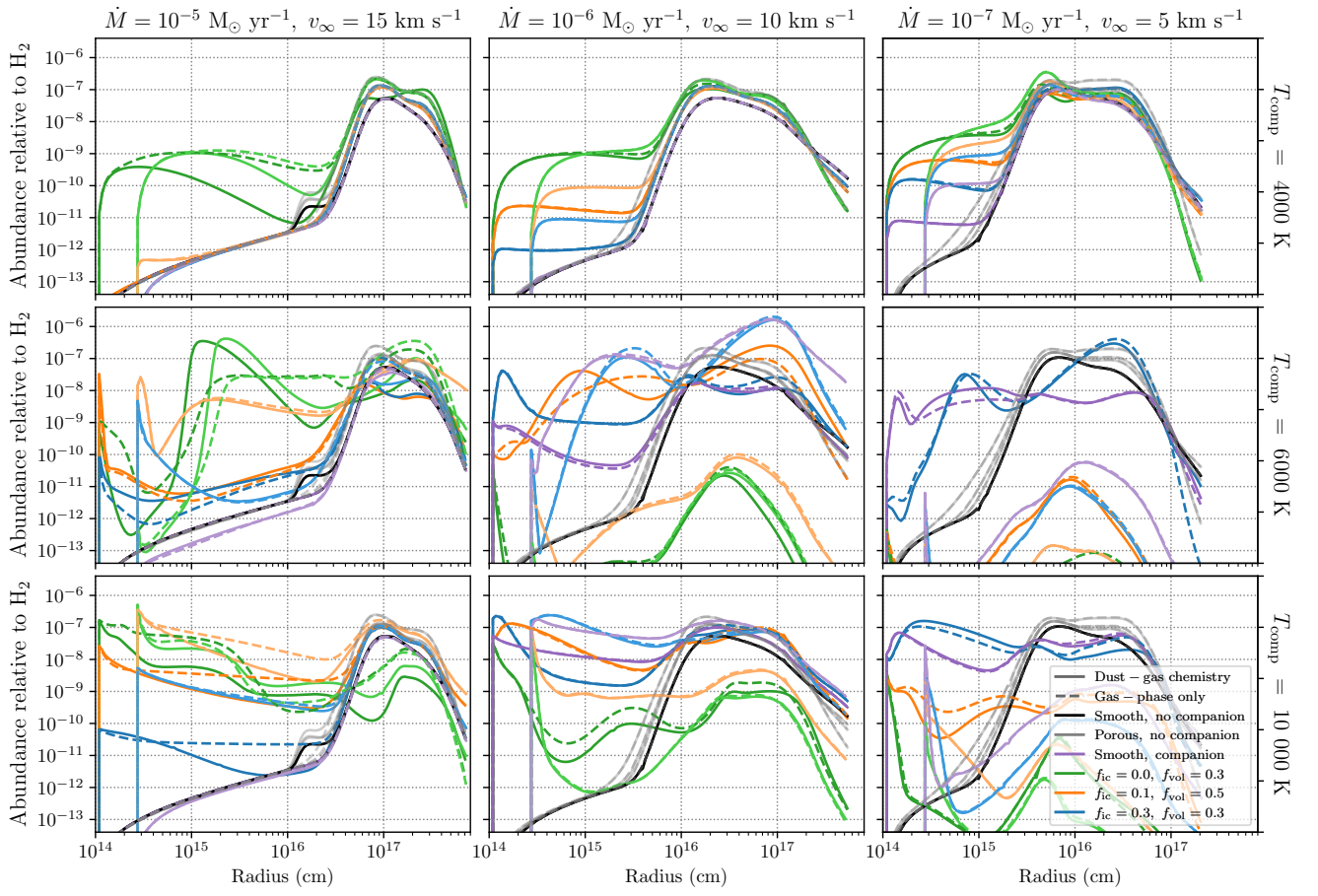


Figure 56: Fractional abundance of C_6H relative to H_2 for a selection of C-rich outflows.

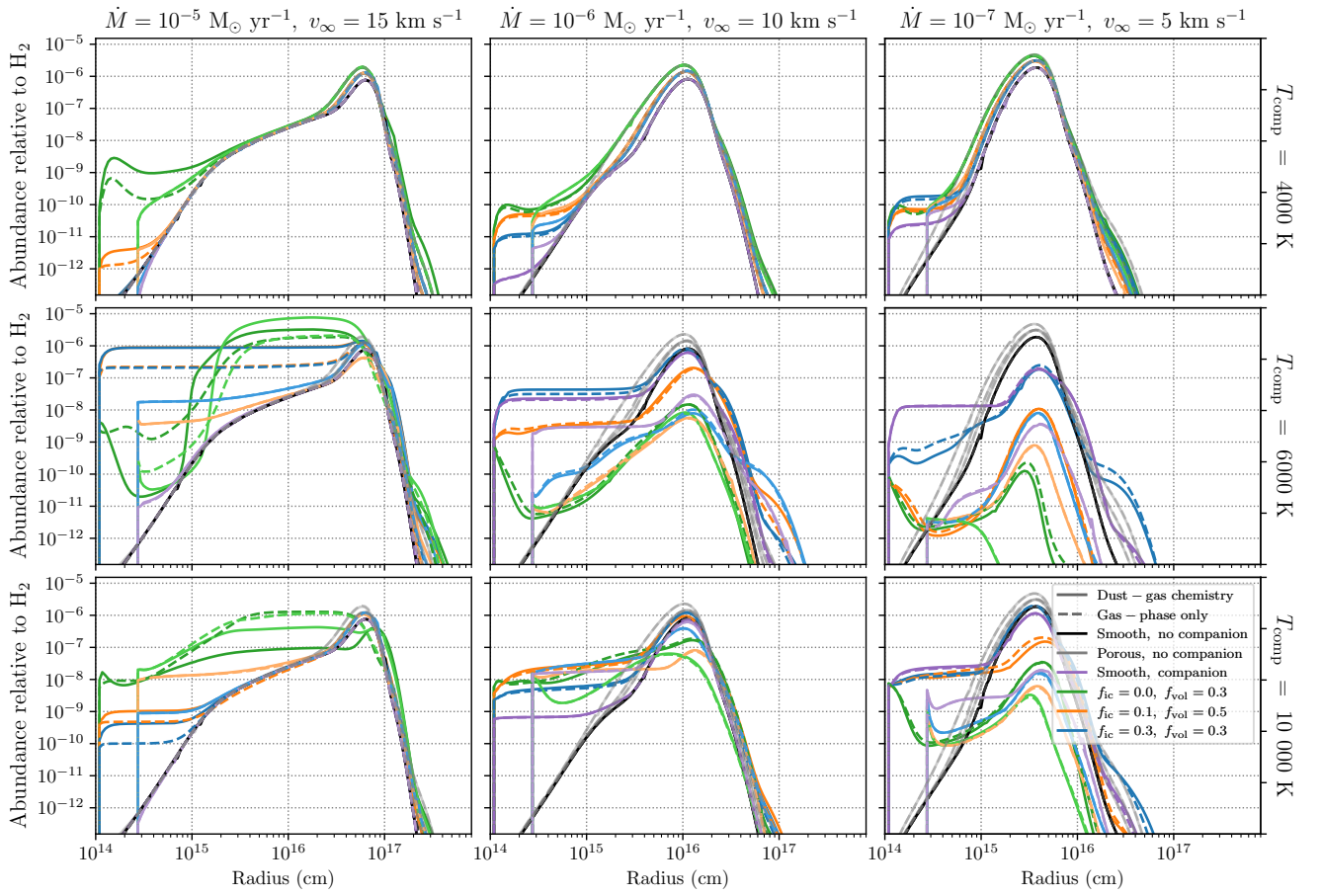


Figure 57: Fractional abundance of HC_3N relative to H_2 for a selection of C-rich outflows.

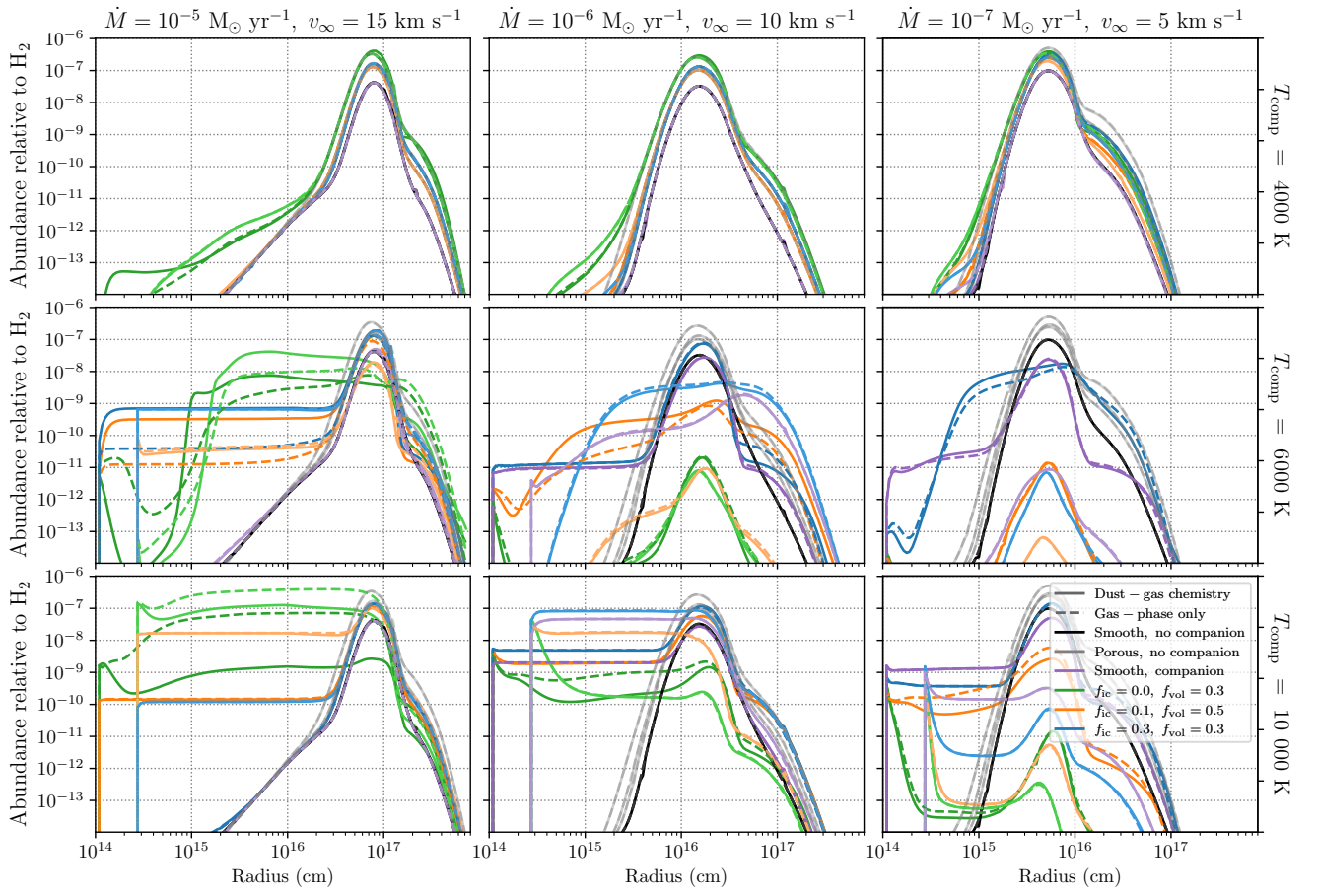


Figure 58: Fractional abundance of HC_5N relative to H_2 for a selection of C-rich outflows.

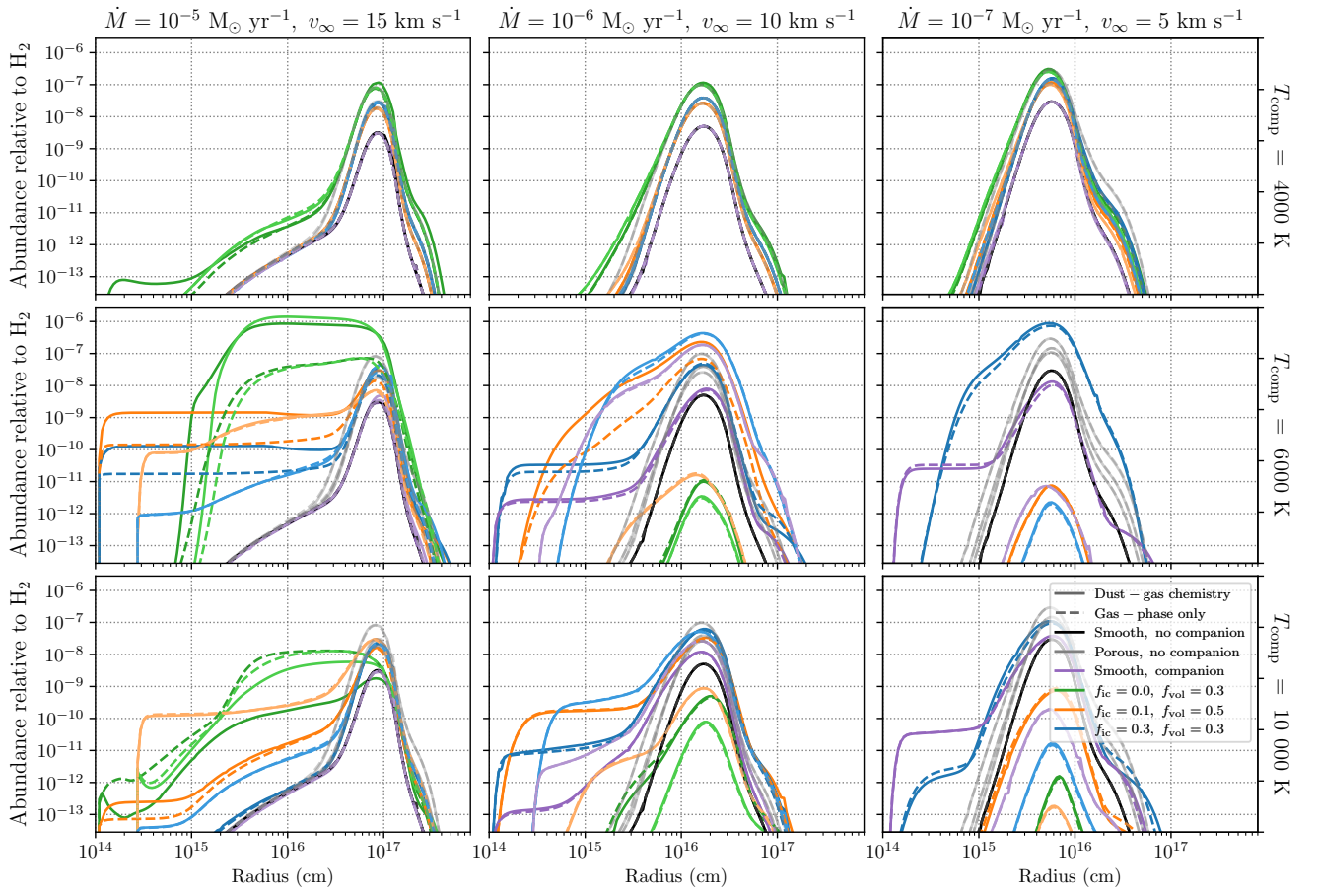


Figure 59: Fractional abundance of HC_7N relative to H_2 for a selection of C-rich outflows.

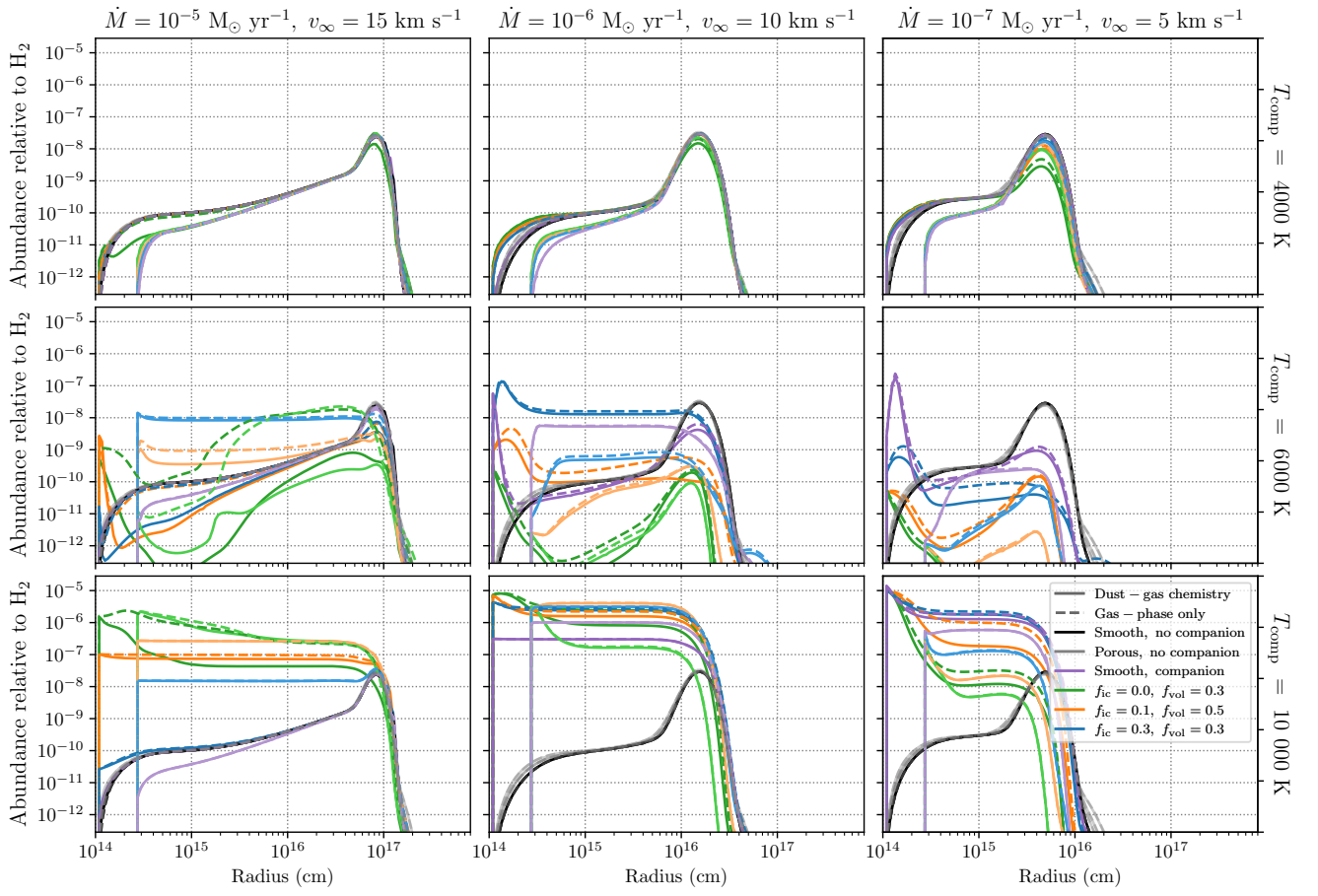


Figure 60: Fractional abundance of CH_3CN relative to H_2 for a selection of C-rich outflows.

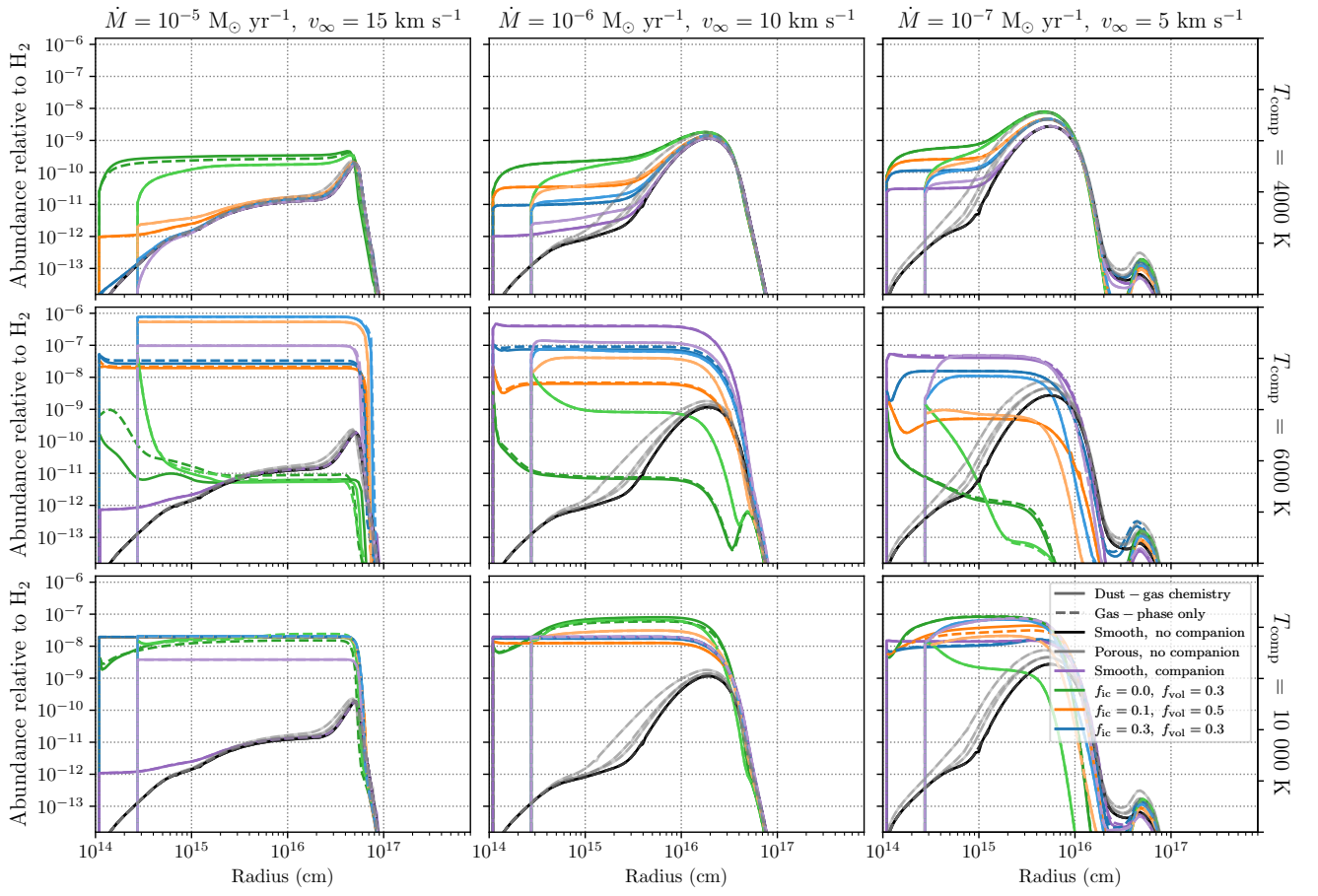


Figure 61: Fractional abundance of CO₂ relative to H₂ for a selection of C-rich outflows.

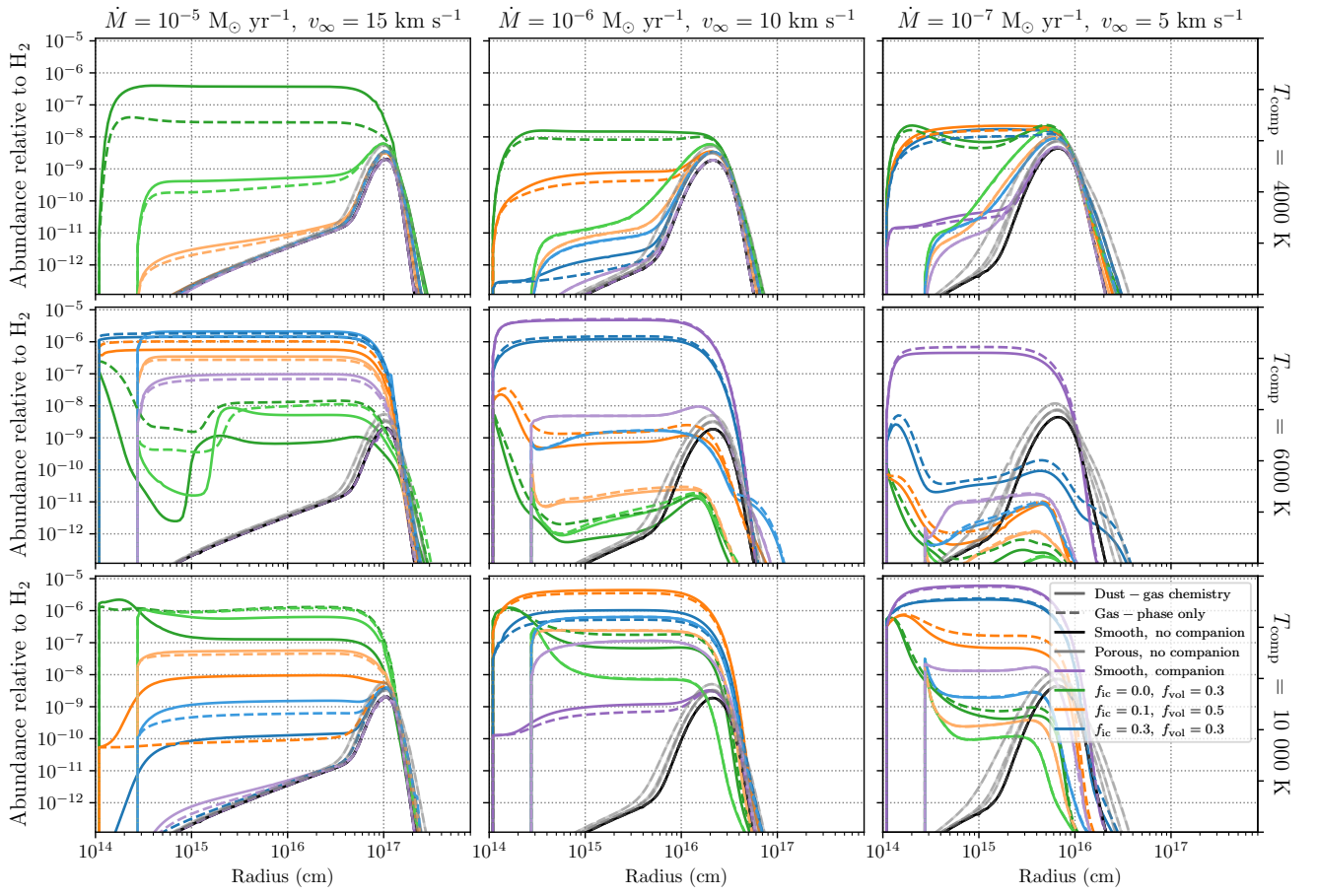


Figure 62: Fractional abundance of H₂CS relative to H₂ for a selection of C-rich outflows.

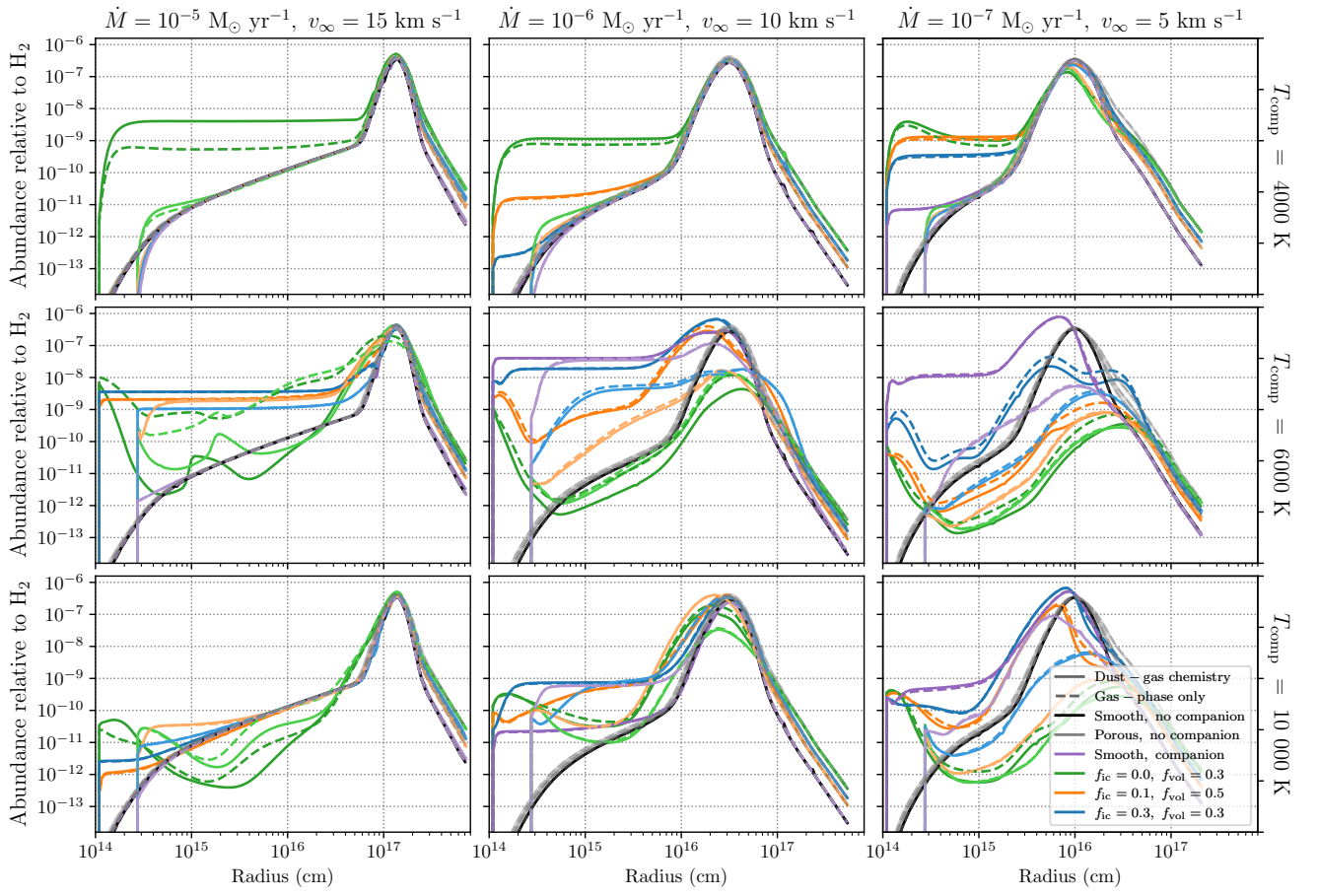


Figure 63: Fractional abundance of HCSi relative to H₂ for a selection of C-rich outflows.

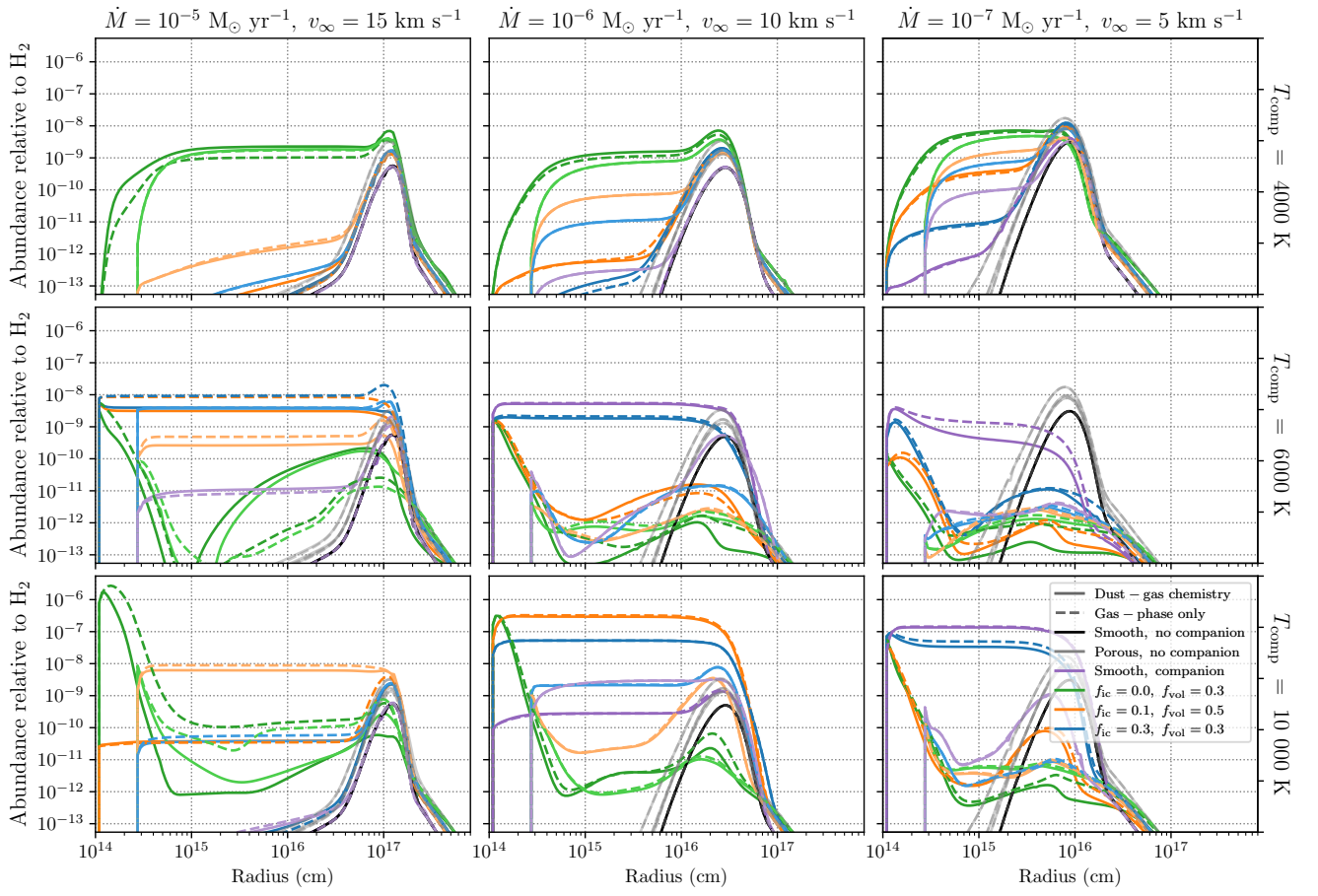


Figure 64: Fractional abundance of NS relative to H_2 for a selection of C-rich outflows.

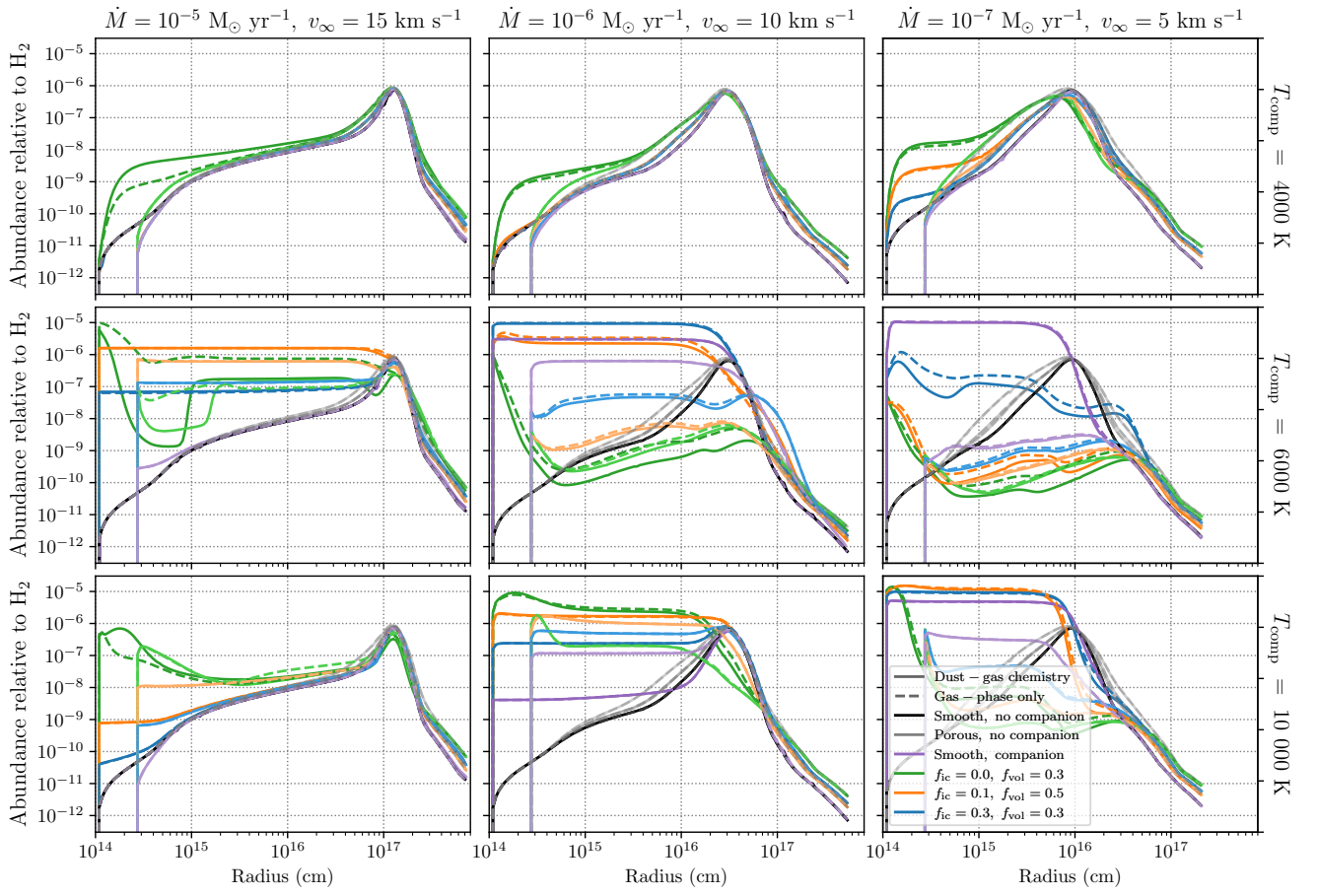


Figure 65: Fractional abundance of SiC relative to H₂ for a selection of C-rich outflows.

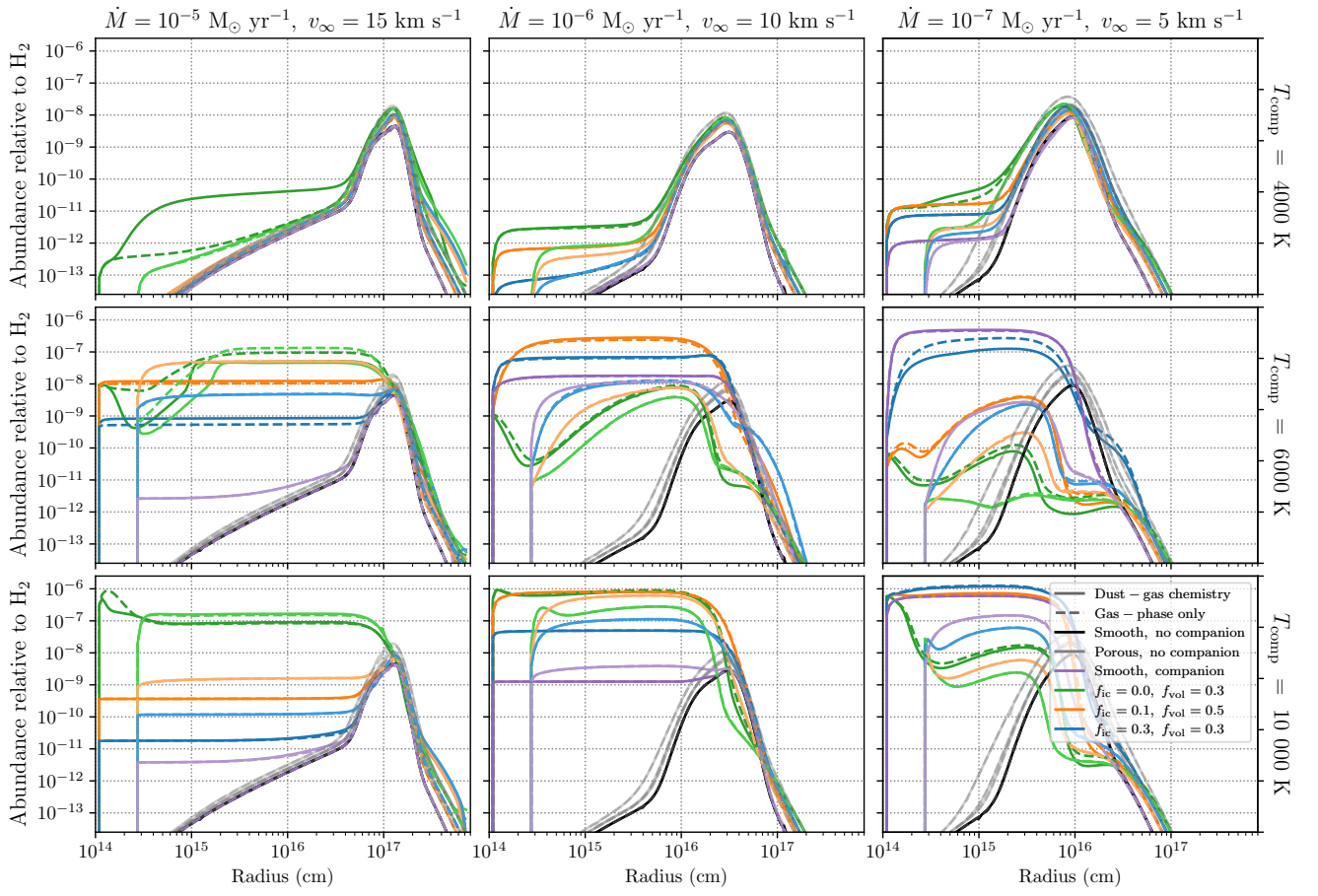


Figure 66: Fractional abundance of SiN relative to H₂ for a selection of C-rich outflows.

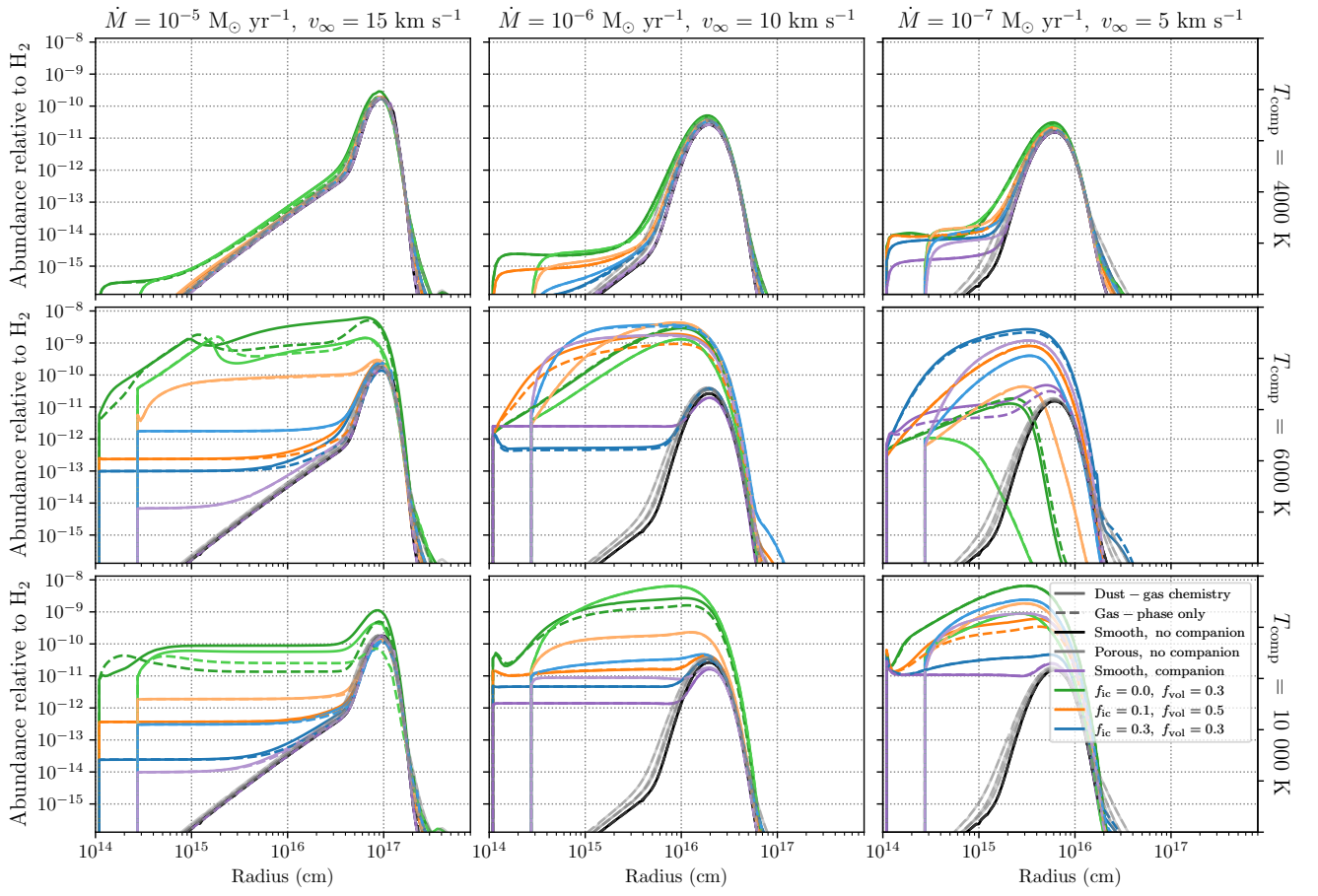


Figure 67: Fractional abundance of SiNC relative to H_2 for a selection of C-rich outflows.

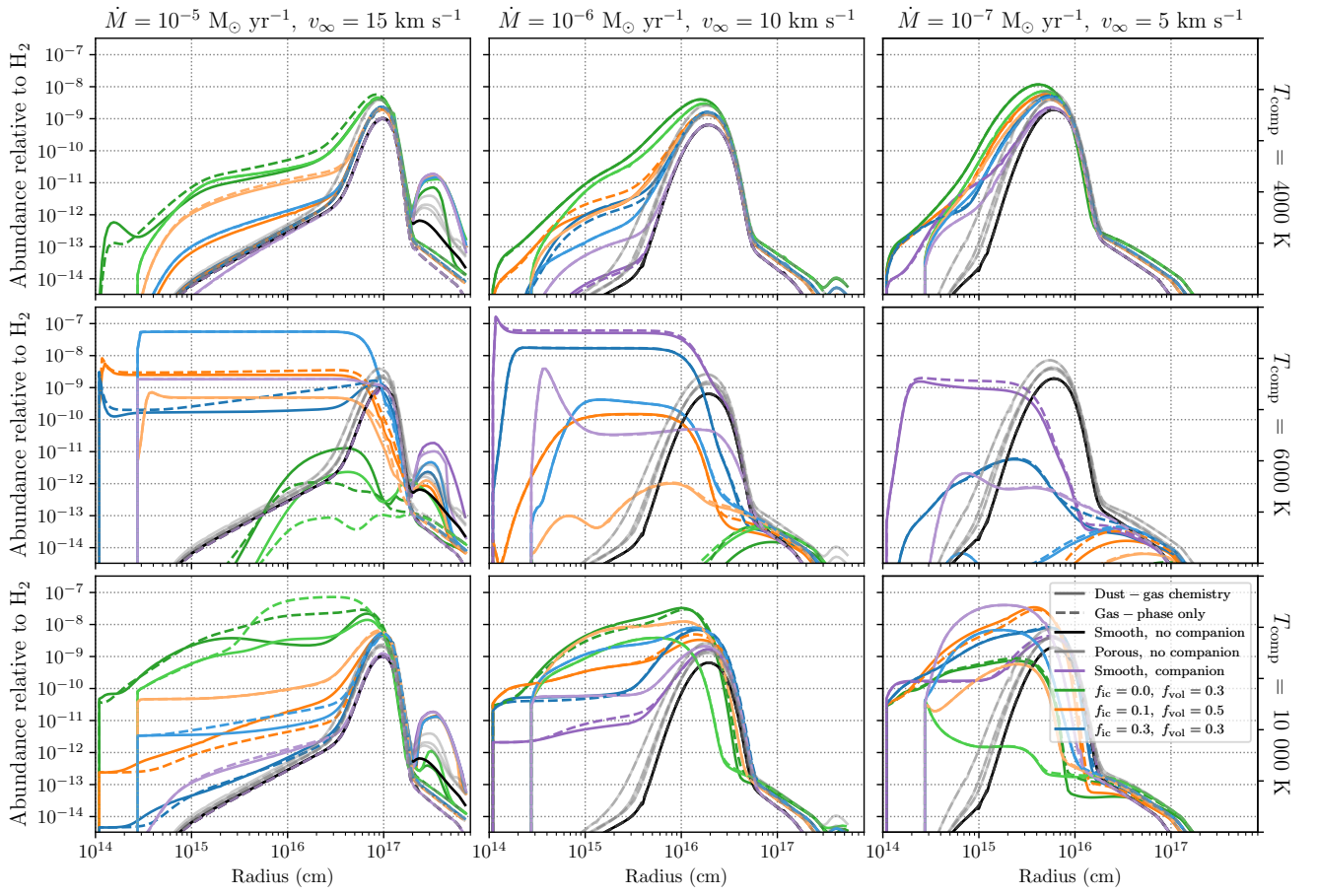


Figure 68: Fractional abundance of SO relative to H₂ for a selection of C-rich outflows.

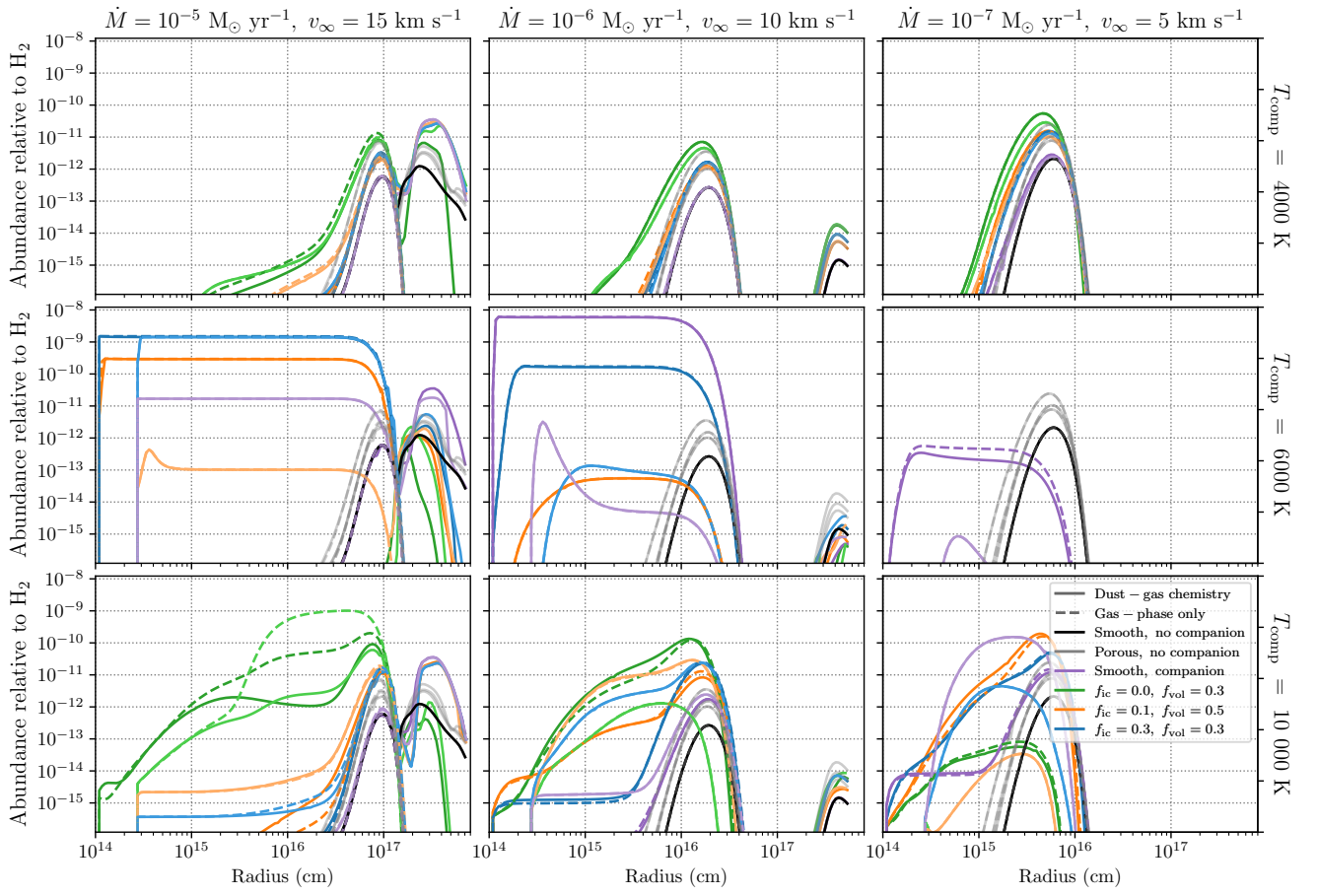


Figure 69: Fractional abundance of SO_2 relative to H_2 for a selection of C-rich outflows.

3 Grain surface coverage with ice and refractory material

The figures show the number of ice or refractory monolayers at the end of the outflow for all calculated outflows with different density structures and companions. The black solid line shows the number of monolayers in a smooth outflow without a companion. Different shapes and colours correspond to different density structures and the presence of a companion. Purple circles: smooth outflow with companion. Grey circles: porous outflows without a companion. The other shapes show the results for porous outflows with a companion. The shape signifies the value of f_{ic} : squares, triangles, hexagons, crosses correspond to $f_{ic} = 0.0, 0.1, 0.3, 0.5$, respectively. The colour signifies the value of f_{vol} : green, blue, red correspond to $f_{vol} = 0.1, 0.3, 0.5$, respectively. Different shades signify different values of l_* . Lighter colour: $l_* = 5 \times 10^{12}$ cm, darker colour: $l_* = 10^{13}$ cm. The edge colour of the shapes shows different values of R_{dust} . Black edge: $R_{dust} = 2 R_*$, grey edge: $R_{dust} = 5 R_*$.

3.1 O-rich outflows

3.1.1 Ice coverage

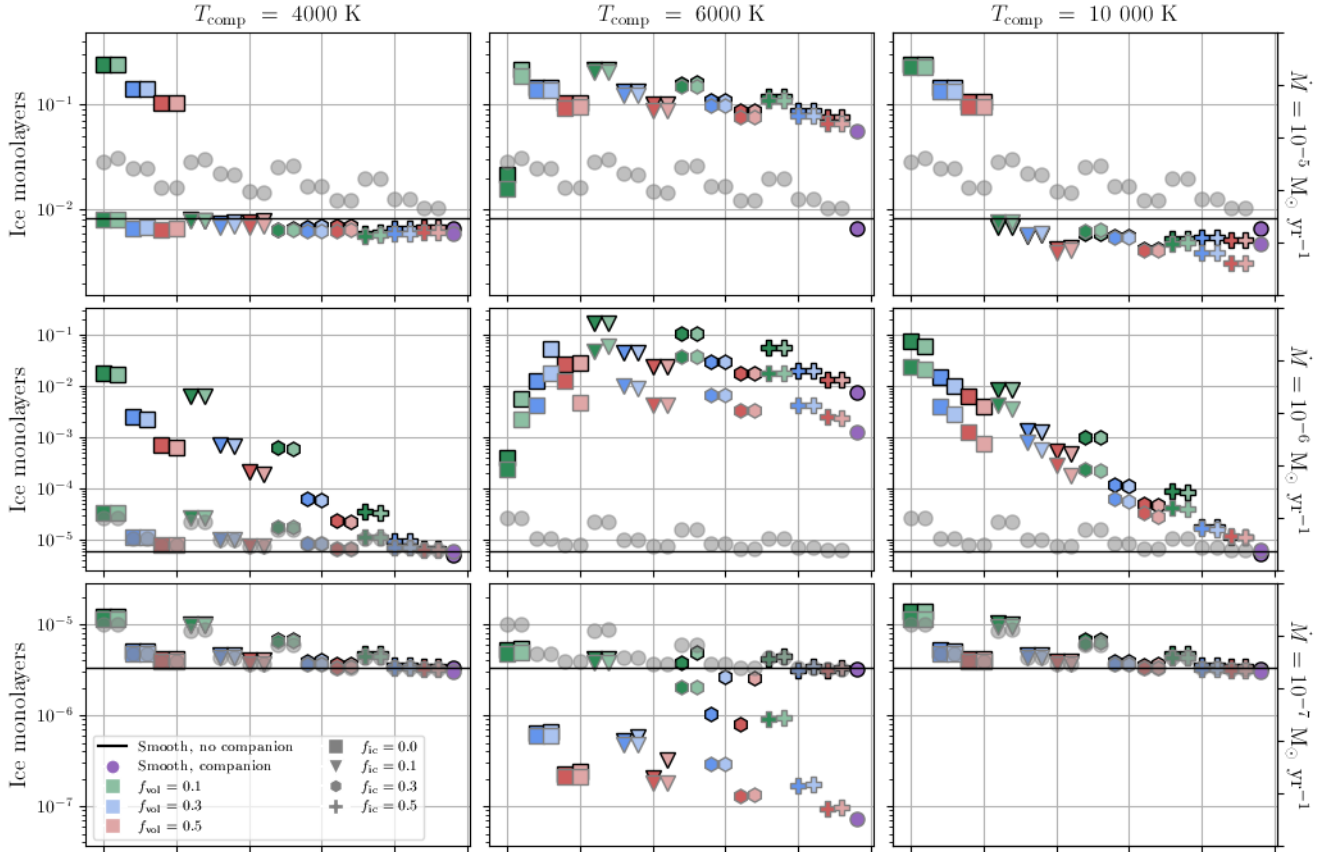


Figure 70: Number of ice monolayers at the end of the outflow for all calculated O-rich outflows, assuming a GSD with smaller grain sizes than the canonical MRN distribution.

3.1.2 Refractory coverage

3.2 C-rich outflows

3.2.1 Ice coverage

3.2.2 Refractory coverage

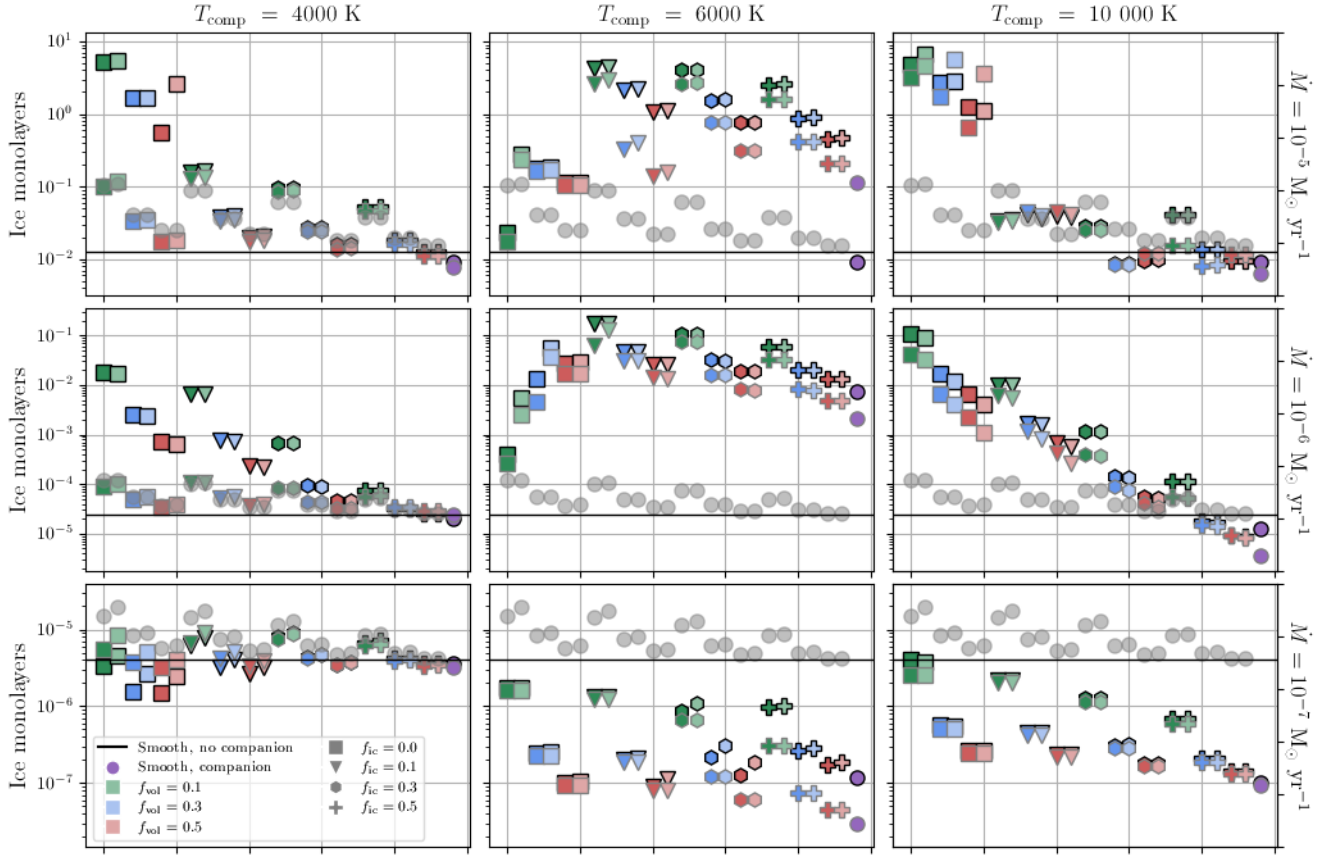


Figure 71: Number of ice monolayers at the end of the outflow for all calculated O-rich outflows, assuming the canonical MRN distribution.

4 Number of monolayers of ice and refractory material throughout the outflow

Number of monolayers of ice or refractory material throughout a selection of outflows with different outflow densities (columns) and companions (rows). Different line styles show different chemistries included. Dashed lines: gas-phase chemistry only, solid lines: including dust-gas chemistry. Different colours show different density structures and the inclusion of a companion. Black: smooth outflow without a companion, gray: porous outflow without a companion. When including a companion, different shades correspond to the value of R_{dust} . Darker shade: $R_{\text{dust}} = 2 R_*$, lighter shade: $R_{\text{dust}} = 5 R_*$. Purple: smooth outflow with a companion. Green: porous outflow with a companion, $f_{\text{ic}} = 0.0$, $f_{\text{vol}} = 0.3$, $l_* = 10^{13}$ cm. Orange: porous outflow with a companion, $f_{\text{ic}} = 0.1$, $f_{\text{vol}} = 0.5$, $l_* = 10^{13}$ cm. Blue: porous outflow with a companion, $f_{\text{ic}} = 0.3$, $f_{\text{vol}} = 0.3$, $l_* = 5 \times 10^{12}$ cm.

4.1 O-rich outflows

4.1.1 Ice coverage

4.1.2 Refractory coverage

4.2 C-rich outflows

4.2.1 Ice coverage

4.2.2 Refractory coverage

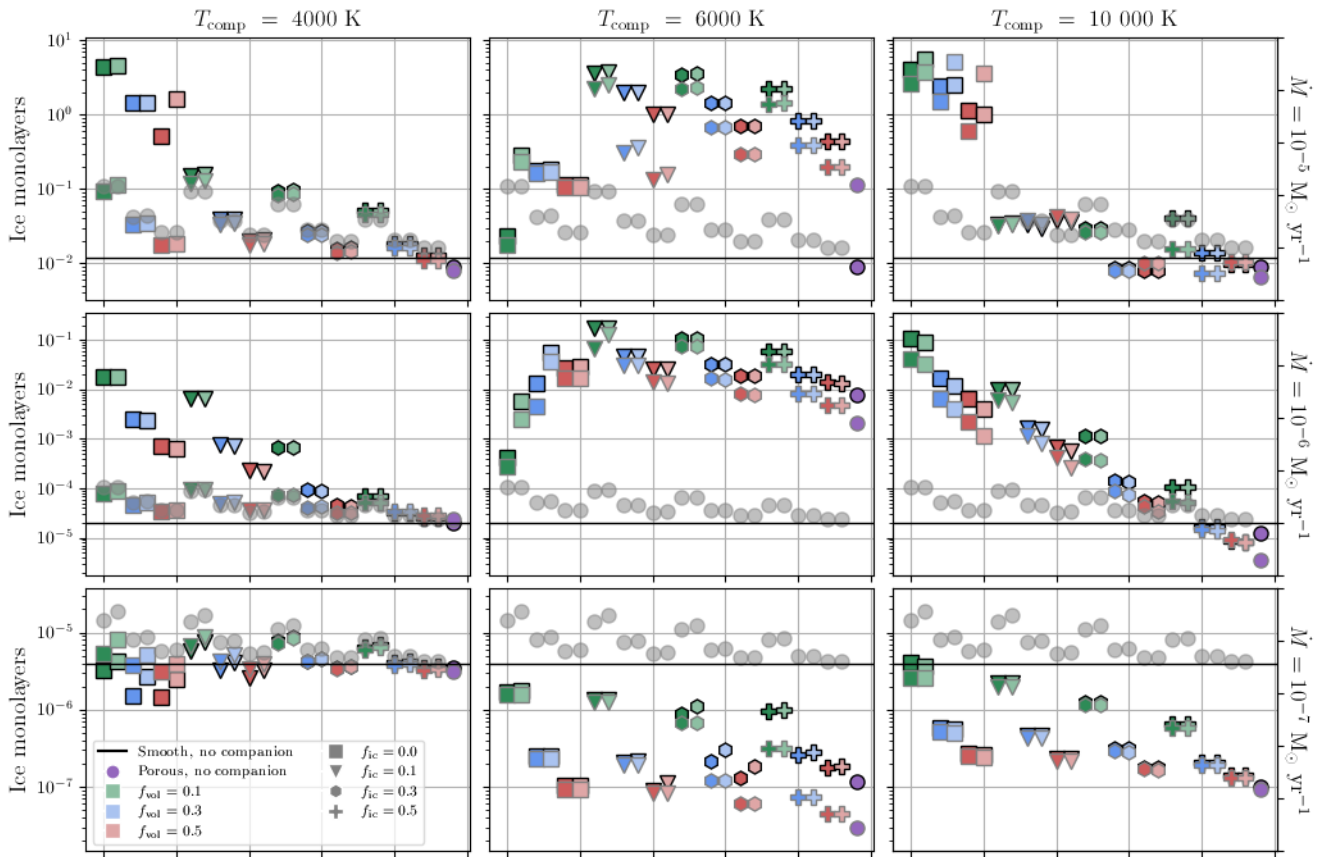


Figure 72: Number of ice monolayers at the end of the outflow for all calculated O-rich outflows, assuming a GSD with larger grain sizes than the canonical MRN distribution.

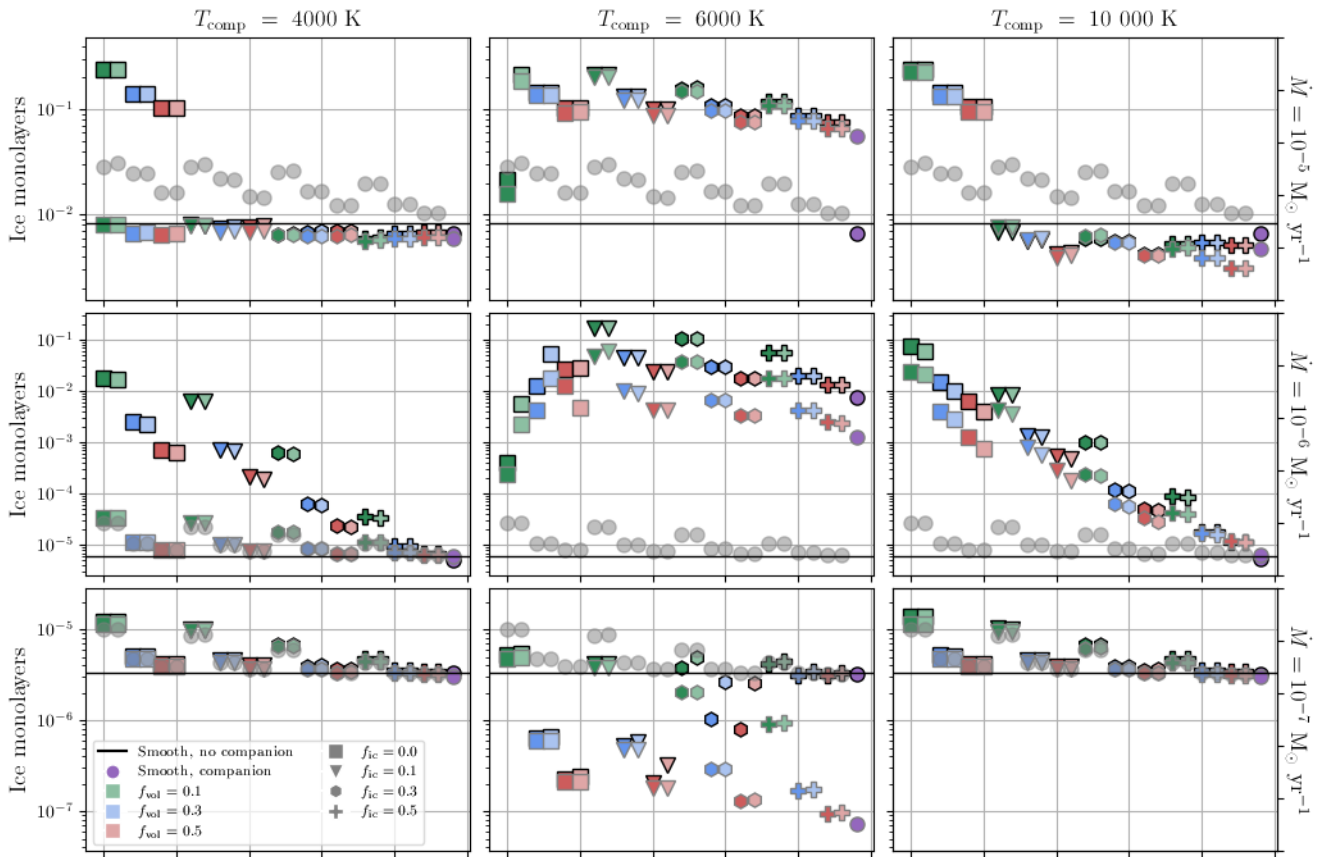


Figure 73: Number of refractory monolayers at the end of the outflow for all calculated O-rich outflows, assuming a GSD with smaller grain sizes than the canonical MRN distribution.

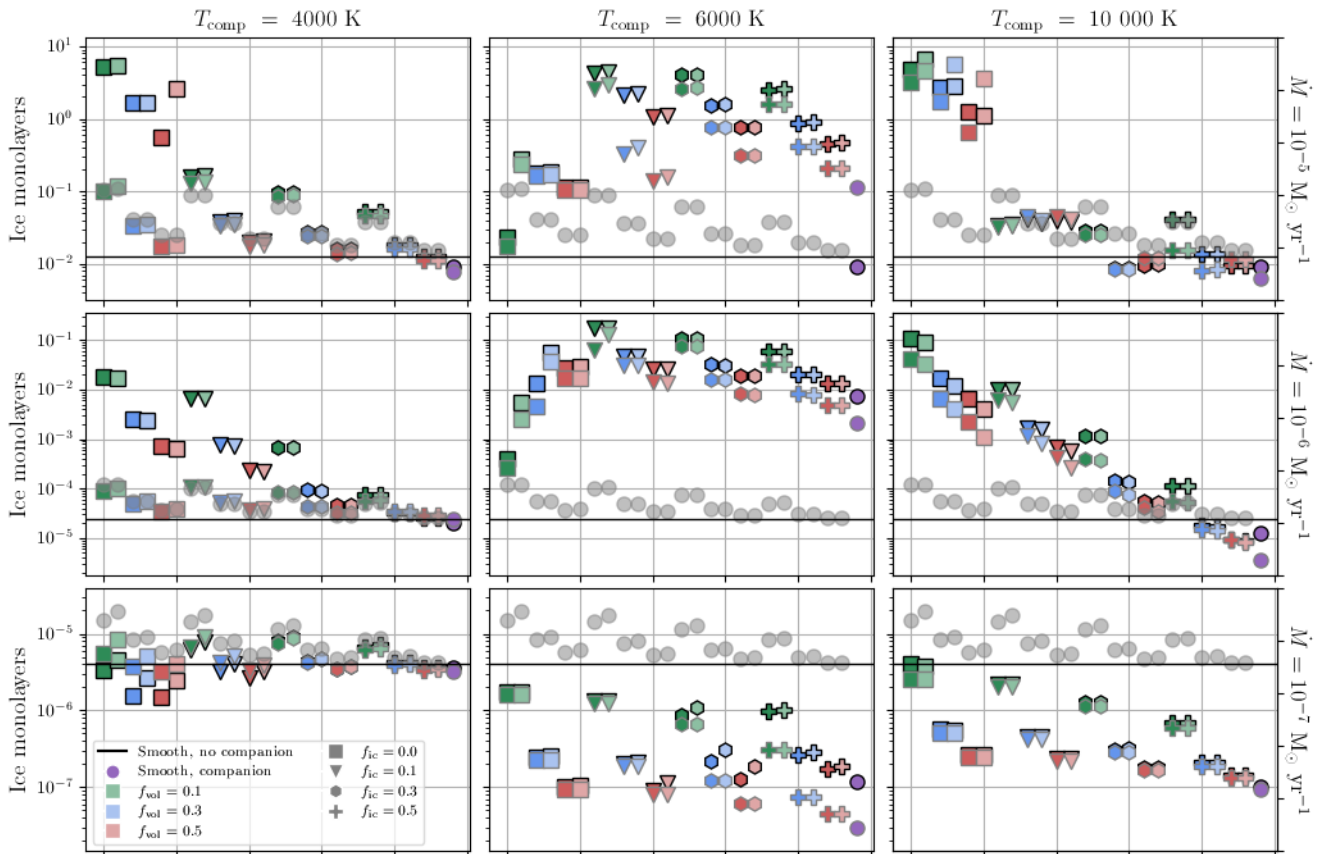


Figure 74: Number of refractory monolayers at the end of the outflow for all calculated O-rich outflows, assuming the canonical MRN distribution.

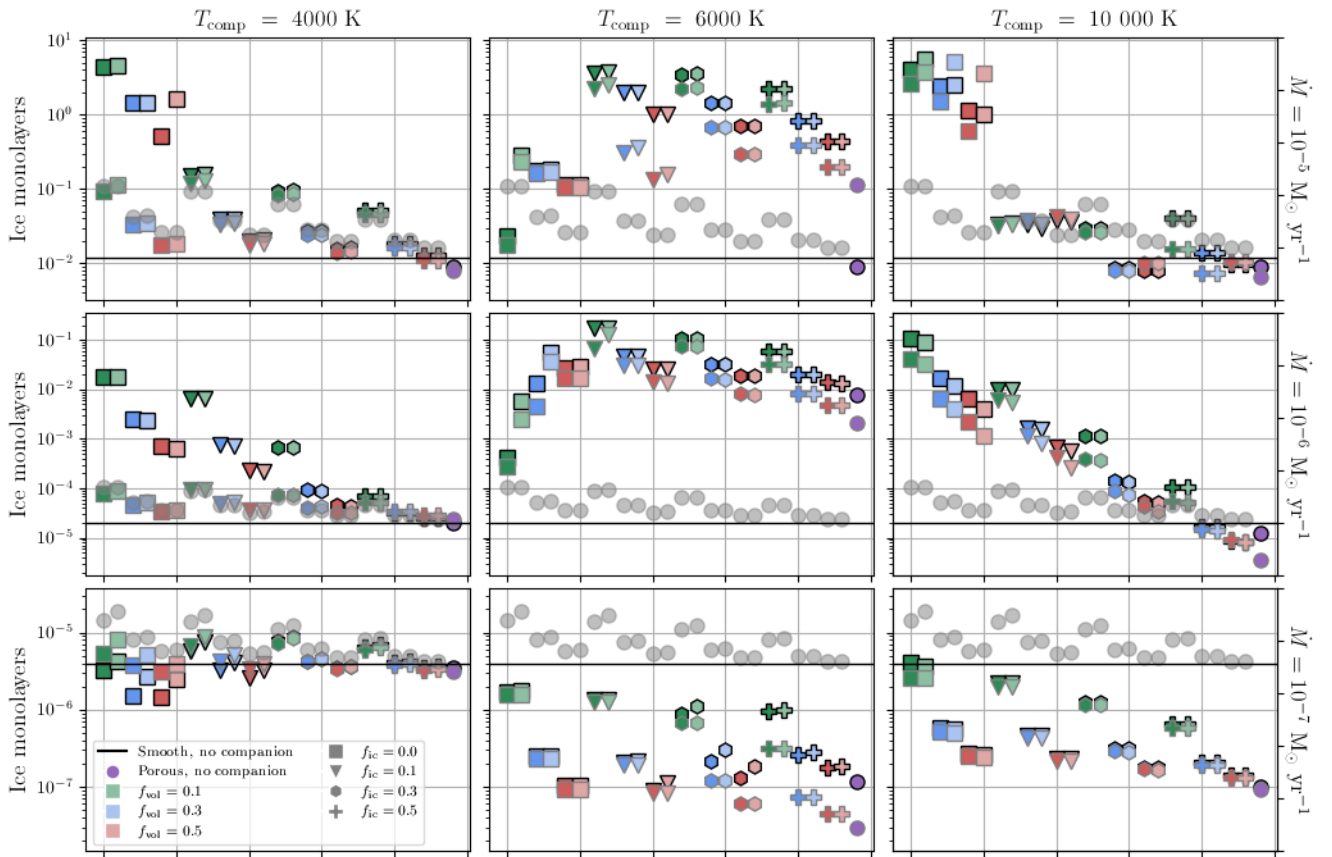


Figure 75: Number of refractory monolayers at the end of the outflow for all calculated O-rich outflows, assuming a GSD with larger grain sizes than the canonical MRN distribution.

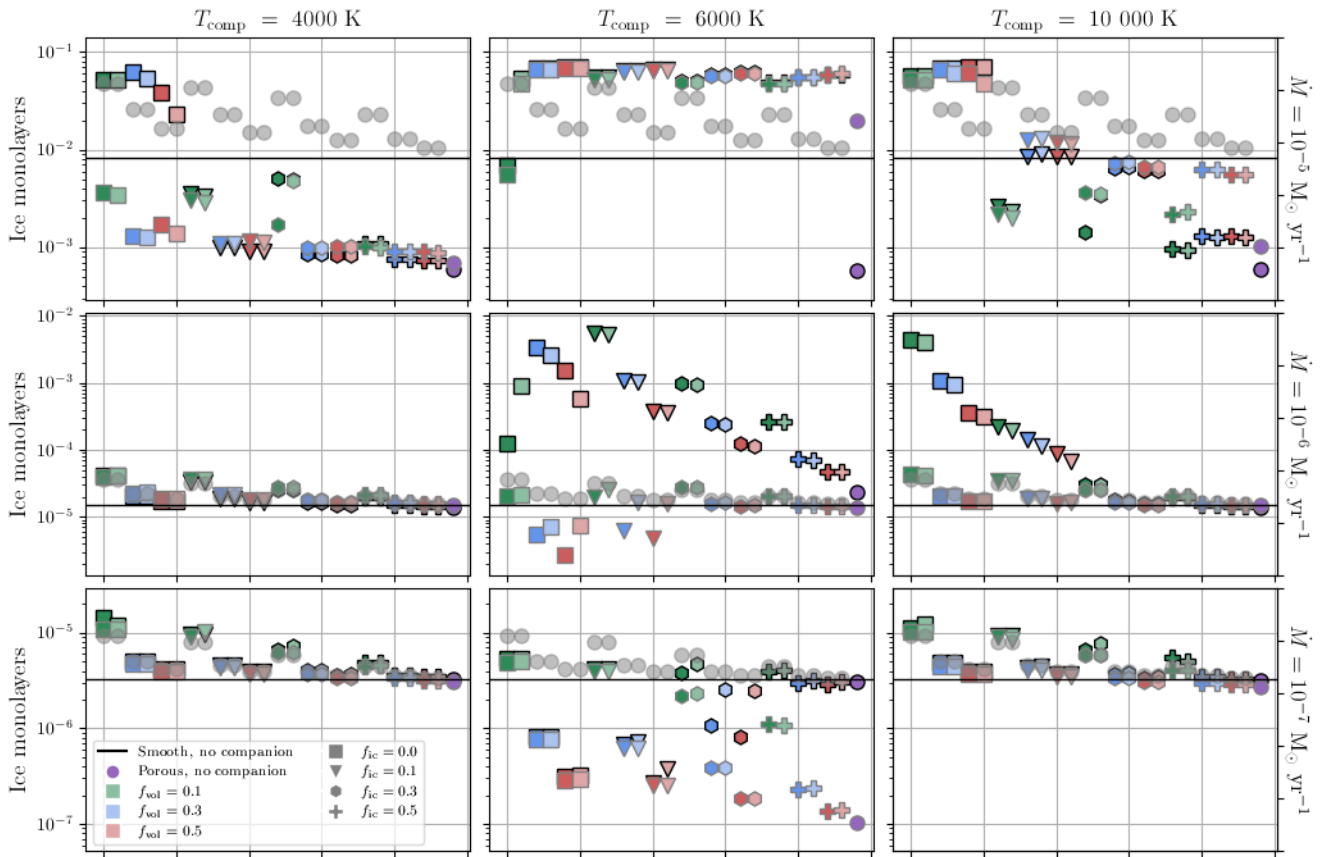


Figure 76: Number of ice monolayers at the end of the outflow for all calculated C-rich outflows, assuming a GSD with smaller grain sizes than the canonical MRN distribution.

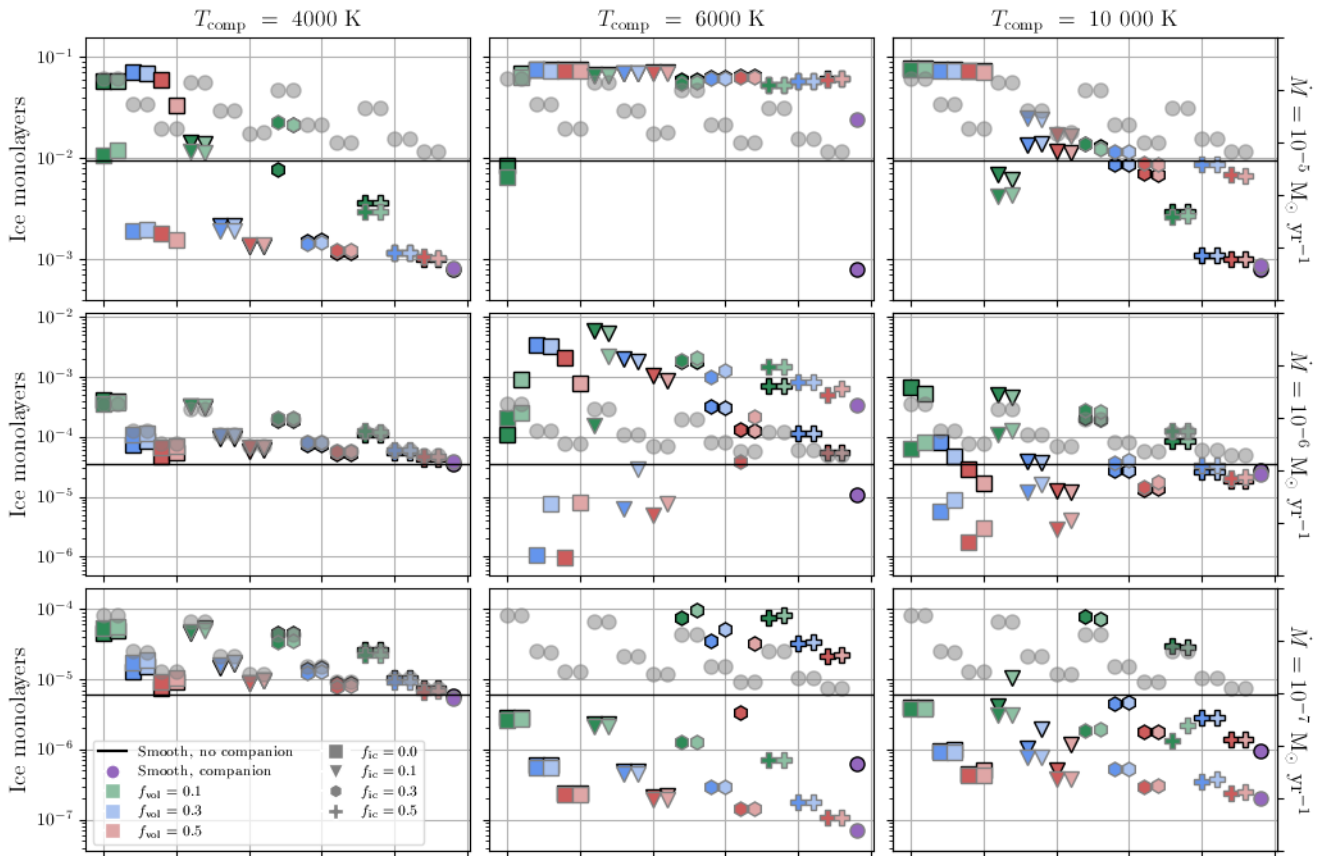


Figure 77: Number of ice monolayers at the end of the outflow for all calculated C-rich outflows, assuming the canonical MRN distribution.

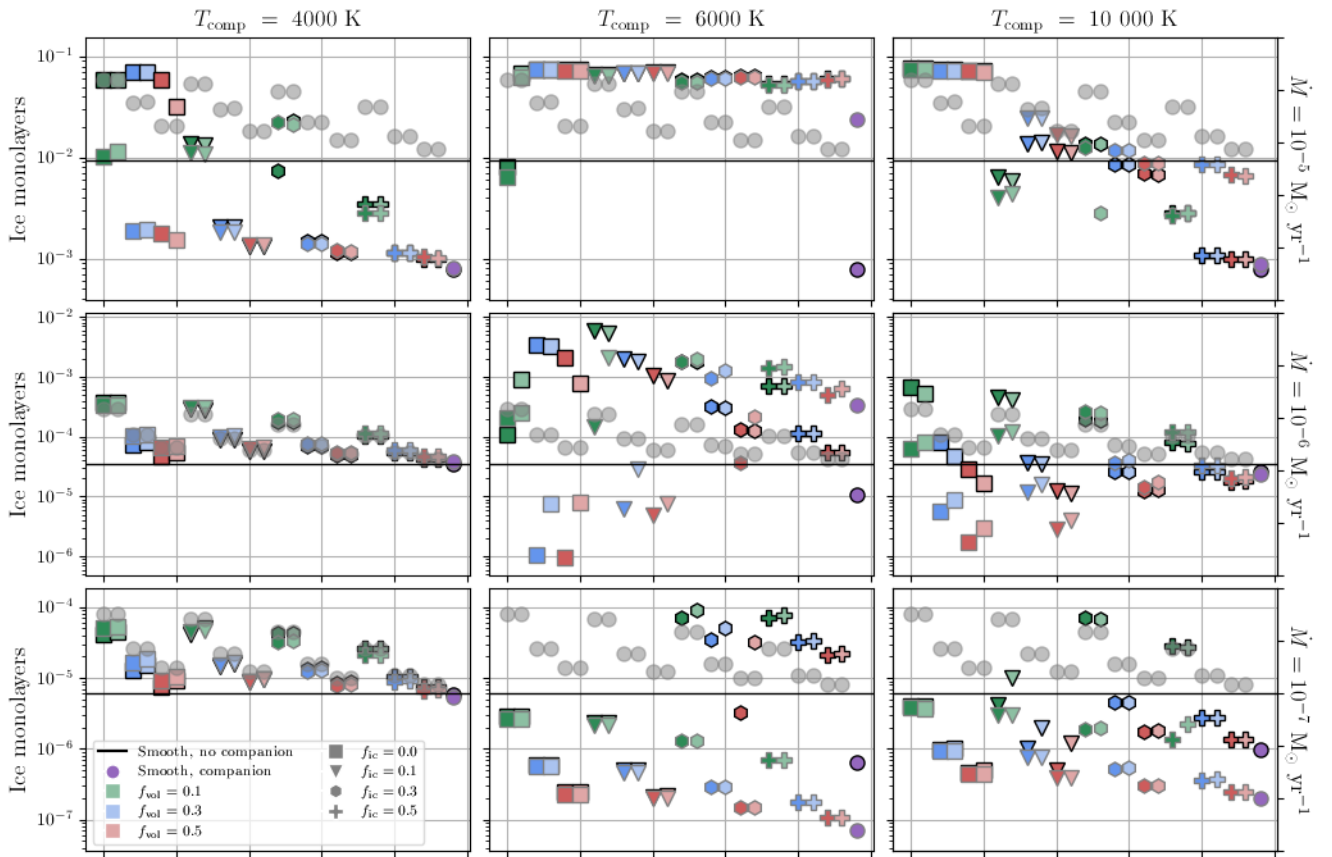


Figure 78: Number of ice monolayers at the end of the outflow for all calculated C-rich outflows, assuming a GSD with larger grain sizes than the canonical MRN distribution.

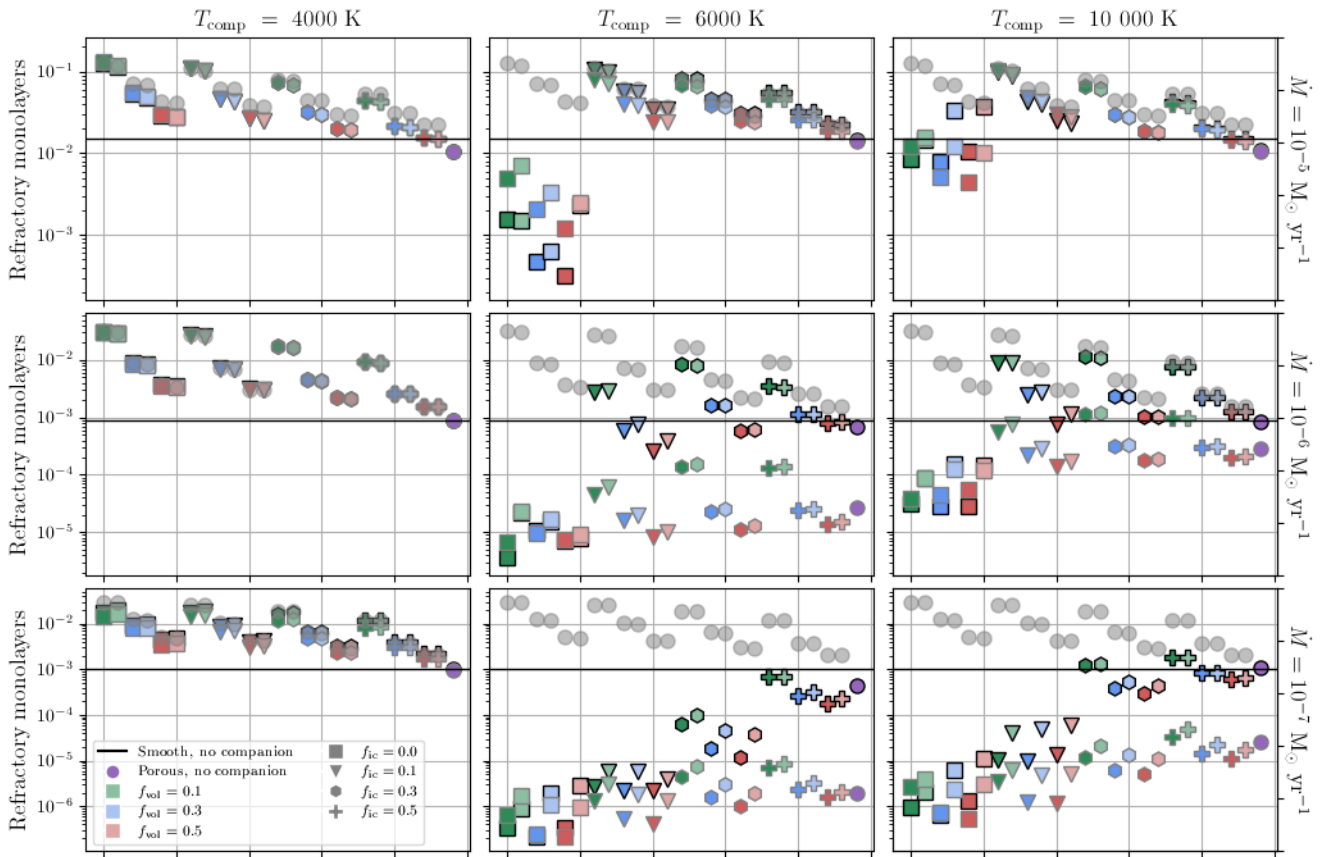


Figure 79: Number of refractory monolayers at the end of the outflow for all calculated C-rich outflows, assuming a GSD with smaller grain sizes than the canonical MRN distribution.

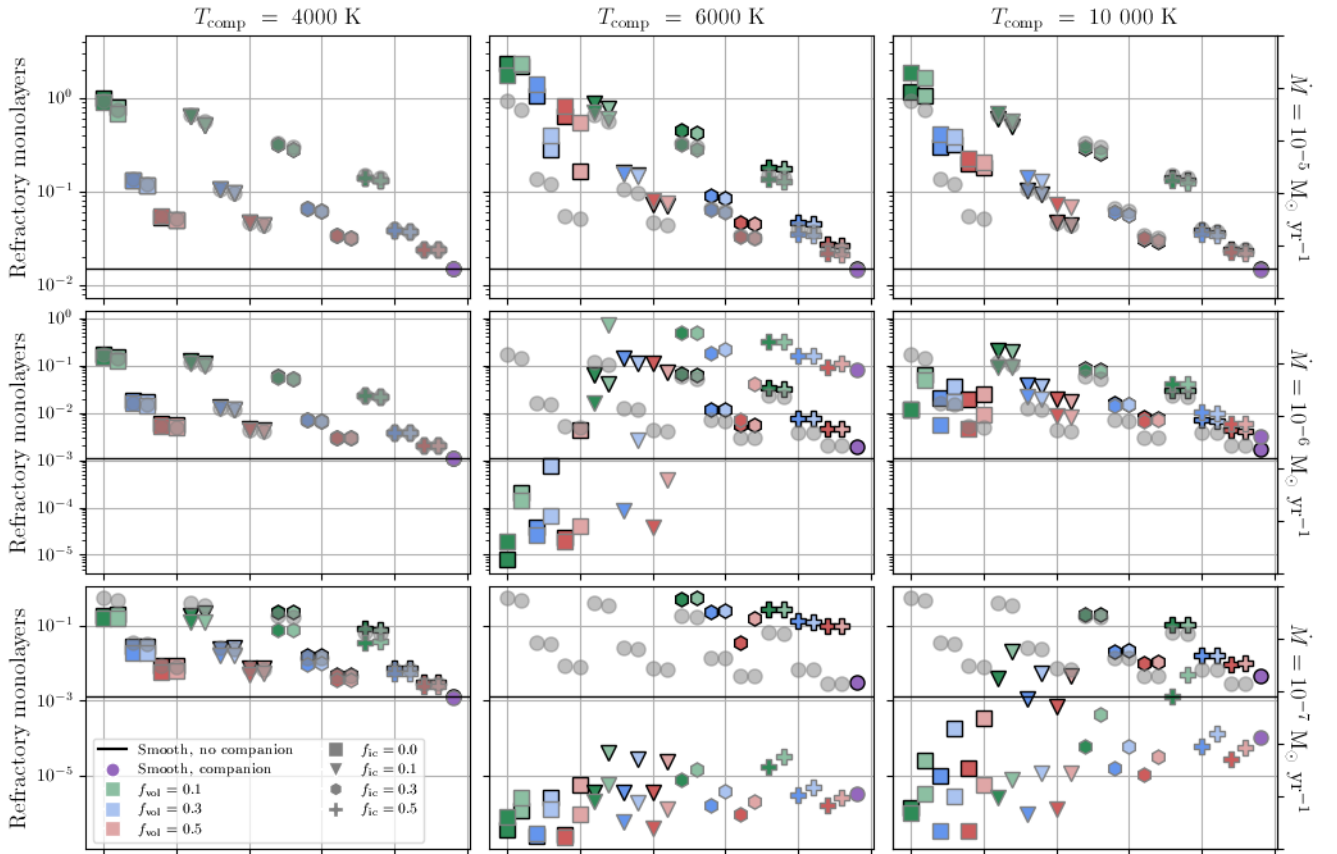


Figure 80: Number of refractory monolayers at the end of the outflow for all calculated C-rich outflows, assuming the canonical MRN distribution.

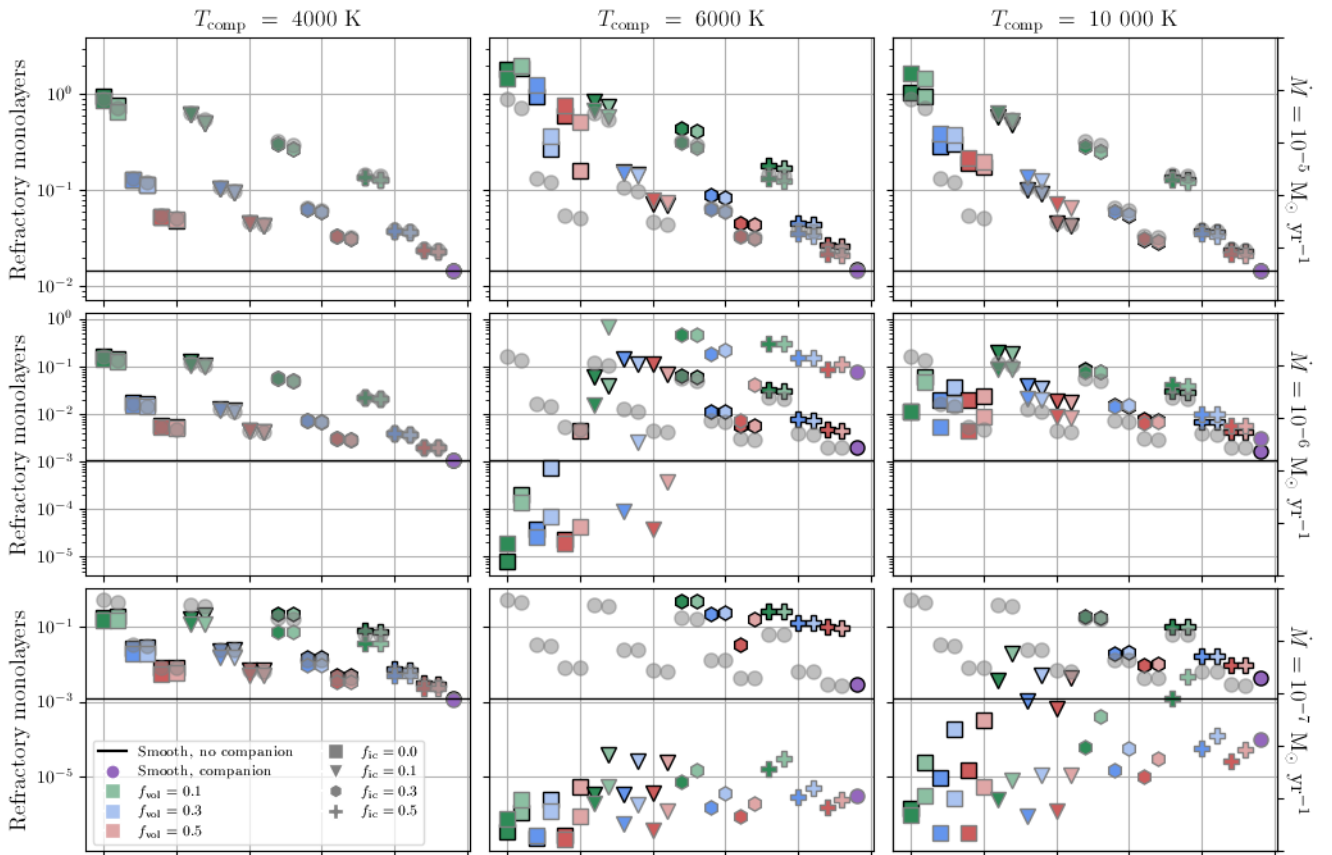


Figure 81: Number of refractory monolayers at the end of the outflow for all calculated C-rich outflows, assuming a GSD with larger grain sizes than the canonical MRN distribution.

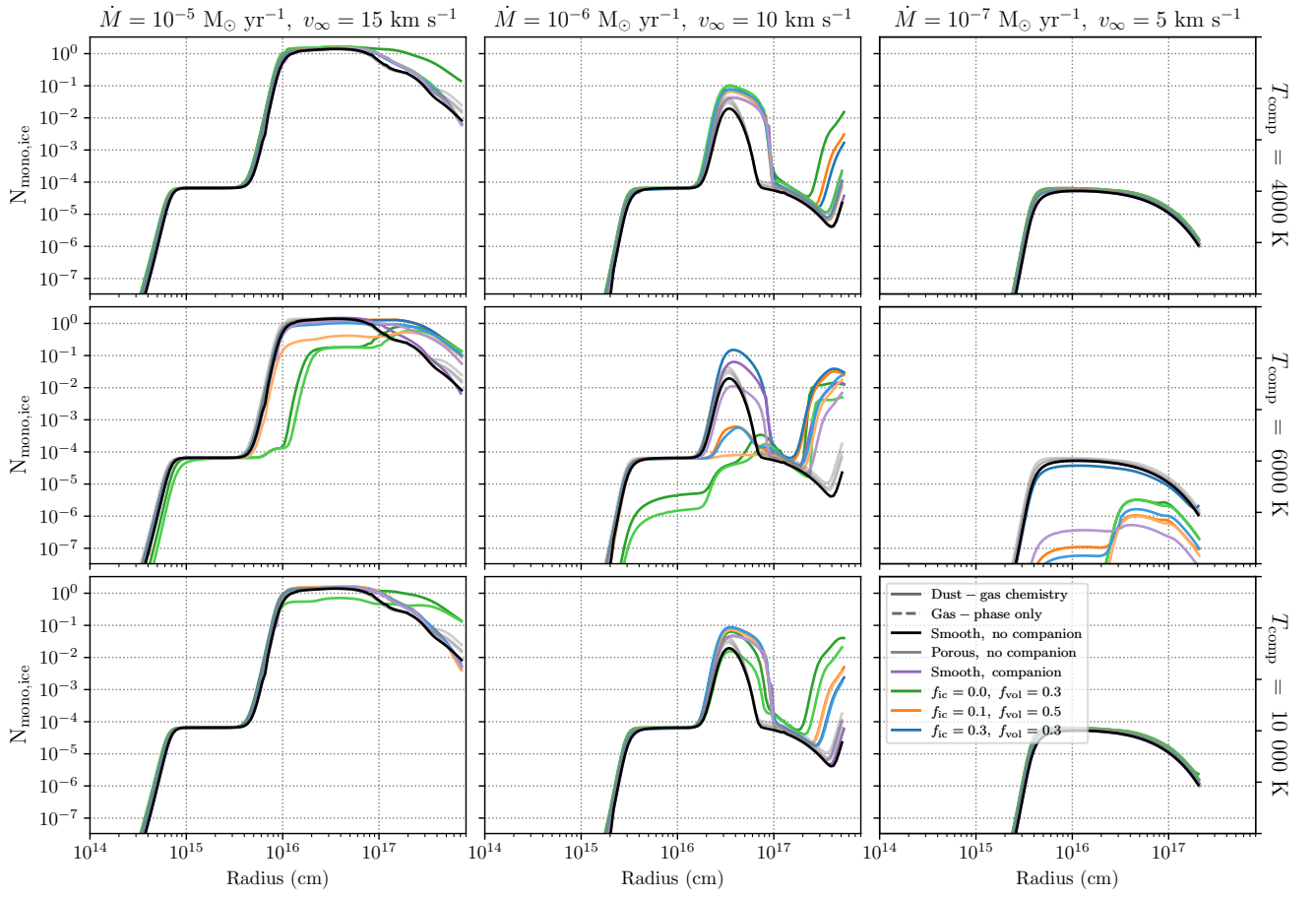


Figure 82: Number of ice monolayers in a selection of O-rich outflows, assuming a GSD with smaller grain sizes than the canonical MRN distribution.

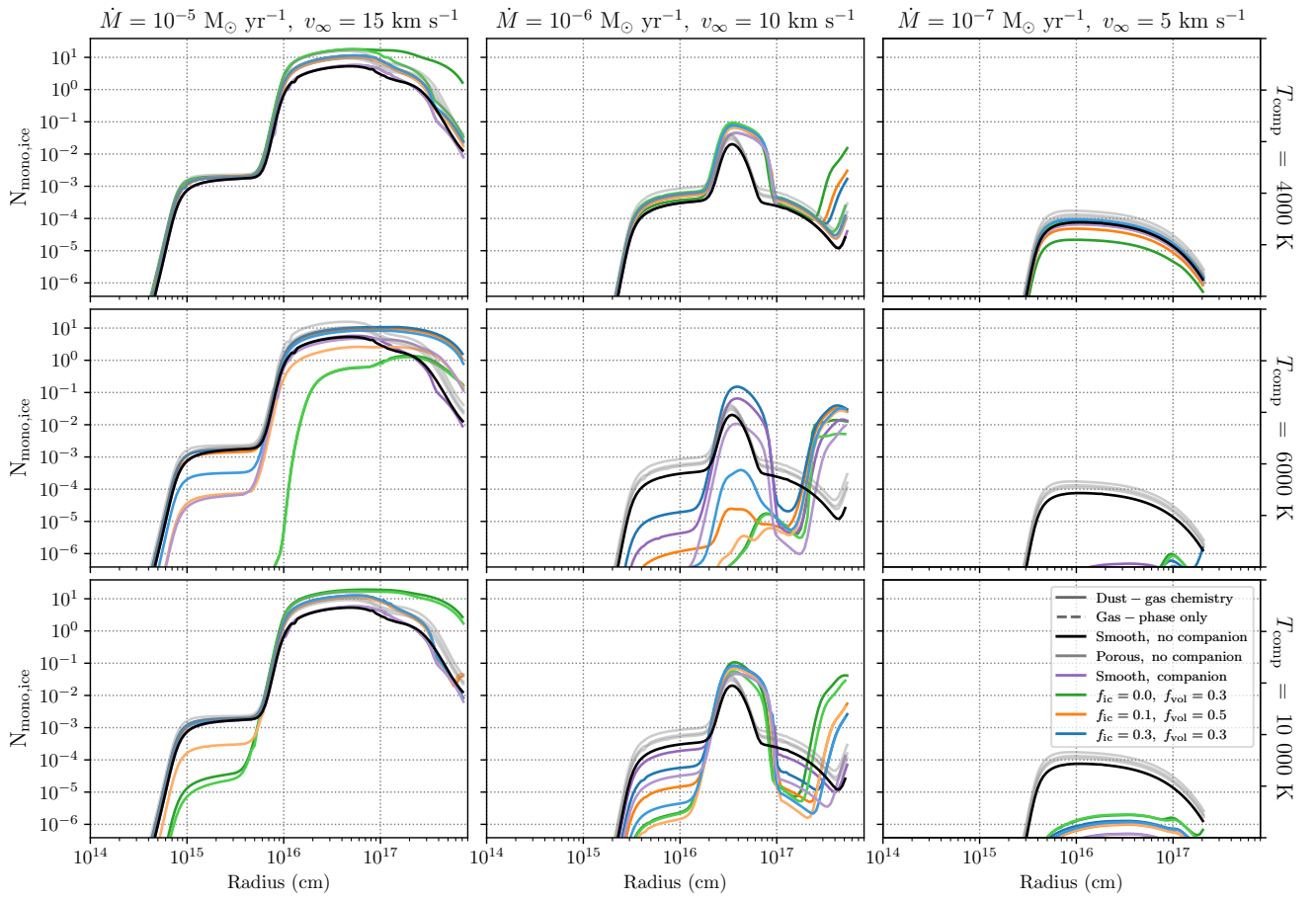


Figure 83: Number of ice monolayers in a selection of O-rich outflows, assuming the canonical MRN distribution.

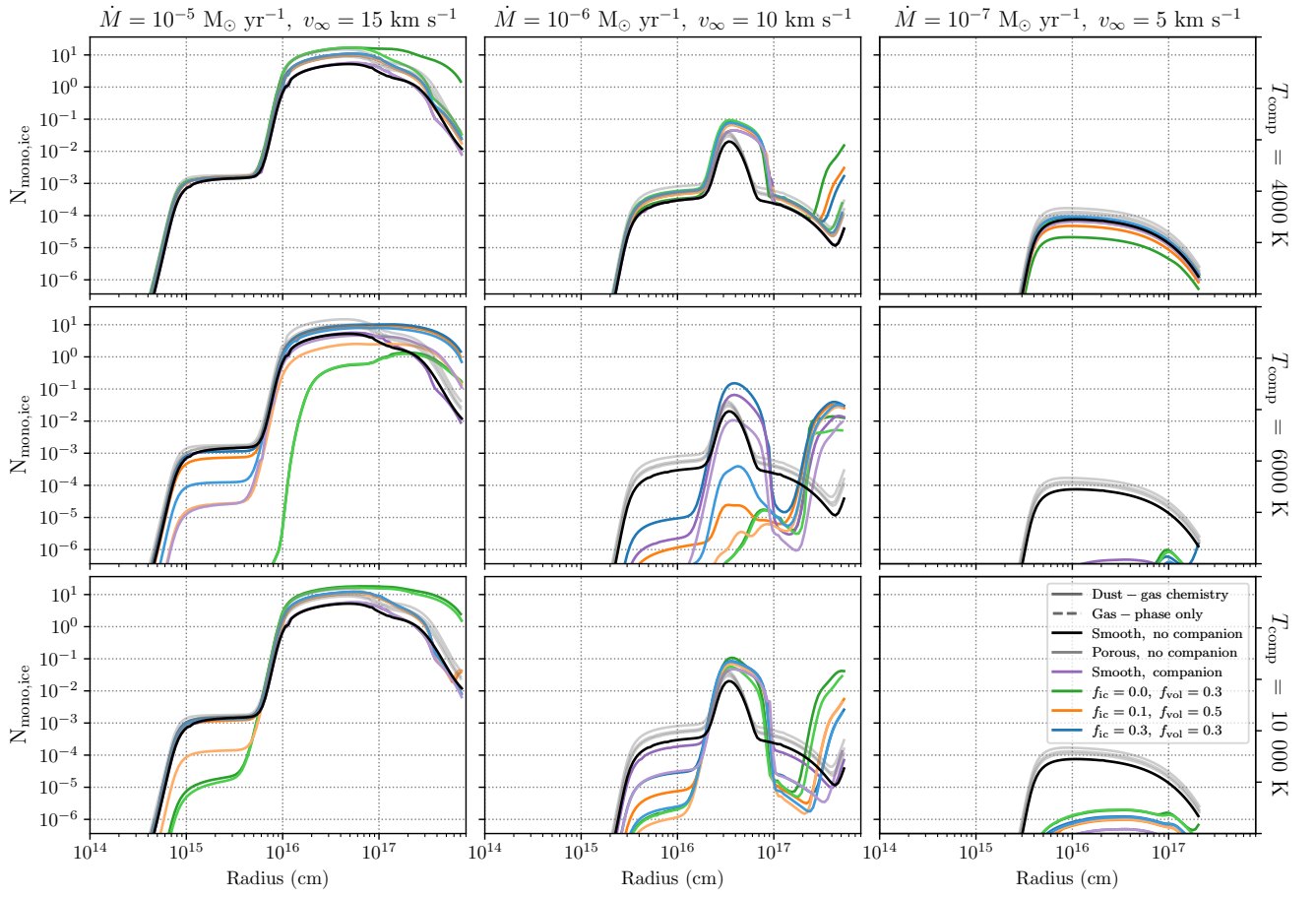


Figure 84: Number of ice monolayers in a selection of O-rich outflows, assuming a GSD with larger grain sizes than the canonical MRN distribution.

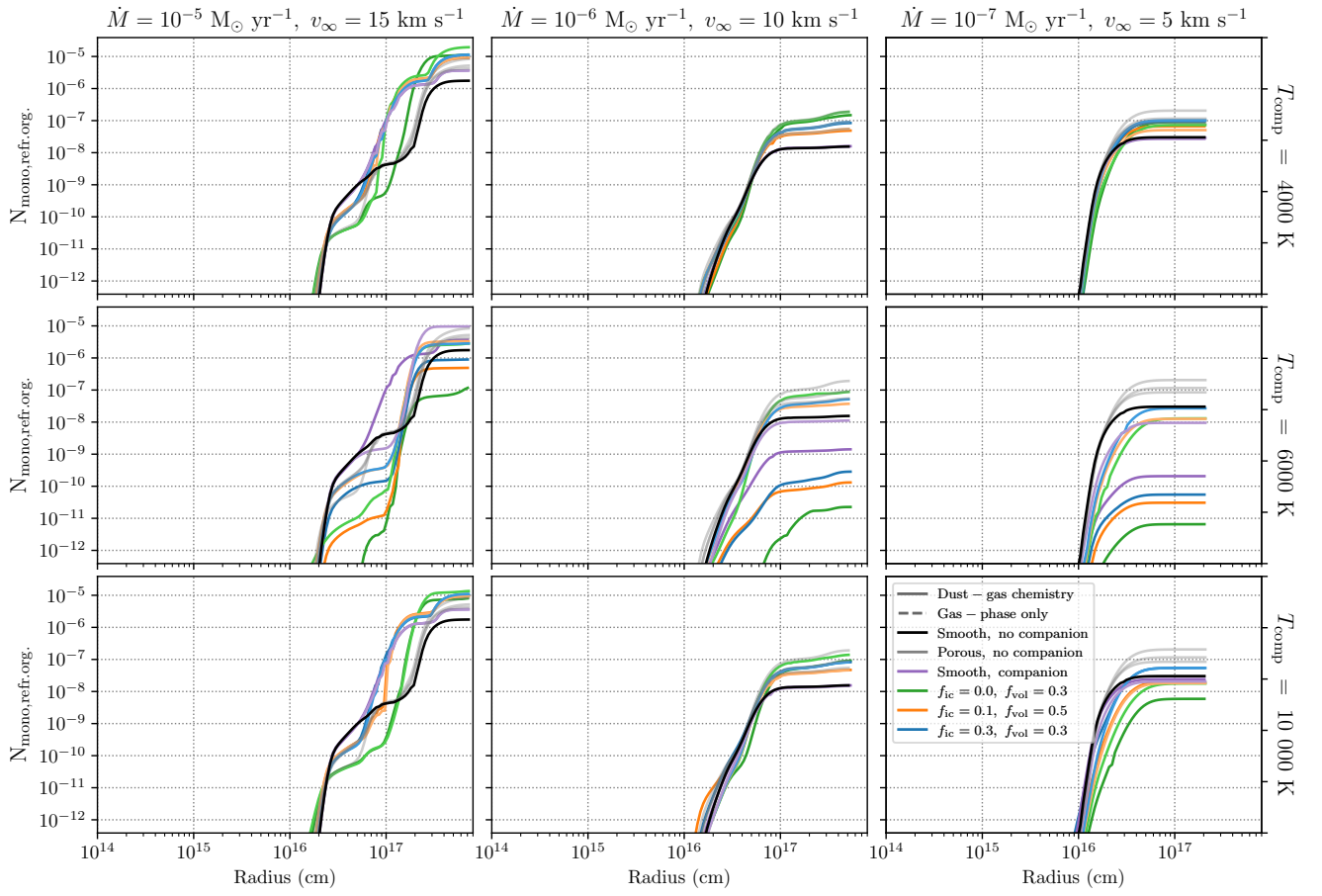


Figure 85: Number of refractory monolayers in a selection of O-rich outflows, assuming a GSD with smaller grain sizes than the canonical MRN distribution.

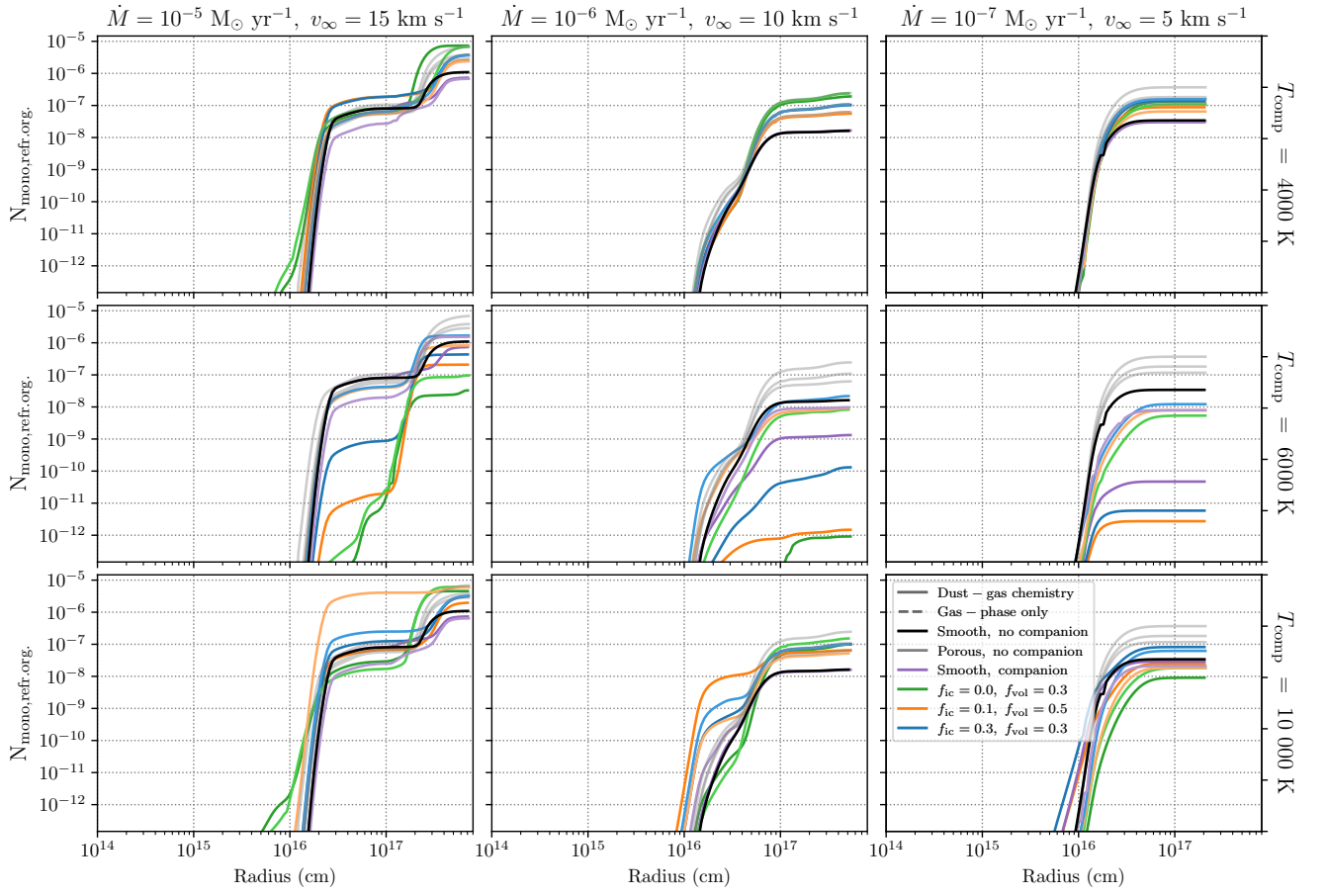


Figure 86: Number of refractory monolayers in a selection of O-rich outflows, assuming the canonical MRN distribution.

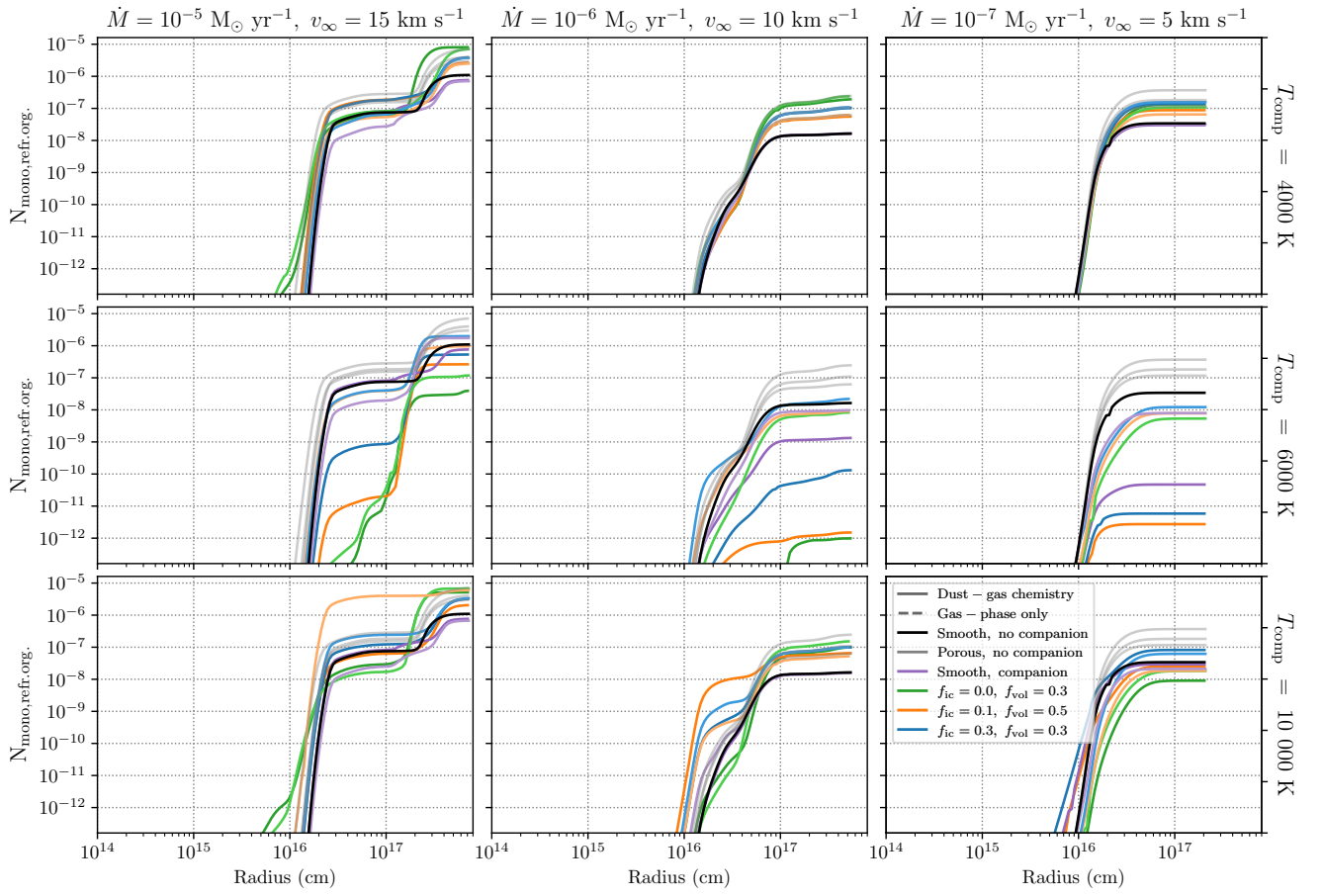


Figure 87: Number of refractory monolayers in a selection of O-rich outflows, assuming a GSD with larger grain sizes than the canonical MRN distribution.

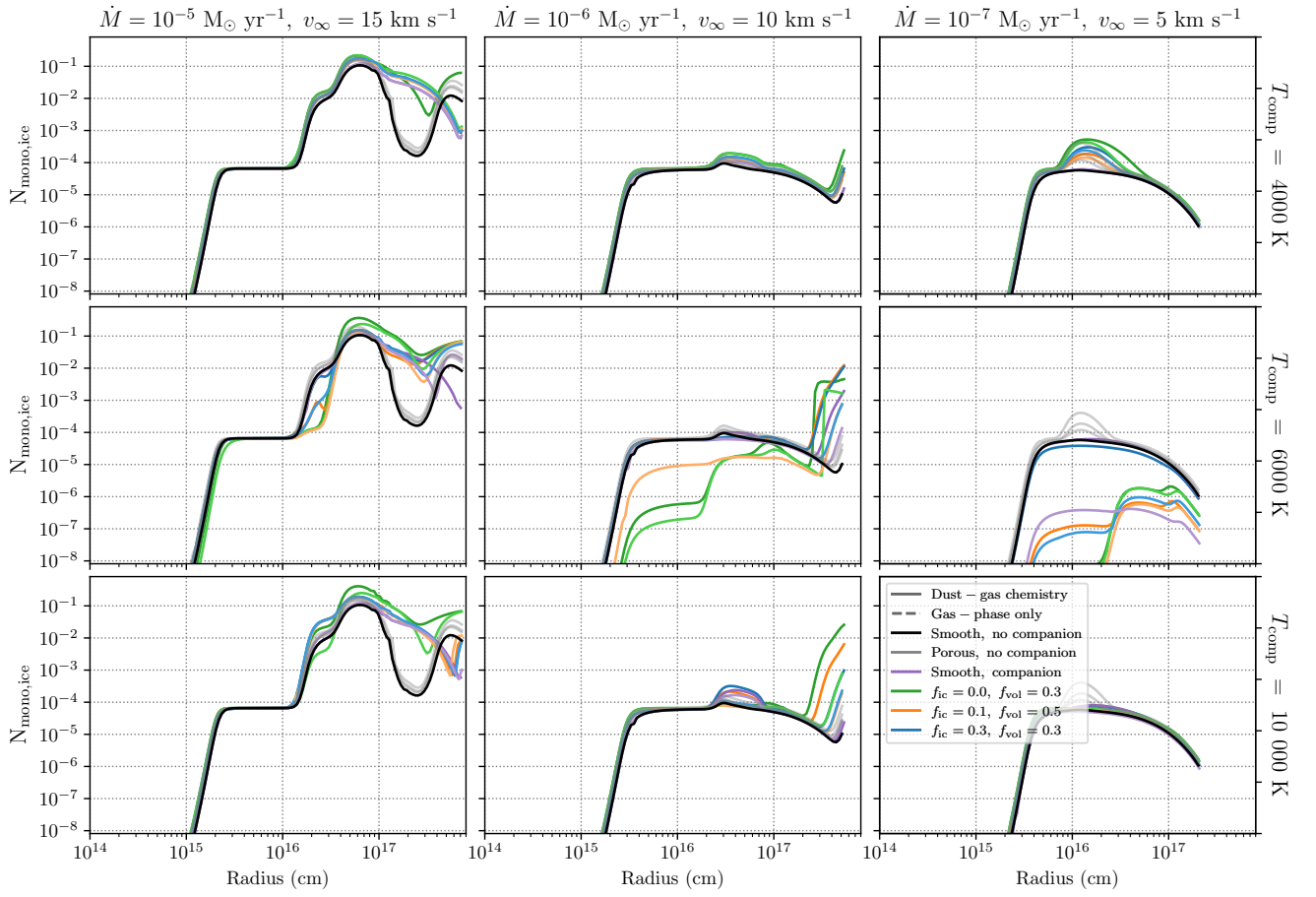


Figure 88: Number of ice monolayers in a selection of C-rich outflows, assuming a GSD with smaller grain sizes than the canonical MRN distribution.

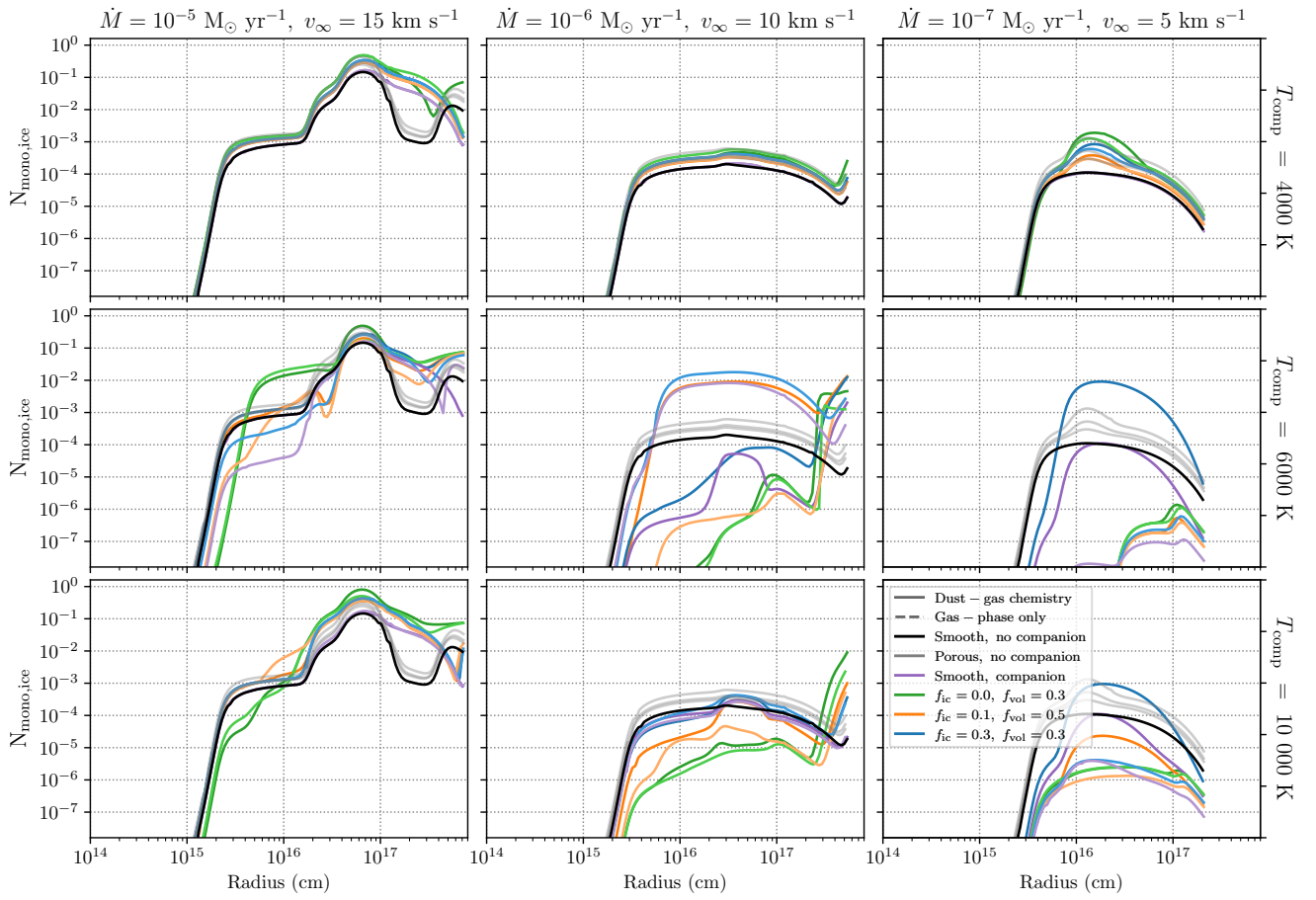


Figure 89: Number of ice monolayers in a selection of C-rich outflows, assuming the canonical MRN distribution.

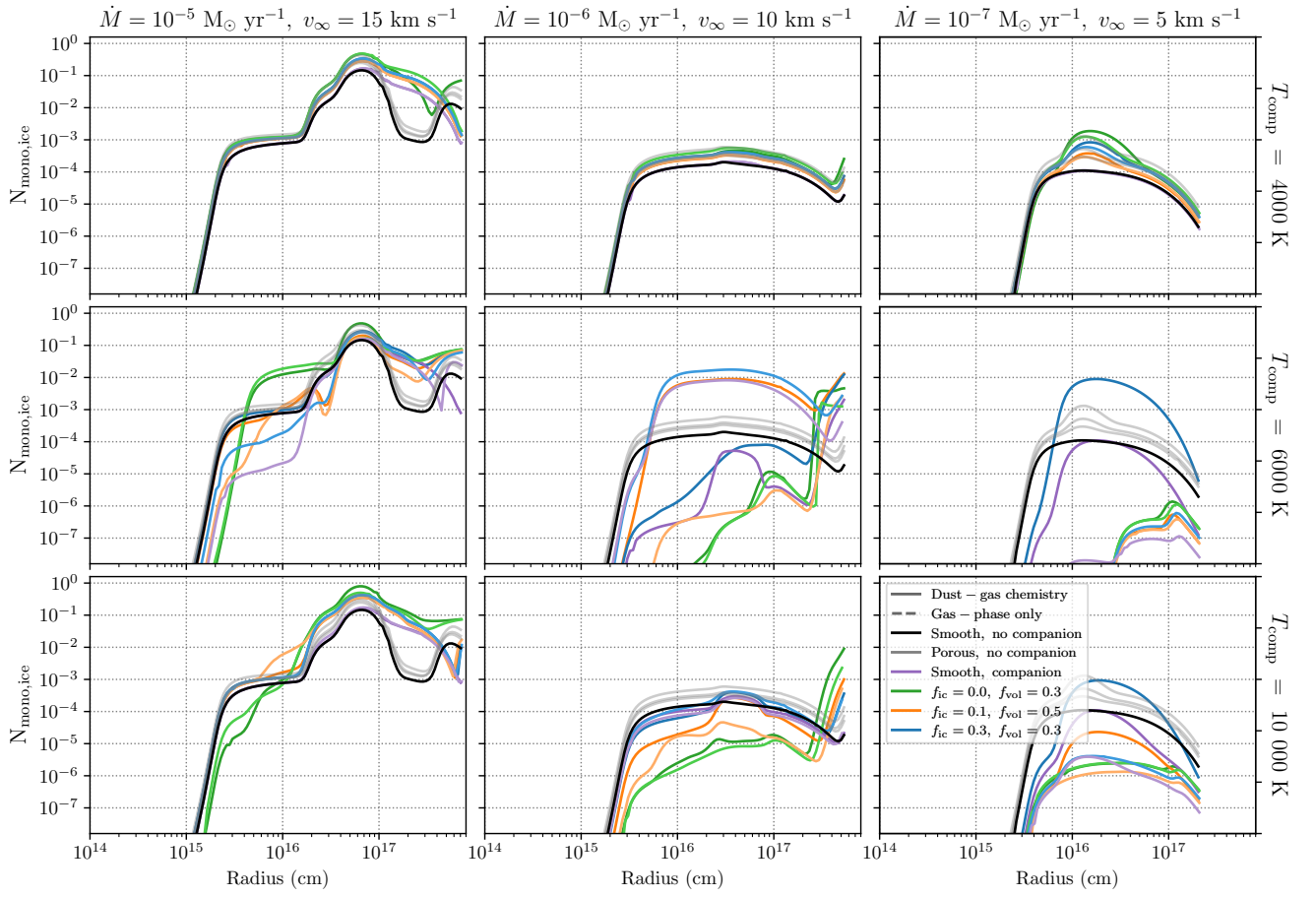


Figure 90: Number of ice monolayers in a selection of C-rich outflows, assuming a GSD with larger grain sizes than the canonical MRN distribution.

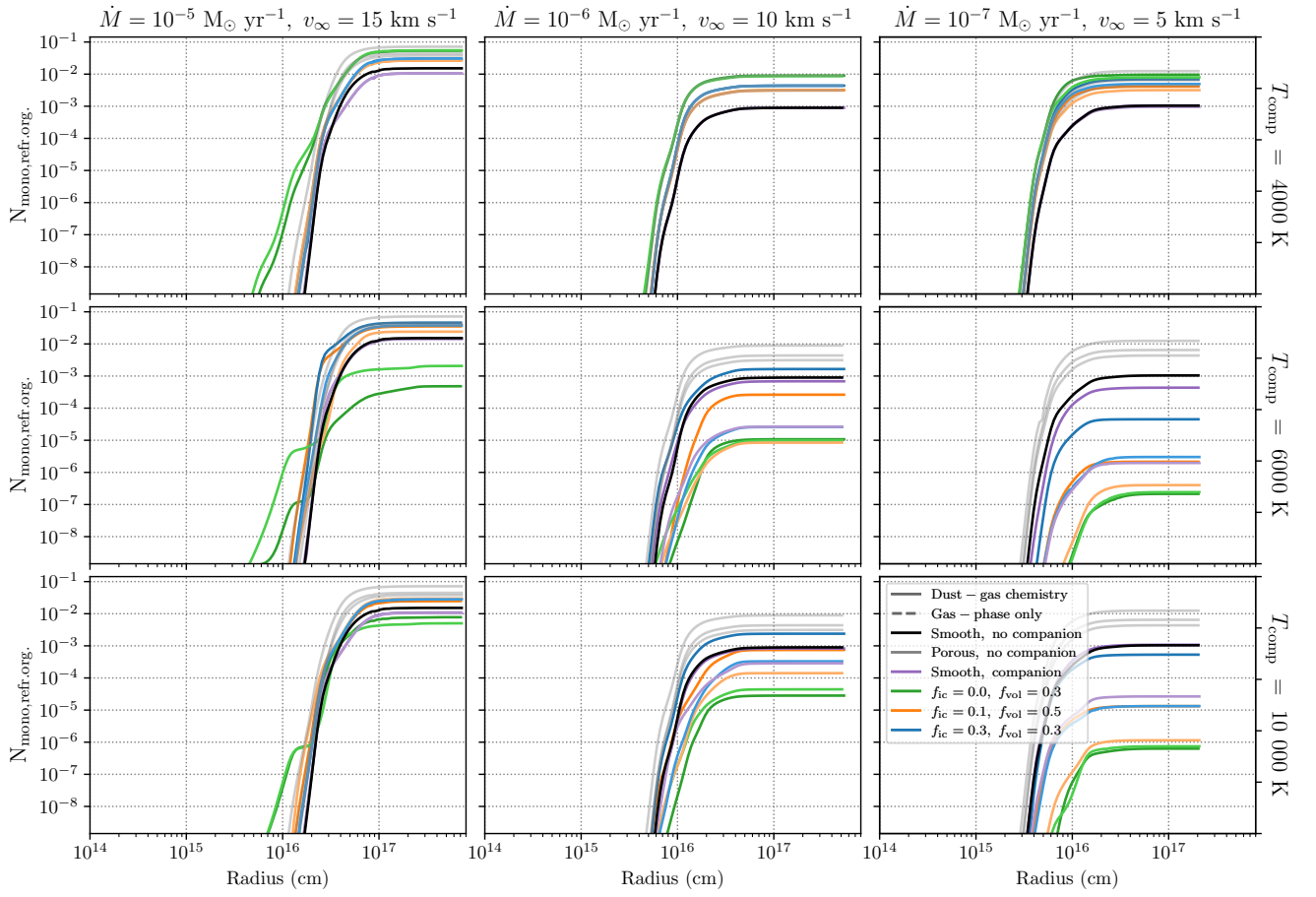


Figure 91: Number of refractory monolayers in a selection of C-rich outflows, assuming a GSD with smaller grain sizes than the canonical MRN distribution.

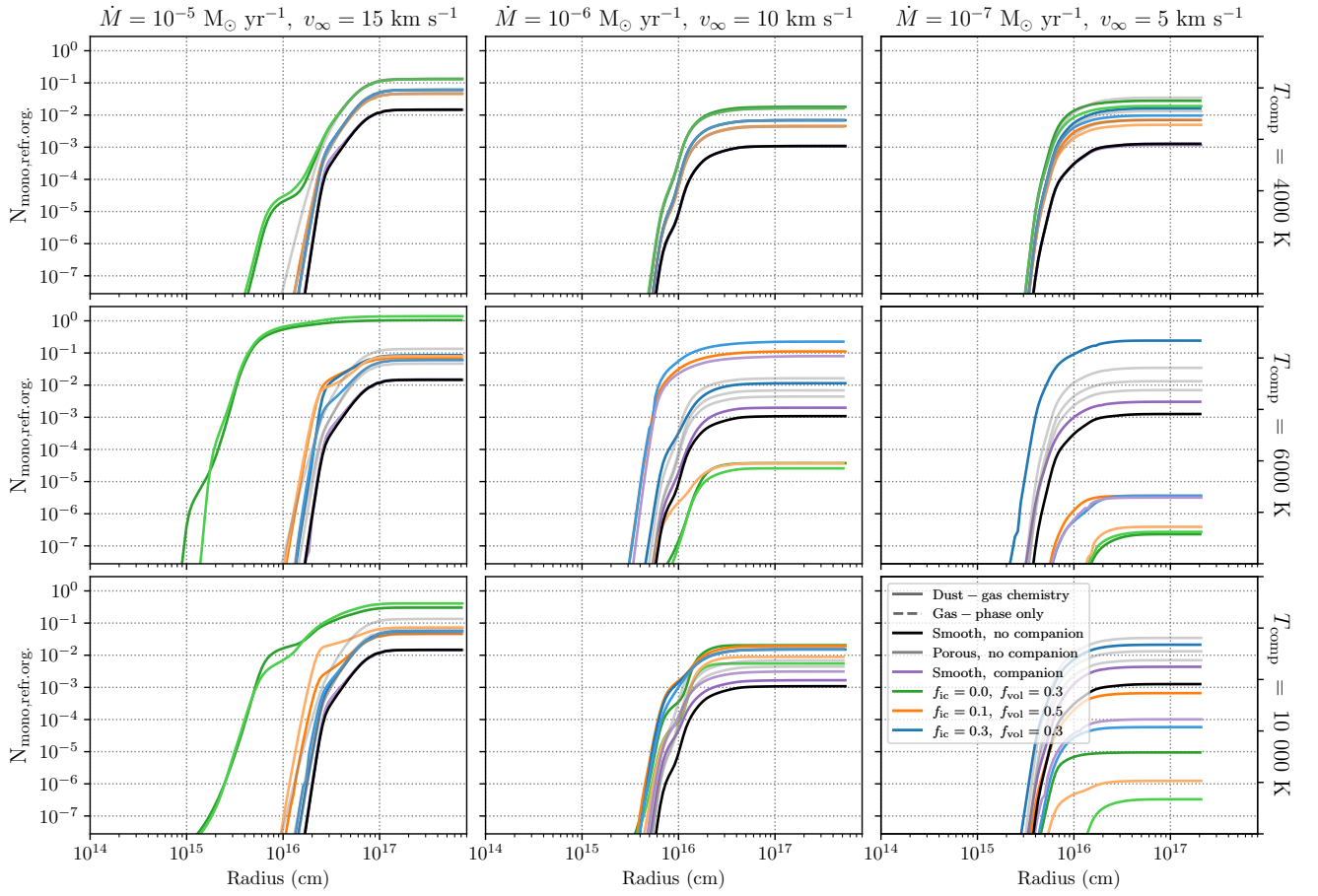


Figure 92: Number of refractory monolayers in a selection of C-rich outflows, assuming the canonical MRN distribution.

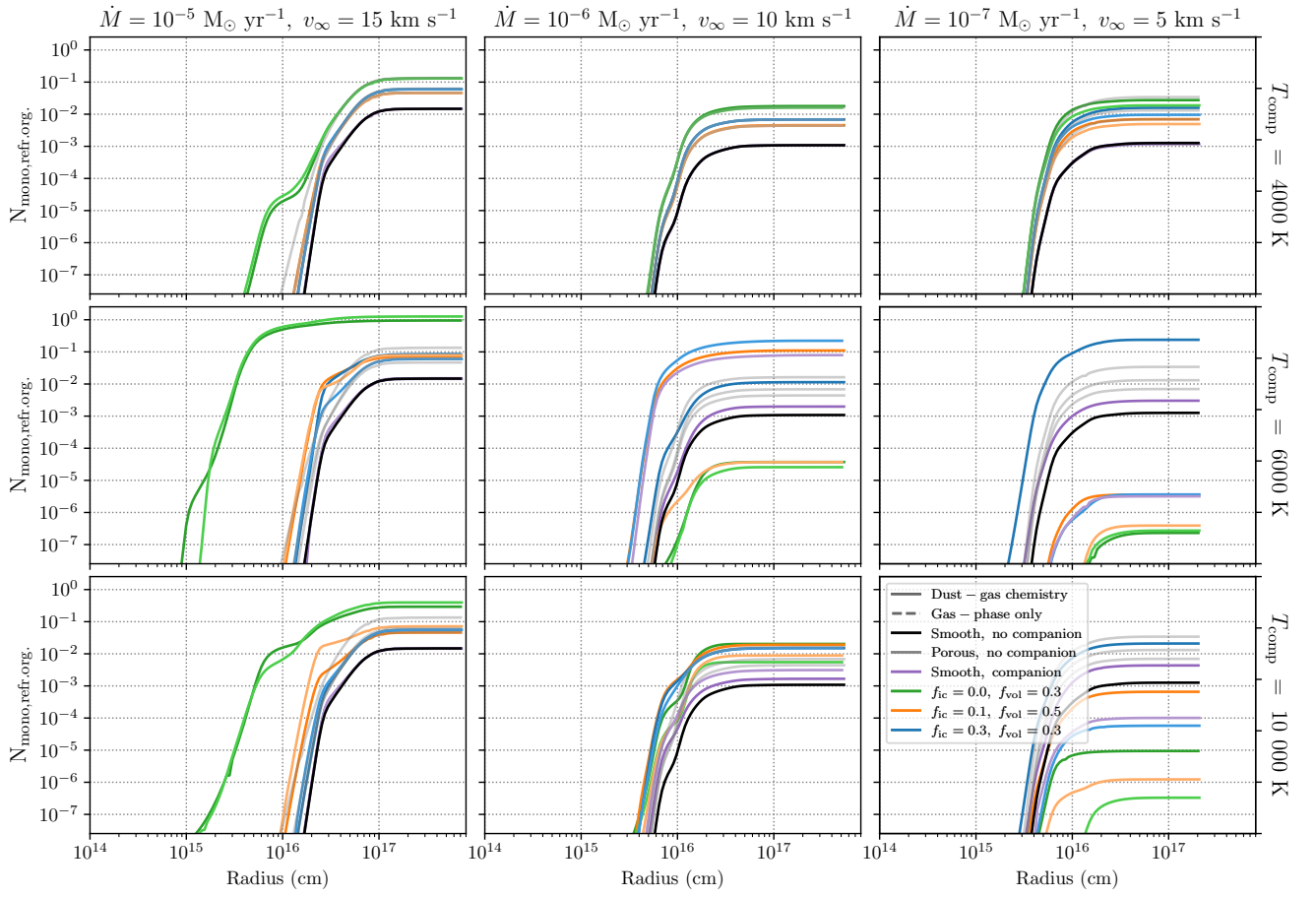


Figure 93: Number of refractory monolayers in a selection of C-rich outflows, assuming a GSD with larger grain sizes than the canonical MRN distribution.